METHODOLOGY FOR DETERMINING THE OPTIMAL OPERATING STRATEGIES FOR A CHILLED WATER STORAGE SYSTEM

A Dissertation

by

ZHIQIN ZHANG

Submitted to the Office of Graduate Studies of
Texas A&M University
in partial fulfillment of the requirements for the degree of

DOCTOR OF PHILOSOPHY

May 2010

Major Subject: Mechanical Engineering

METHODOLOGY FOR DETERMINING THE OPTIMAL OPERATING STRATEGIES FOR A CHILLED WATER STORAGE SYSTEM

A Dissertation

by

ZHIQIN ZHANG

Submitted to the Office of Graduate Studies of
Texas A&M University
in partial fulfillment of the requirements for the degree of

DOCTOR OF PHILOSOPHY

Approved by:

Chair of Committee,	William D. Turner
Committee Members,	David E. Claridge
	Charles H. Culp
	Warren M. Heffington
Head of Department,	Dennis L. O'Neal

May 2010

Major Subject: Mechanical Engineering

ABSTRACT

Methodology for Determining the Optimal Operating Strategies

for a Chilled Water Storage System. (May 2010)

Zhiqin Zhang, B.S.; M.S., Tsinghua University

Chair of Advisory Committee: Dr. William D. Turner

This dissertation proposed a new methodology for determining the optimal operating strategies for a chilled water storage system under a Time-of-Use electricity rate structure. It is based on a new classification of operating strategies and an investigation of multiple search paths.

Each operating strategy consists of a control strategy and the maximum number of chillers running during the off-peak and on-peak periods. For each month, the strategy with the lowest monthly billing cost and minimal water level higher than the setpoint is selected as the optimal operating strategy for the current month. A system model is built to simulate the tank water level at the end of each time step and the system total power during each time step. This model includes six sub-models. Specifically, the plant model is a forward model using a wire-to-water concept to simulate the plant total power. For the Thermal Energy Storage (TES) model, the tank state is described with total chilled water volume in the tank and its derivation is the tank charging or discharging flow rate. A regression model is adopted to simulate the loop supply and return temperature

difference as well as the loop total flow rate demand. In the control strategy sub-model, except for three conventional control strategies and the operation without TES, a new control strategy is advanced to load the chiller optimally. The final results will be a table showing the monthly control strategy and maximal number of chillers staged on during the off-peak and on-peak periods, an approach which is easy for the operators to follow.

Two project applications of this methodology are introduced in this dissertation. One is an existing TES system with state-of-the-art control and metering systems. The monthly optimal operating strategies are generated, which will achieve significant savings. The comparisons among different control strategies are also provided. The other application consists of multiple plants with little data. The purpose of the study is to evaluate the economic feasibility of designing a new chilled water storage tank and sharing it among four plants. This problem can be solved with a simplified system model, and an optimal tank size is recommended.

DEDICATION

To my wife Jingjing, my son Jason, and my parents

ACKNOWLEDGEMENTS

First of all, I would like to express my sincere gratitude to my advisor, Dr. William D. Turner, for his great guidance and support throughout my research. From literature review, proposal, to dissertation and presentation slides, Dr. Turner reviewed them word-by-word, time and time again, and gave me alot of insightful comments and advice. I greatly benefited from his guidance. I also wish to thank my committee, Dr. David E. Claridge, Dr. Charles H. Culp, and Dr. Warren M. Heffington, for their careful reviews and comments on this dissertation.

I am also grateful to Energy Systems Laboratory for providing me continuous financial support and such a great academic environment in which to finish this research. The appreciation is extended to Continuous Commissioning® group members: Song Deng, Darren Chen Xu, Daniel Qiang Chen, Dr. Hui Li, Dr. Lei Wang, and Liang Ma. Without their advice and help, I could not have finished this research.

In addition, I want to thank Diane McCormick and Connie Clarno for their great encouragement and thoughtful coordination efforts.

Finally, I am forever grateful to my wife Jingjing, my son Jason, my parents, and my parents-in-law, who encouraged me to pursue my dreams, and gave me the love, confidence, and abilities to realize those dreams. All of this is for them.

NOMENCLATURE

4CP	Four Coincident Peak
AHU	Air Handling Unit
CHLR	Chiller
ChW	Chilled Water
ChWLT	Chilled Water Leaving Temperature
COP	Coefficient of Performance
C-P	Chiller-Priority
CPP	Sam Houston Central Plant
CSB-SQP	Complete Simulation-Based Sequential Quadratic Programming
CT	Cooling Tower
CV	Coefficient of Variation
CVRMSE	Coefficient of Variation of the Root Mean Squared Error
CW	Condenser Water
CWET	Condenser Water Entering Temperature
CWLT	Condenser Water Leaving Temperature
CWP	Condenser Water Pump
DB	Dry-Bulb
DCS	Dynamic Chiller Sequencing
DDC	Direct Digital Control

DDP	Differential Dynamic Programming
DFW	Dallas-Fort Worth
DP	Differential Pressure
EMPP	Equal Marginal Performance Principle
EP	Energy Plaza
ERCOT	Electric Reliability Council of Texas
FCV	Flow Control Valve
FOM	Figure-of-Merit
F-S	Full-storage
GPM	Gallons per Minute
GRG	Generalized Reduced Gradient
HHW	Heating Hot Water
HVAC	Heating, Ventilating, and Air Conditioning
LP	Loop
M	Million
NCDC	National Climatic Data Center
NCP	Non-Coincident Peak
NLP	Non Linear Programming
NTU	Number of Transfer Units
OCL	Optimal Chiller Loading
OCS	Optimal Chiller Sequencing
OLS	Ordinary Least Squares

OM	On-site Manufacture
PCA	Pre-cool Air
PID	Proportional Integral Derivative
PLR	Part Load Ratio
PPMP	Primary Pump
PSV	Pressure Sustaining Valve
Re	Reynolds number
REJ	Robert E. Johnson Plant
RMS	Root Mean Square
RPM	Revolutions per Minute
RTP	Real-Time-Pricing
SA	Simulated Annealing
SFA	Stephen F. Austin Plant
SG	Specific Gravity
SP	Setpoint
S-P	Storage-Priority
SPMP	Secondary Pump
TDC	Target Demand Cost
TES	Thermal Energy Storage
TFC	Texas Facility Commission
TFM	Transfer Function Method
TMY	Typical Meteorological Year

TOU	Time-of-Use
VSD	Variable Speed Drive
WB	Wet-Bulb
WPC	William P. Clements Plant
WTW	Wire-to-Water

TABLE OF CONTENTS

Page

Page

Page

Page

Page

LIST OF FIGURES

Page

Page

Page

LIST OF TABLES

Page

1. INTRODUCTION

1.1 Background

Thermal Energy Storage (TES) is a concept of generating and storing energy in the form of heat or cold for future use. This concept has been used for centuries, but only recently have large electrical users taken advantage of this technique for demand side management and cost reduction. This work focuses on a Chilled Water (ChW) system with a naturally stratified ChW storage tank, which is a subclass of TES systems. The advantages of a TES system are summarized by the following three concepts.

Except for capital cost savings due to reduced equipment size, the TES system is designed to avoid high electric utility energy or demand charges. Cooling buildings is a major contributor to the high electricity demand during the summer time, especially during the on-peak hours. It is estimated that the cooling of buildings contributes about 35% to the U.S. peak electrical power consumption in the summer (Henze 1995). Demand charges with Time-of-Use (TOU) rates as well as Real-Time-Pricing (RTP) rates have been designed to stimulate the application of electrical load shifting technologies, such as the TES system. The basic idea of a ChW storage system is to run chillers during the time of low utility system demand and energy costs and store the produced chilled water in a tank. During the time of high electrical demand and energy

---

This dissertation follows the style of *ASHRAE Transactions.*

costs, all or part of the plant chillers are shut down while the tank is discharged to meet the cooling load of the facility. As a result, the electricity load of a ChW plant is shifted and operation costs are minimized. This is the general design purpose of a ChW TES system, and most systems are operated following this strategy.

Secondly, a TES system provides an opportunity to decouple the production and the consumption of the chilled water. This decoupling effect could be utilized to provide increased flexibility, reliability, or backup capacities for the control and operation of the system (ASHRAE 2003a). A conventional ChW plant must handle the cooling demand as it occurs. This forces the ChW plant to operate in a load following mode, varying the output of the system in response to fluctuations in the cooling requirements. TES acts as a buffer in the system, and can produce much of the cooling at night when the ambient wet bulb (WB) temperature is low, and chiller efficiency is improved.

The third concept is that the plant performance can also be improved by loading chillers at the optimal Part Load Ratio (PLA). The extreme low or extreme high loading operations, where chiller efficiency is degraded, can be avoided or optimized. Sometimes, the plant efficiency can be further improved by shifting the cooling load to more efficient chillers (such as new electric centrifugal chillers), thus avoiding the operation of less efficient chillers.

Consequently, TES is not only cost-effective but it also could be energy-effective if operated properly. At the same time, improving the performance of a ChW plant will reduce the demand and energy usage and cut the total cost further.

In practice, many ChW storage systems are manually operated based on operators' experiences. The operating strategies target some simple objectives, such as avoiding chillers running during the on-peak hours and charging the tank as soon as possible during the off-peak hours. The operators determine the control strategies based on their instincts and the utility rate structures. A good example is to start charging the tank right after the end of on-peak hours until the tank is full, fully loading the chillers for the initial loading period. During the winter months when utility rate structures change, many ChW storage tanks are not in use. Such kinds of operations may reap part of the benefits from the thermal storage tank but they cannot make full use of the advantages of a TES system.

The energy performance of most existing ChW plants is not very efficient. It was estimated that about 90% of water-cooled, centrifugal, central plants operated in the 1.0-1.2 kW per ton "needs improvement" range, while a highly efficient plant can reach 0.75 kW per ton (Erpelding 2006). All kinds of problems are to blame, such as the low delta-T syndrome (Kirsner 1995), low part load ratio, significant mixing, valve and pump hunting, higher than needed pump pressure, etc. In addition, there are other reasons for plant optimization, such as equipment performance degrading with age, load changes (Taylor 2006), plant expansion in an unorganized manner, and energy cost fluctuations. Therefore, enhancing the performance of cooling plants is an urgent and important task.

There are many reasons why the TES capabilities are not fully exploited. One reason could be that sophisticated controllers and adequate controls sensors are not available. The fear of prematurely depleting the tank during the on-peak hours also

forces the operators to take a more conservative attitude in tank operations. The various operation modes together with complicated rate structures also enhance the difficulties and complexities of determining the optimal operating strategies.

Consequently, a rigorous and systematic methodology is needed to help TES operators and energy managers determine cost-effective and reliable operating strategies for a TES system. Such a method should not only be able to capture the main characteristics of the system performance and rate structures but also be easily followed. It should be able to be generalized to some popular systems and find the optimal operating strategies quickly. The control strategies can maximize the benefits of the tank operations and be easily implemented into the control system if the hardware requirements are met. In addition, the safety considerations should be included and be adjustable to accommodate a conservative or an aggressive operating attitude. A good operating strategy should be a trade-off among cost savings, reliability, and feasibility. The method of searching for the best overall strategy should be able to depict the relationships among these three factors and find the right balance point.

1.2 Research Objective

The goal of this dissertation is to propose a generic methodology for determining the optimal operating strategies for a chilled water storage system under a Time-of-Use utility rate structure. This objective is achieved in the following four steps:

1. Define the classification of operating strategies and construct a detailed search procedure to explore different strategies. A tank level safety threshold and an electricity rate model will be defined to filter the options and compare the total costs of all possible

combinations. The search is conducted month by month and the optimization target function is the monthly utility billing cost.

2. Build a system model to simulate the tank water level and the total system power of the system at the end of each time step. Determine the plant controlled variables to be optimized as well as the optimization method.

3. Build appropriate sub-models for the plant, loop, TES, control strategies, and non-plant power, and connect them together based on the relationships among them. Each sub-model could be revised or replaced with new ones without affecting other sub-models. The loop model calculates the total loop ChW flow demand and ChW return temperature. The plant model simulates the ChW production-related total power at a given ChW demand. The TES model gives the tank water level and the non-plant power model calculates other electricity consumptions. A chiller model is needed to provide the optimal and maximal chiller ChW flow rate.

4. Design a new control strategy to make full use of the energy and cost saving potential of a TES system. The control strategy model determines the plant total ChW production and on-stage chiller number at each time step. The model on the controller design is also introduced to show how this control strategy will be implemented.

Two project applications are introduced in the dissertation to illustrate how this methodology is applied in practice. One is an existing TES system with state-of-the-art control and metering systems. The monthly optimal operating strategies with plant optimization are generated to achieve significant utility billing cost savings. The comparisons among different control strategies are also provided. The other one is an old

ChW system with little operating data. The purpose is to evaluate the economic feasibility of designing a new ChW storage tank and sharing it among four utility plants. This problem can be solved with a simplified plant and loop model for preliminary assessment purposes. The most cost-effective tank size is provided.

1.3 Problem Statement

1.3.1 Basic system configuration

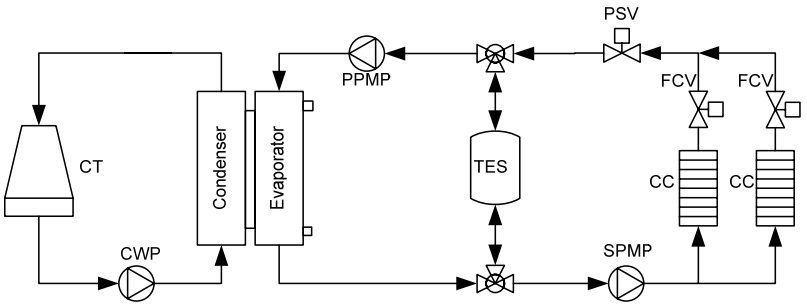

Figure 1 Basic configuration of a stratified chilled water storage system

Figure 1 shows the basic configuration of a naturally stratified ChW storage system. A primary-secondary pump system is designed with variable-speed secondary pumps (SPMPs) and constant-speed primary pumps (PPMPs). The TES tank parallels the chillers and functions like a bypass with an extremely large volume. The water level in the tank also serves as a constant pressure point when the tank is vented. A pressure sustaining valve (PSV) is necessary to avoid a vacuum in the pipes above the water level. If the elevation of a user is much higher than the tank water level, heat exchangers will be designed to transfer the cooling from the tank loop side to the user loop side. This system configuration is the most popular because it is easy to control. In retrofit

projects, such a configuration is often adopted since the least system changes have to be made. As a result, this study will focus on this configuration.

There are no modulating devices on the tank in this configuration. The tank charging or discharging flow rate is the difference between the plant side total flow and the loop side total flow. Since the loop side flow rate can not be controlled by the plant, the TES charging or discharging flow rate is determined by plant total ChW flow rate, and it can be controlled by modulating or sequencing the PPMPs and chillers. The TES operation profile is, in fact, a profile of chilled water total flow rate supplied by the plant. The plant total flow rate is also constrained by some limits, such as chiller evaporator maximum (avoiding erosion) and minimum (avoiding freezing) flow rates, PPMP maximum flow rate, and tank design maximum charge or discharge flow rate to avoid intense mixing.

1.3.2 TES control strategies

The TES control strategies are classified as conventional and non-conventional. Conventional tank control strategies include full storage and partial storage. The partial storage can be further divided into chiller-priority (C-P) and storage-priority (S-P). Demand limiting control or load-limiting control may be combined with any of the above control strategies (ASHRAE 2003b). These strategies are often used as benchmarks compared with non-conventional control strategies. Forecasts of building cooling requirements and weather conditions are not required for chiller priority control but required for other strategies.

The non-conventional control strategies include optimal strategies and near-optimal strategies or rule-based control strategies. An optimal TES control strategy is a sequence of plant flow rate operations which can minimize the operating cost of the targeted system region. It is a complicated function of several factors, such as utility rates, load profiles, plant characteristics, tank performance, loop characteristics, and weather. The definition of the operation cost will vary with different utility rate structures and the billing coverage period.

Dynamic programming or some direct search methods can be used to find the globally optimal solution in a reasonable amount of time. The optimal results from dynamic programming may maximize the savings. However, in most cases, such an optimal sequence is difficult to follow since there is no clear control logic inside. Some researchers developed heuristics by studying the optimal trajectories and summarizing them into some rule-based control strategies or so-called near-optimal controls. They consist of different conventional control strategies with some judgment clauses.

1.3.3 Differences between water storage and ice storage

A basic review of the current TES studies shows that ice storage has become the most prevalent (ASHRAE 2006). However, large-scale applications (over 10,000 ton-hours) are dominated by the use of ChW storage systems (Andrepont 2006). While many different types of ChW storage systems have been applied in the past, including membranes, baffles, and multiple tanks, naturally stratified tanks are the primary TES method used today. It uses the principle that warm return water and cool stored water tend to stratify due to the density differences. This tends to keep the water from mixing.

Although they share the same idea of shifting electrical load, there are still obvious differences between chilled water and ice storage systems. Compared to an ice storage system, the primary advantage of a chilled water storage system is that the produced ChW temperature can be the same (39 °F to 42 °F normally) when the system shifts between charging and discharging modes. Standard commercial chillers can be used and the control is much easier. A chilled water storage system has no efficiency penalty since it is not necessary to produce extremely low temperature water (22 °F to 26 °F normally). There will be more capacity loss, however, due to mixing effects and heat loss through the tank wall. A second difference is that the charging and discharging rate of a ChW storage system is determined by the acceptable ChW flow rate and stored warm and cool water temperatures all the time. The heat transfer rate for an ice storage system is limited by the heat exchanger area, secondary fluid flow rate and inlet temperature, and the thickness of ice at any time. Complicated correlations are required to calculate the charging and discharging effectiveness (Drees and Braun 1995). In addition, the actual inventory of the water tank is dependent upon the temperature difference between the tank inlet and outlet while the capacity of the ice tank is determined by the ice volume.

The experiences on an ice storage system may be used as a good reference for a water storage system. However, these differences indicate that it is not rigorous to transfer the conclusions from an ice storage system to a ChW storage system without a thorough analysis.

2. LITERATURE REVIEW

The studies on the TES tank are first introduced, followed by the plant simulation and optimization research. Loop side performance has a significant impact on tank operations and will be reviewed as well. Equipment modeling, electrical utility rate structures, and load and weather predictions are covered in the end.

2.1 TES Study

An in-depth literature search and study shows that most research is focused on ice storage systems since it is the most popular TES system. The studies on ChW storage systems are mainly concentrated on field experiment testing and numerical simulations of the tank performance.

2.1.1 Application and economics benefits of TES

A chiller plant with an ice storage system utilizes modular components and shows relatively constant unit capital costs (in $ per ton) regardless of the installed TES capacity. But a larger water storage system has a lower unit capital cost (in $ per ton-hr and in $ per ton of peak discharge capacity).Therefore, very large applications (over 10,000 ton-hours) are dominated by the use of a sensible heat TES. Some representative examples include Reedy Creek-Disney World, FL (57,000 ton-hours), DFW Int'l Airport, TX (90,000 ton-hours), Calpine Cogen-Pasadena, TX (107,000 ton-hours),

Toyota-Georgetown, KY (126,000 ton-hours), and OUCooling-Orlando, FL (160,000 ton-hours) (Andrepont 2006).

The unit power consumption (kW per ton) and unit capital cost ($ per ton) of TES with low supply temperatures are higher than that with traditional supply temperatures, but significant benefits in terms of reduced size and capital cost for chilled water pumps and piping, and other equipment can be achieved. Accordingly, the overall system optimization has led system designers to employ increasingly lower supply temperatures (Andrepont 2006).

Except for capital cost savings due to reduced equipment size, significant reduction of time-dependent energy costs, such as electric demand charges and on-peak Time-of-Use energy charges, can also be achieved. Although TES experiences tank thermal losses that typically range between 1% and 5% per day and lower chiller efficiency when lower chilled water is produced, it can help reduce energy consumption because of lower condensing temperatures at night, less electricity transmission and distribution losses, better chiller load allocation, and flexible plant operation. Documented examples include chilled-water storage installations that reduce annual energy consumption on a kWh basis for air conditioning by up to 12% (Bahnfleth and Joyce 1994).

In general, a chilled water storage system becomes more attractive for facilities with a high load factor, high ratio of peak to average electric demand, very high peak demand charges that are applied as a penalty for several months, and ample space to accommodate a storage tank. The electric rate demand penalty that applies over a several

month period is often called a ratchet clause and will be discussed later under utility rate structures. Effective system control, including reasonably accurate load forecasting at least half a day ahead of time, is a key to reaping the operating cost savings of TES (Roth, Zogg, et al. 2006).

Much of the success experienced by TES technology in the past can be attributed to electric demand charges and to capital cost incentives offered through utility rebate programs. Concerns are that TES is not a green technology and that changes in the power production industry may eliminate both demand charges and rebates. However, using an example facility, Caldwell and Bahnfleth (1997) found that, without electric rebate incentives or rebates, stratified chilled water TES yielded a first cost savings of 9-17% and a life-cycle savings of 33-36% over two non-TES plant alternatives for the example facility. It was concluded that stratified chilled water TES was a viable technology even without the presence of electric rebate incentives or rebates, and it was a sustainable technology for the foreseeable future.

2.1.2 Chilled water storage tank thermal performance index

Several metrics have been used to quantitatively describe the performance of a chilled water tank.

The cycle thermal efficiency of a stratified tank is the ratio of the integrated discharge capacity for a complete discharge process to the integrated charge capacity for the preceding complete charge process for a true cycle in which initial and final states of the tank are identical (Wildin and Truman 1985). It is extremely difficult to obtain measurements of efficiency for single cycles in operating full-scale systems due to the

requirement of identical initial and final conditions. This index is useful as a measure of long-term tank performance because the small differences between the initial and final states of water in the tank become insignificant compared to these much larger capacities. However, it measures only capacity losses through the tank wall and does not account for mixing internal to the tank.

Tran and Kreider et al. (1989) tested several large chilled water storage systems and proposed a Figure-of-Merit (FOM) to reflect the loss of usable capacity. The FOM is the ratio of integrated discharge capacity for a given volume to the ideal capacity that could have been withdrawn in the absence of mixing and losses to the environment. The liquid volumes in the discharge and charge cycles are identical. FOM may be difficult to measure in the field because many operating chilled-water storage sites cannot conduct full-cycle tests running for 24 hours or longer. A "half-cycle Figure of Merit" has been defined as the ratio of integrated charge or discharge capacity to the theoretical capacity contained in one tank volume (Bahnfleth and Musser 1998). It measures capacity lost to mixing in a half-cycle (single charge or discharge process) rather than a full cycle.

A lost capacity in a charge process was defined as the capacity that could not be stored because the system could not continue to cool water as it approached the inlet temperature (Bahnfleth and Musser 1998). It is defined relative to an application-specific limiting temperature. Capacity is "lost" in a discharge half-cycle when water in the tank exists at a temperature above the upper limit that can be utilized by the process served.

A mixing effect leads to a reduction of usable ChW volume while a heat loss to the environment results in an increase of the ChW bulk temperature. It is necessary to treat these two kinds of capacity losses in different ways for a ChW storage system.

2.1.3 Field experiment and simulation research

Field experiments provide a direct and practical understanding of the performance and characteristics of a stratified ChW storage system.

Tran and Kreider et al. (1989) tested six chilled water storage systems and found that well-designed storage tanks had an FOM of 90% or higher for daily complete charge and discharge cycles and between 80% and 90% for partial charge and discharge cycles. Bahnfleth and Musser (1998) found that the lost capacity was roughly 2% of the theoretical capacity available when a minimum outlet temperature limit was applied while as much as 6% could be lost for discharge processes performed at the same flow rate for typical limiting temperatures. Discharge cycle lost capacity was significantly decreased by reducing the inlet flow rate. In a dynamic mode of operation, the effects of mixing overtook the influence of other parameters but the effect of wall materials could not be neglected when the tank was in an idle status (Nelson, Balakrishnan, et al. 1999b). Caldwell and Bahnfleth (1998) found that mixing was localized near the inlet diffuser and directly related to flow rate. Nelson and Balakrishnan et al. (1999a) proposed the definition of the mixing coefficient, which was expressed as a function of Reynolds number (Re) and Richardson number (Ri).

Some researchers built dynamic or static simulation models to study the thermal performance of a stratified ChW storage tank. Gretarsson and Pedersen et al. (1994)

derived a fundamental energy balance model based on a one-dimensional plug-type flow approach. Studies showed that the thermocline thickness could be 3% to 7% of the water height. Homan and Sohn et al. (1996) grouped the capacity loss into heat transfer through the tank walls, conduction across the thermocline, and the flow dynamics of the charge and discharge process and found that the flow dynamics were generally orders of magnitude more important than the other factors. Published data showed current storage tanks generally operated at efficiencies of 50% to 80%.

This research indicates that considerable capacity loss may occur when a minimum outlet temperature limit is applied, especially during a discharge cycle at higher flow rate. The tank discharge rate should be controlled to minimize the mixing effect near the inlet diffuser. These findings could place some constraints on the optimization of the TES system and also provide insights to simply quantify the tank performance.

2.1.4 TES control strategies

TES control can be divided into charging and discharging strategies. Most systems share the same charging strategies. Charging should be initiated when the building load is lower, and off-peak electrical rates are in effect. The discharging strategy could be different for various systems when different control strategies are adopted.

Chiller-priority control operates the chiller, up to its available capacity, to meet loads. It is the most simple and most commonly applied with the chiller in series upstream of storage, but it minimizes the load shifted by the TES system and works well

economically when the utility rate does not include demand charges or Time-of-Use (TOU) electricity rates (Henze 2003b). Storage-priority control meets the load from storage up to its available discharge rate. This allows for maximal load shifting, but comes with the risk of depleting the storage capacity prematurely by under-predicting loads (Henze 2003b). Load forecasting is required to maximize its benefits (Wei, Liu, et al. 2002). Simpler storage-priority sequences using constant discharge rates, predetermined discharge rate schedules, or pseudo-predictive methods have also been used (ASHRAE 2003a). Full storage control strategy only applies when the tank capacity is large enough to ensure running chiller during the on-peak period is not necessary. It could be regarded as a special case for the storage-priority strategy.

In general, these control strategies are appropriate for systems with utility rate structures that include TOU energy and demand charges, but would not be appropriate in conjunction with real time pricing (RTP) rates (ASHRAE 2003b). Braun (2007a) developed a simple algorithm that provides near-optimal control of cool storage systems with RTP rates. It is an extension of methods developed and evaluated by Drees and Braun (1996). For a range of partial-storage systems, load profiles, and utility rate structures, the monthly electrical costs were, on average, within about 3% of the optimal costs.

These conventional control strategies are easy to follow and can reap part of the cost saving benefits. They will be used as a benchmark when it comes to calculating the savings potential of new strategies.

2.1.5 TES optimization methods

TES optimization is finding a combination of different control strategies during specific periods to achieve minimal energy consumption or demand cost over a utility billing period. Similar to chiller plant optimization, TES optimization can be divided into component-based optimization and system-based optimization. For component-based optimization, each component is represented as a separate subroutine with its own parameters, controls, inputs, and outputs. The models used by Henze and Krarti et al. (1997b) predict cooling plant and distribution system power with a component-based simulation that is appropriate for simulation studies. Alternatively, for system-based optimization, plant and distribution system power can be simplified with empirical correlations, such as Braun (2007a). Drees (1994) used curve-fits of plant power consumption in terms of cooling load and ambient wet-bulb temperature.

The optimal supervisory control for storage is a dynamic optimization problem and is a complex function of such factors as utility rates, load profiles, chiller characteristics, storage characteristics, and weather conditions. Two types of solutions to the optimization problem are of interest: (1) minimum billing-period operating cost and (2) minimum energy cost for a specified target demand cost (TDC) and short-term horizon (e.g., a day) (ASHRAE 2003b). The first problem is useful for benchmarking the best control and minimum cost through simulations, but is not useful for online control because forecasts beyond one day are unreliable. The second solution can be used for online control in conjunction with a system model and forecaster. For a given value of

TDC, minimization of cost may be accomplished using dynamic programming (Bellman 1957) or some other direct search methods.

2.1.6 Research on TES optimization

Most references are related to an ice storage system but several chilled water storage cases can still be found.

Braun (1992) described a comparison of control strategies for a partial ice-storage system installed in an office building located in Milwaukee, Wisconsin. The results indicate that the load-limiting strategy provides a near-optimal control in terms of demand costs for all environmental conditions considered. Dorgan and Elleson (1993) used the term operating strategy to refer to full-storage and partial-storage operation. That discussion focuses on design-day operation and does not discuss operation under all conditions. Krarti and Brandemuehl et al.(1995) evaluated chiller-priority and storage-priority control strategies for ice systems as compared with optimal control for a wide range of systems, utility rate structures, and operating conditions. Similar to Braun (1992), they concluded that load-limiting, storage-priority control provided near-optimal performance when there were significant differentials between on-peak and off-peak energy and demand charges. However, without Time-of-Use energy charges, chiller-priority control did provide good performance for individual days when the daily peak power was less than the monthly peak.

Drees and Braun (1996) found that, for ice storage, a simple and near-optimal approach was to set TDC to zero at the beginning of each billing period. The optimization results were used to develop a rule-based discharge strategy that is

introduced in ASHRAE. Henze and Krarti et al. (1997b) developed a simulation environment that determined the optimal control strategy to minimize operating cost, including energy and demand charges, over the billing period. The simulation tool was used to compare the performance of chiller-priority, constant-proportion, storage-priority, and optimal control.

Henze and Dodier et al. (1997a) presented a predictive optimal controller for use with RTP structures. For the RTP structure considered, the demand charge disappears and the optimization problem only involves a 24 h period. The controller calculates the optimal control trajectory at each time step (e.g., 30 min), executes the first step of that trajectory, and then repeats that process at the next time step. The controller requires a model of the plant and storage, along with a forecast of the future cooling loads. The efficiencies of the cooling plant in the chilled water mode and ice-making model are assumed constant. The component-based plant optimization is described in detail by Krarti and Brandemuehl et al. (1995). The state of the ice storage tank is defined by state-of-charge and rate of change variables with constraints. Dynamic programming is used to find the optimal control trajectory.

Hajiah (2000) investigated the effects of using simultaneously building thermal capacitance and an ice storage system to reduce total operating costs (including energy and demand costs) of a central cooling plant while maintaining adequate occupant comfort conditions in buildings. An optimal controller of a central cooling plant using both an ice storage system and building thermal capacitance was developed using the results from a simulation environment. It was implemented and tested.

Yoshida and Goto (1999) previously proposed a basic methodology for the optimal operation of a thermal storage water tank but instability and local minima were found. Load prediction safety factor was included in a new method (Yoshida and Yamaguti 2001). The total HVAC system, including major components, such as a storage tank, air-handling units, cooling towers, and water pumps, was modeled to simulate the performance by MATLAB/ SIMULINK environment. The variables to be optimized are the chilled water temperature and the duration of chiller operation. It is found the tank could be depleted due to load prediction error, and room temperatures may be out of acceptable comfort levels.

A neural network-based optimal controller has been developed by Massie (2002) to control a commercial ice storage system for least cost. It is robust in finding solutions given any price structure, building cooling load and equipment operating conditions. Because of its ability to learn patterns, it self-calibrates to equipment operating characteristics and does not require an expert to fine tune. This feature insures that the controller will operate optimally as a building or equipment undergoes a retrofit. A RTP structure is applied in this research.

Henze and Schoenmann (2003c) presented a model-free reinforcement learning controller for optimal operation of thermal energy storage systems. The reinforcement learning controller learned to charge and discharge a thermal storage tank based on the feedback it received from past control actions. The performance of this controller was evaluated by simulations, and the result showed that it had strong capability to learn a

difficult task of controlling thermal energy storage with good performance. However, cost savings were less when using a predictive optimal controller.

Henze (2003a) investigated whether thermal storage systems could be controlled effectively in situations where cooling loads, non-cooling electrical loads, weather information, as well as the cost of electricity were uncertain and had to be predicted. The analysis shows that the reduction in achievable utility cost-savings is small when relying on RTP electricity rates that are made available by the utility only 1 h ahead instead of an entire day-ahead. Consequently, uncertain electrical utility rates do not imperil the superior cost-saving benefits of cool storage when governed by predictive optimal control.

A module for ice-based TES systems was developed and integrated within EnergyPlus by Ihm and Krarti et al. (2004). The TES module uses building load and system thermodynamics (BLAST) models for two direct ice systems (ice-on-coil external melt and ice harvester) and one indirect ice system (ice-on-coil internal melt). The integration of a TES module in combination with the integration of optimization routines within EnergyPlus provides HVAC designers and facility operators with an effective simulation environment to determine the best control strategy for a building equipped with a TES system.

A near-optimal control method was developed for charging and discharging of cool storage systems when real-time pricing (RTP) electric rates were available (Braun 2007a). The model includes a correlation for plant cooling capacity as a function of chiller supply temperature and ambient wet-bulb temperature and a correlation for plant

power consumption as a function of chiller cooling load, chiller supply temperature, and ambient wet-bulb temperature from simulations that incorporated individual equipment models. A model was developed for the time dependence of typical RTP rates that depends on time of day and maximum temperature for the day. For charging of storage, it was found that a very simple, near-optimal strategy is to fully recharge storage with the chiller operating at maximum capacity during a period defined by when the RTP rates are lowest and the building is unoccupied. For discharging of storage, it was found that the best strategy is to use a storage priority control that maximizes the discharge rate of storage during a period defined by when RTP rates are highest, the building is occupied, and it is economical to utilize storage. For all other times, it is best to use chiller-priority control that minimizes the discharge rate of storage. The simplified method worked well in all cases and gave annual costs within approximately 2% of the minimum possible costs associated with optimal control.

Braun (2007b) evaluated the operating cost savings associated with employing the strategy developed by Braun (2007a) as compared with using chiller-priority control. In addition, operating cost savings associated with employing ice storage in combination with RTP rates were evaluated for both the near-optimal and chiller-priority strategies. For a range of systems employing ice storage with RTP rates, the cost savings associated with the near-optimal strategy compared to chiller-priority control were found to be as high as 60% with typical savings between 25% and 30%. These savings are much more significant than savings associated with employing near-optimal control for cool storage systems when typical Time-of-Use utility rates are employed with demand charges. A

similar level of savings was determined when comparing costs for the near-optimal control strategy applied to ice storage systems with costs for systems not employing cool storage. However, relatively small savings were determined for use of ice storage when chiller-priority control is utilized. In many situations, the use of storage with chiller-priority control can actually result in higher costs than without storage. It can be concluded that chiller-priority control should not be employed in combination with RTP rate structures for cool storage systems. With conventional rates, the largest part of the cost savings opportunity is associated with reduced demand due to downsizing of the peak chiller cooling capacity. For application of cool storage with RTP utility rates, the opportunity for cost savings is much more sensitive to the control strategy employed.

Henze and Biffar et al. (2008) described the investigation of the economic and qualitative benefits of adding a chilled water thermal energy storage system to a group of large buildings in the pharmaceutical industry in Southern Germany. It is found that the adoption of a chilled water thermal energy storage system is expected to provide economic benefits as measured in energy cost savings, as well as qualitative merits such as the avoidance of numerous safety measures necessary for a chilled water plant without storage (e.g., always operating at least two chillers), and a cost effective addition of supplemental chilled water plant cooling capacity. Moreover, the overall system reliability and availability will be significantly improved through the addition of a thermal energy storage system. The near-optimal heuristics suitable for implementation in the actual pharmaceutical buildings is an on-going task.

Based on the reviews above, the current research can be summarized as follows:

(1) Most TES operating and control researchers emphasize an ice-storage system or combining ice-storage active storage with building passive thermal storage. Considering the differences of these two systems introduced above, it is not appropriate to generalize the conclusions and experiences of an ice storage system to a ChW storage system without a thorough study.

(2) Current studies on TES system are on a case by case basis, and there is not a general method to find the optimal operating strategy. It is hard to apply the conclusions and experiences on one project to other ones.

(3) Dynamic programming is used to obtain the optimal control strategies. Then, the near-optimal strategies are induced from the optimal trajectories. Such sophisticated routines are not easy to follow. It is also difficult to induce some logic from the optimal control strategies. In addition, the cost-saving benefits of such optimal strategies are often small in comparison to a well-designed logic that makes full and appropriate use of the principles described previously (Drees 1994). Some optimal controllers were developed to control TES operations. However, most controllers were evaluated by simulations, and their practical applications seemed to be missing.

(4) It is shown that the TES system provides a good opportunity to save billing costs by shifting electricity load during on-peak hours to off-peak hours and leveling the peak demand or reducing the on-peak demand. But studies on

utilizing TES to enhance ChW plant performance are rare. Some researchers used constant plant efficiency or regression models while others selected a modular-based steady-state model, which was time-consuming. The TES is regarded as more of a cost management tool than an efficiency enhancement tool.

(5) All studies used the dimensionless state-of-charge x of the storage tank to depict the tank inventory. The primary control variable u (ton) is defined as the rate of change of the state-of-charge x. The state transition equation can be stated as (Henze, Biffar, et al. 2008):

$$x_{k+1} = x_k + \varphi u_k \frac{\Delta t}{SCAP},$$

where SCAP is the capacity of the chilled water storage tank (ton-hr), Δt is the time interval of the calculation. A Figure-of-Merit (ϕ) was suggested by Dorgan and Elleson (1993) to describe chilled water tank performance. Such a description method comes from the study on an ice storage system, but it is not necessarily a good choice for a water storage system. The main problem is that it combines the chilled water flow rate, and supply and return water temperatures into the rate change of the tank. It is acceptable for an ice storage tank because the tank inventory is not affected by water temperatures but by the ice volume in the tank. The tank available cooling capacity is equal to the latent heat of the ice. However, for a water storage tank, there is no explicit definition for the tank available capacity before

discharging since the total cooling provided by the tank is determined by the discharging water flow rate as well as the supply and return water temperatures. The return temperature may fluctuate a lot diurnally or seasonally. Consequently, such a description method will lead to inconsistent results.

2.2 Plant Side Simulation and Optimization

The plant side includes condenser water loop, chillers, and primary and secondary chilled water pumps. Two kinds of research methods are used: component-based and system-based.

2.2.1 Chiller plant configuration

A typical chilled water system consists of an indoor air loop, chilled water loop, refrigerant cycle loop, condenser water loop, and outdoor air loop (Lu, Cai, et al. 2005a). Primary electricity consumption components include cooling tower fans, condenser water pumps, chillers, primary and secondary chilled water pumps, and air handling unit fans.

A primary-secondary pumping configuration is most prevalent, where a VSD is installed on the secondary-loop chilled water pumps while the primary chilled water and condenser water flow are kept constant. Recently, there is a trend to apply VSDs on all components to achieve higher operation performance, when specially tailored operating strategies are incorporated (Hartman 2001a).

Durkin (2005) introduced the evolution of the chiller plant design. Ever since 1990, traditional chilled-water plant design has begun utilizing a primary-secondary loop configuration. The low-head primary loop pump provides a constant flow through the chiller, while the high-head variable-flow secondary loop pumps modulate to adjust secondary chilled water flow to meet the actual cooling demand. The imbalance in flow between the primary and secondary circuits results in flow through the bypass piping circuit. While this configuration satisfies the objective of maintaining constant chilled-water flow through the chiller, it may not achieve the highest chiller efficiency at part loads and can limit chiller capacity. At low demand for cooling, the flow in the primary loop is substantially higher than that in the secondary, which adversely impacts the overall chiller operating efficiency at part load conditions. At high loads, the flow of the primary circuit is likely to be less than the maximum flow capacity of the chiller, so that return water from the load is mixed with chilled-water supply, leading to a higher supply temperature and the low delta-T syndrome. The appearance of variable primary flow in 1996 made the bypass line unnecessary. But another bypass line may be designed at loop end to make sure the chiller minimum flow rate is guaranteed. The low delta-T can be overcome by over-pumping the chiller.

Hartman (1996) discussed the benefits and problems associated with a single circuit variable chilled water flow system, and he offered a chiller plant control strategy that could provide safe, stable, and reliable chiller operation over the entire operating range employed in typical HVAC applications. The integrated control strategies can be employed to operate variable-flow chilled water distribution systems at much higher

efficiencies by coordinating the pump speed directly to the load demands without employing pressure control (Hartman 1993). But several basic requirements must be met. The cooling requirement must be above the lowest stable chiller operating load, and the water flow through the chiller evaporator must always be sufficient to maintain evaporator temperature within suitable limits. Finally, chilled water temperature can rise and the condenser water temperature can drop as the load decreases, such as comfort air conditioning. In addition, the direct digital control (DDC) system has the capacity to integrate the operation of the chillers, pumps, and the loads the system serves with high-performance control algorithms. In typical North American single-building applications, it is usually a good candidate for effective and economical space cooling. Coordinated chiller and pump control is used to establish smooth chiller and pump control under varying flow conditions. Pump speed and chiller capacity are adjusted in unison by setting percent chiller electric load proportionately to the pump motor load. Chilled water temperature adjustment could also be included.

2.2.2 Chiller plant control methods

Automatic control systems have been widely applied in central chiller plants to achieve robust, effective, and efficient operation of the system on the basis of ensuring thermal comfort of occupants and satisfying indoor air quality. All the variables associated with the optimization problems are classified into uncontrolled variables, discrete and continuous control variables, and controlled variables. The typical uncontrolled variables in HVAC systems are ambient air WB and DB temperature, and building cooling load. The load distributions in each zone and sensible-latent load ratio

all belong to secondary uncontrolled variables and are ignored normally. The typical discrete control variables are the numbers of on-stage equipment, and the continuous control variables are speed (or capacity) of components in operation. The controlled variables in HVAC systems could be the temperature setpoints, pressure setpoints, flow rates, and the rate at which energy is added or removed from storage, etc. As the subsystems in HVAC systems interact with each other, the optimal solution for the related control variable is the trade-off among the energy input or operating cost of each subsystem.

Generally, all the control methods used in HVAC systems can be divided into supervisory control and relational control. Supervisory control, often named optimal control, seeks stable and efficient operation by systematically choosing properly controlled variables setpoints, such as flow, pressure or temperature. These setpoints can be reset when uncontrolled variables are changed, and they are maintained by modulating control variables through PID controllers or sequencing. This method is easy to understand and implement in practice. Relational control is to determine continuous and discrete control variables directly according to uncontrollable variables (cooling load and ambient weather conditions) or equipment power input, such as demand-based control (Hartman 2001b) and load-based control (Yu and Chan 2008). It was claimed by the authors that these controls could realize tremendous energy savings.

Supervisory control can be further classified into four categories: model-based, hybrid, performance map, and model-free supervisory control method (Wang 2008). Many efforts in the control of building HVAC systems are typically made on local level

controls. Local control is the lowest level control, which is designed to guarantee robust operation and track the setpoint, while considering the dynamic characteristics of the local process environment. Local control functions can be further subdivided into two groups, including sequencing control and process control. Sequencing control defines the order and conditions associated with bringing equipment online or moving them offline. Process control adjusts the control variables to achieve well-defined process objectives in spite of disturbances, using measurements of state and/or disturbance variables (Ramirez 1994). The typical process control used in the HVAC field is proportional-integral-derivative (PID) control, ON/OFF control (or bang-bang control), step control, and modulating control. Normally, only certain subsystem performance optimization can be achieved by such control settings.

Supervisory control is the high level control, which is designed to utilize global optimization techniques to find energy or cost-efficient control settings (i.e., operation modes and setpoints) for all local controllers, taking into account the system level or subsystem level characteristics and interactions. In most cases, an energy consumption objective function or cost objective function is defined with equality or inequality constraints and minimized through specific optimization algorithms. Due to the electricity rate structure diversity, minimizing system operation energy consumption is not always equivalent to minimizing system energy input.

The fundamentals of supervisory control strategies have been comprehensively introduced in the ASHRAE Handbook (2003b) and are widely applied in practice. Most of these controls originated from the supervisory control methodology developed by J.E.

Braun. Based on model-based simulation, the optimal setpoint reset and equipment sequencing can be related to uncontrollable variables. The parameter estimate methods and implementation algorithms are also presented. These general optimal or near-optimal control guides for a typical chiller plant are widely accepted due to their simplicity and effectiveness.

Typically, the condenser water pump control is dedicated to the chiller control to provide relatively constant flow for individual chillers. The chiller condenser water supply temperature set point is usually held constant, but it is better to maintain a constant approach by modulating fan speed. A dead band for the condenser water setpoint should be adopted to avoid fan cycling. Braun and Diderrich (1990) demonstrated that feedback control for cooling tower fans could be eliminated by using an open-loop supervisory control strategy. This strategy requires only measuring chiller loading to specify the control and is inherently stable.

The tower fan control is separated into two parts: tower sequencing and optimal airflow. For a given total tower airflow, general rules for optimal tower sequencing are used to specify the number of operating cells and fan speeds that give the minimum power consumption for both the chillers and tower fans. The optimal tower airflow is estimated with an open-loop control equation that uses design information for the cooling tower and chiller. For variable-speed fans, minimum power consumption results when all cooling tower cells are operated under all conditions. For a multi-speed fan, when additional tower capacity is required, Braun and Klein et al. (1989b) showed that, in almost all practical cases, the speed of the tower fan operating at the lowest speed

(including fans that are off) should be increased first. Near the optimum, the total power consumption is not very sensitive to the control but higher flow is preferred. They showed that the tower control that minimized the instantaneous power consumption of a cooling plant varied as a near-linear function of the load over a wide range of conditions. Although optimal control depended on the ambient wet-bulb temperature, this dependence was small compared to the effects of load. High and low limits are applied to condenser water temperature.

For constant speed chilled water pumps, a two-way bypass valve is controlled to maintain a fixed pressure difference between the supply header and return header. Ideally, the chilled-water temperature should be adjusted to maintain all discharge air temperatures with a minimal number of cooling-coil control valves in a saturated (fully open) condition. One difficulty of this control approach is that valve position data are often unreliable. This problem can be overcome by also monitoring discharge air temperatures.

For VSD-controlled pumps with primary-secondary chilled water loops, the primary pumps are fixed speed and are generally sequenced with chillers to provide a relatively constant flow of water through the chiller evaporators. The secondary chilled-water pumps are variable speed and are typically controlled to maintain a specified set point for pressure difference between supply lines and return lines for the cooling coils. But the best strategy for a given chilled-water set point is to reset the differential pressure set point to maintain all discharge air temperatures with at least one control valve in a saturated (fully open) condition.

The optimal chilled water supply temperature at a given load results from a tradeoff between chiller and pumping power. The minimum total power occurs at a point where the rate of increase in pumping power with chilled-water temperature is equal to the rate of decrease in chiller power. This optimal set point moves to lower values as the load increases. Braun and Klein et al. (1989b) demonstrated that the optimal chilled-water set point varied as a near-linear function of both load and the average WB temperature entering the cooling coils over a wide range of conditions.

In most cases, controlling for identical chiller set temperatures is the best and simplest strategy. With this approach, the relative loading on operating chillers is controlled by the relative chilled-water flow rates. However, this is typically not done and it is probably sufficient to establish the load distributions based on design information and then balance the flow rates to achieve these load distributions. In general, the condenser water flow to each chiller should be set to give identical leaving condenser water temperatures. Braun and Klein et al. (1989b) showed that for chillers with identical design COPs and part-load characteristics, a minimum or maximum power consumption occurred when each chiller was loaded according to the ratio of its capacity to the total capacity of all operating chillers. This solution gives a minimum when the chillers are operating at loads greater than the point at which the maximum COP occurs (i.e., chiller COP decreases with increased loading). For the general case of chillers with significantly different part-load characteristics, a point of minimum or maximum overall power occurs where the partial derivatives of the individual chiller's power consumption with respect to their loads are equal. The individual chiller loads must be constrained to

be less than the maximum chiller capacity at these conditions. The distribution of chiller loads could be changed for a fixed-flow distribution by using different chilled water setpoint temperatures because it is not typical to control the flow by a two-way valve.

For chillers with similar efficiencies, the order in which chillers are brought online and offline may be dictated by their cooling capacities and the desire to provide even runtimes. However, whenever beneficial and possible, chillers should be brought online in an order that minimizes the incremental increase in energy consumption. A chiller should be shut down when its load drops below the spare capacity load of the current number of online chillers. For chillers with similar design cooling capacities, the chiller with the highest peak COP can be brought online first. The maximum COP for each chiller can be evaluated using manufacturers' design and part-load data or from curve-fits to in-situ performance. In general, chillers should be brought online at conditions where the total power (including pumps and tower or condenser fans) of operating with the additional chiller would be less than without it. In practice, the switch point for bringing a chiller online should be greater than that for bringing that same chiller offline (e.g., 10%), to ensure a stable control. The optimal sequencing of chillers depends primarily on their part-load characteristics and the manner with which the chiller pumps are controlled. For dedicated pumps, where individual condenser and chilled water pumps are dedicated to the chiller, Hackner and Mitchell et al.(1985) and Braun and Klein et al. (1989b) showed that a chiller should be brought online when the operating chillers reached their capacity. For systems without dedicated chiller pumps (e.g., variable-speed primary systems), the optimal load conditions for bringing chillers

online or offline do not generally occur at the full capacity of the chillers. A chiller should be brought online whenever it would reduce the overall chiller power (e.g., 5%) or if the current chillers can no longer meet the load.

Hartman is a pioneer in research on chiller water plant control and optimization. Based on system analysis, he pointed out the importance of implementing DDC systems to the concept of global optimization (Hartman 1995) and promoted all-variable speed chiller plants where all the chillers, condenser pumps and tower fans were driven by VSDs (Hartman 2001a). However, the huge amount of data accumulated and employed in calculations for large systems could place huge burdens on the communication network and computing capacities of DDC systems.

Hartman advanced LOOP^{TM} technology and claimed that it could reduce total chiller plant energy use by about 20-25% percent (depending on climate and application)(Hartman 1999a). The core ideal of LOOP^{TM} technology is to slow equipment speed instead of shedding it before the low limit is reached, such as about 20% load (depending on the exact configuration of equipment).

Hartman explained the operation of LOOP^{TM} plants in another paper (Hartman 1999b). Constant speed compressor power requirements vary approximately proportionately with capacity down to about 70%. But below 70%, power no longer falls proportionately as load is further reduced. Aggressively reducing compressor head pressure requirements at part load conditions rather than reducing capacity by closing compressor vanes or shedding chillers can make chillers work in the high efficiency zone. For comfort conditioning, it is almost always possible to reduce the condensing

temperature and raise the chilled water temperature at low loads since cooling load usually decreases as outdoor temperature drops. A single circuit variable chilled water flow system is sometimes adopted to make the secondary pump serve as a booster pump. A modulating bypass valve at the end of the distribution line is designed to ensure a minimum flow rate.

Hartman also introduced relational control concepts and pointed out the difference between relational control and PID control (Hartman 2006). To assist in improving the electrical efficiency of HVAC systems, Hartman (2005) developed a general system analysis principle, namely Equal Marginal Performance Principle (EMPP), to help in optimizing the system design, and to ensure optimal operation of nearly any modern HVAC system. This technology has been transferred into products (Armstrong 2006) and applied in some central chilled water plants successfully (Erpelding 2006).

Some remarks on using EMPP to implement system optimization were made by Yu and Chan (2008). It needs much effort and time to create the system output expressions and determine the marginal COP for a large system with many staging patterns of the power components. To obtain the power relationships in mathematical form, a curve fitting technique is needed, which indicates that the EMPP is viable for the post-operation stage when enough trend data are available. It is more desirable to apply it in the design stage to facilitate optimum equipment selection. In addition, outside wet-bulb temperature may also change the interaction between power input and cooling output. This may complicate the control. Also, each system component has to be sized

and optimized in its operation using identical methodologies. All these limits make this technology more suitable for modular products.

There are some other control methods, such as a four-level control structure for a chiller system(Kaya and Sommer 1985), a predictive control approach by Ling and Dexter (1994), load-based speed control by Yu (2008), etc. But the applications of these methods are not found.

Kaya and Sommer (1985) presented a four-level control structure for a chiller system. The first-level controls are local controllers for chilled-water temperature, vane position, and condenser water temperature. All the first-level controls are supervised by the second-level control to provide reasonable setpoints. The third-level control is used to optimally allocate the total load for each operating chiller and pump. The fourth-level control is used for supervisory coordination of the chilled-water temperature and scheduling of the chiller system operation. There is no actual energy savings due to the application of the supervisory control strategy.

An expert controller for a building HVAC system was designed by Ling and Dexter (1994) using a predictive control approach. The design of the predictive control algorithm was based on prior knowledge of the system. A rule-based supervisory method was used to optimize the control performance. Experimental results showed that the use of rule-based supervisory control could lead to significant cost savings without unacceptable increases in the level of discomfort. The result also demonstrated that this expert controller was able to compensate day-to-day variations in control performance.

Wang and Burnett (2001) have developed a novel control strategy using a system approach for optimizing variable-speed pumps of indirect water-cooled chilling systems. This strategy included an adaptive and a derivative method to optimize the speed of pumps by resetting the pressure setpoint according to the estimated derivative of the total instantaneous powers of chillers and water pumps with respect to pressure. The adaptive strategy identified the changes of the system parameters essential for the control strategy and updated the control accordingly. Simulation results showed that proper reset of seawater pressure control setpoint could provide up to 10% of the savings in total chilling system electricity consumption, while 5% of the savings could be expected in most of cases investigated.

Yu (2008) presented the use of load-based speed control to enhance the energy performance of water-cooled chiller systems. Thermodynamic-behavior chiller and cooling tower models have been developed to investigate how the energy and water uses vary for a chiller system operating under various controls of condenser water pumps and cooling tower fans. The optimum operation of the system can be achieved simply and directly by the load-based speed control under which the speed of the tower fans and condenser water pumps is regulated as a linear function of the chiller part load ratio. The superiority of such control rests on its coherence with typical sequencing of chillers based entirely on their load conditions and on eliminating the need for high quality humidity sensors for the reset of cooling water temperature. The system COP under the optimal control could increase by 1.4-16.1% relative to the equivalent system with fixed temperature and flow rate controls for the cooling water leaving from cooling towers. A

case study showed that the payback could be two years or less. This is a simple and direct means to achieve optimal operation of all the variable speed equipment. But only condenser water loop and chiller operation are optimized while the chilled water flow rate and supply temperature are constant.

2.2.3 Chiller plant control optimization

Optimization is an area of mathematics that is concerned with finding the "best" points, curves, surfaces, etc (Hull 2003). In general, chiller plant optimization can be divided into static optimization and dynamic optimization depending on if there is considerable storage system. The optimization related to the systems without storage is a quasi-steady, single-point optimization, while the optimization associated with the systems with storage is the dynamic optimization determining a trajectory of setpoints. Dynamic programming or some direct search methods can be used for the dynamic optimization, while static optimization techniques can be used for the quasi-steady, single-point optimization. In this section only static optimization is reviewed and dynamic optimization will be covered in the TES section.

All the optimization techniques could be summarized into two categories: linear and nonlinear. The linear optimization technique, such as direct method, recursive method, and iterative method, etc., is the most simple and straightforward technique since there is always a unique optimum in a linear optimization problem. Compared to linear optimization techniques, nonlinear optimization techniques are complex and sophisticated since many local optimums exist in a nonlinear optimization problem and the difficulties in finding the global optimum increase greatly. Nonlinear optimization

techniques can be further subdivided into two categories, including nonlinear local and global optimization (Nelles 2001).

Optimization problems of building HVAC systems are often characterized with discretization, nonlinearity, and high constraints. Nonlinear optimization techniques are more powerful and useful and can be divided into local and global optimization.

Nonlinear local optimization techniques include direct search (Sreedharan and Haves 2001), sequential quadratic programming (SQP) (Sun and Reddy 2005), Lagrange method (Chang 2004), and univariate search. Nonlinear global optimization techniques includes branch and bound (B&B) (Chang, Lin, et al. 2005), simulated annealing (SA) (Chang 2006), evolutionary algorithms, and genetic algorithm (GA) (Chow, Zhang, et al. 2002; Lu, Cai, et al. 2004; Nassif, Kajl, et al. 2005). The existing approaches to evolutionary algorithms include evolution strategy (ES), evolutionary programming (EP), genetic algorithm (GA), and genetic programming (GP). Other optimization techniques include recursive numerical algorithm and Newton-Raphson solution methods but they may not be efficient and reliable for highly nonlinear and complicated optimization problems in typical building HVAC systems. Among all of these techniques, genetic algorithm (GA) is attracting growing attention. Further research on the robustness and feasibility of this technique for practical applications is essentially required (Wang 2008).

2.2.4 Component-based plant research

The ASHRAE Handbook (ASHRAE 2003b) presents a framework for determining optimal controls and a simplified approach for estimating control laws for

cooling plants. General static optimization problems are mathematically stated as the minimization of the sum of the operating costs of each component with respect to all discrete and continuous control variables, subject to equality constraints and inequality constraints. Typical input and output stream variables for thermal systems are those controlled variables, such as flow, pressure, and temperature. Static optimization is applied to all-electric systems without significant storage, leading to minimization of power at each instant in time.

This expression summarizes the basic characteristics of the component-based plant optimization and can be achieved with proper optimization techniques. Literature reviews show that some optimization research only covers part of system or subsystem of the condenser water loop, chillers, and chilled water loop. Sometimes, the air distribution system can also be included to get a more comprehensive coverage. The conclusions drawn from the subsystem optimization results may be valid for local optimization but need further verification on a global viewpoint. Following are some studies on local optimization of HVAC sub-systems:

Graves (2003) presented a thermodynamic model for a screw chiller and cooling tower system for the purpose of developing an optimized control algorithm for the chiller plant. A wet bulb temperature and cooling tower setpoint correlation coupled with a fan speed and condenser water pump speed correlation obtained a 17% reduction in the energy consumption. However, chilled water loop and building air side are excluded in the optimization.

Lu and Cai et al. (2004) presented a model-based optimization strategy for the CW loop of centralized HVAC systems. A modified generic algorithm for this particular problem was proposed to obtain the optimal set points of the process. Simulations and experimental results on a centralized HVAC pilot plant showed that the operating cost of the condenser water loop could be substantially reduced compared with conventional operation strategies.

Chang and Lin et al. (2005) proposed a method for using the branch and bound (B&B) method to solve the optimal chiller sequencing (OCS) problem and to eliminate the deficiencies of conventional methods. The proposed method consumes much less power than the conventional method and is very appropriate for applications in air conditioning systems.

Furlong and Morrison (2005) studied the optimization of CW system cooling tower and chiller combination. The conclusions only applied to design conditions. The influence of other variables, such as compressor type, variable speed capabilities for both the compressor and tower, and off-peak loading are not considered.

Xu and Luh et al. (2005) presented a daily energy management formulation and the corresponding solution methodology for HVAC units. A method that combines Lagrangian relaxation, neural networks, stochastic dynamic programming, and heuristics was developed to predict system dynamics and uncontrollable load and to optimize the setpoints. Numerical testing and prototype implementation results showed that this method could effectively reduce total costs, manage uncertainties, and provide for load shedding.

Chang (2006) has attempted to solve the optimal chiller loading (OCL) problem by utilizing simulated annealing (SA). The case study analysis demonstrates that this method solves the Lagrangian problem and generates highly accurate results.

Bahnfleth and Peyer (2006; 2007) investigated the economics of variable primary flow chilled water pump systems via a parametric modeling study. Evaporator flow varies between 30% and 120%. It is found that variable primary flow systems reduced total annual plant energy use by 2-5%, first cost by 4-8%, and life-cycle cost by 3-5% relative to equivalent primary-secondary systems for the assumptions and range of parameters considered.

Yu and Chan (2007) recommended using uneven load sharing strategies for multiple chillers to enhance their aggregate COP. It is found that for two equally sized chillers operating, one should carry a full load and the other should be partially loaded to meet the system load. It is expected that the uneven load sharing strategy is applicable to chiller plants with air-cooled reciprocating chillers, given that their COP increases with chiller part load ratios and approaches the highest level at full load for any given outdoor temperature.

It is easier to study the performance of a subsystem and the conclusions drawn may provide some insights into the local optimal control. However, when these conclusions are extended to whole systems, the global optimization is not guaranteed. The following researchers tried to find some general optimal control rules on the whole system level:

Hackner and Mitchell et al. (1985) and Lau (1985) utilized component models to simulate and search the minimum power consumption for the operation of building HVAC systems. The comparison studies showed that these techniques could save more energy as compared to local optimization methods.

Braun (1988) and Braun and Klein et al.(1989c) presented a component-based nonlinear optimization and simulation tool and used it to investigate optimal performance. The results showed that optimal set points could be correlated as a linear function of load and ambient wet-bulb temperature.

Cumali (1988) presented a method for real-time global optimization of HVAC systems including the central plant and associated piping and duct networks. The objective function was minimized using the reduced gradient method, subject to constraints on comfort and equipment operation. Electrical demand reductions of 8% to 12% and energy savings of 18% to 23% were achieved in practical applications.

Zaheer-uddin and his collaborators demonstrated that multi-stage optimal control technique was an effective and useful tool for computing supervisory control profiles for building systems subject to time-of-day operating schedules (Zaheer-uddin and Patel 1993) (Zaheer-uddin and Zheng 2000) (Zaheer-uddin and Zheng 2001).

Olson (1993) presented dynamic chiller sequencing (DCS), an algorithm for controlling the HVAC equipment necessary to cool non-residential buildings. This is accomplished by forecasting the cooling loads expected through a planning horizon, determining the minimum cost way of meeting the individual loads with various combinations of equipment, and using a modified shortest path algorithm to determine

the sequence of equipment selection that will minimize the cost of satisfying the expected loads for the entire planning horizon.

The performance of the differential dynamic programming (DDP) technique applied to optimal control of building HVAC systems was studied by Kota and House et al. (1996). It was showed that DDP was more efficient compared with non linear programming (NLP) for the example problems, while NLP was more robust and could treat constraints on the state variables directly.

Lu and Cai et al. (2005b) have presented the optimal set point control for the global optimization problem for overall HVAC systems using a modified generic algorithm. The mixed integer nonlinear constraint optimization problem was solved to minimize the overall system energy consumption by appropriately setting the operating point of each component. However, it is very difficult to get the sufficiently well-tuned controllers to complete the ideal local control loops.

For real-time control applications, Sun and Reddy (2005) suggested using the simple control laws for near-optimal control of HVAC systems. Based on the developed complete simulation-based sequential quadratic programming (CSB-SQP), optimal control maps could be generated using detailed simulations. The regression model for each control variable can then be developed from the control map of the corresponding control variable and was used for near-optimal control of the operation of HVAC systems.

2.2.5 System-based plant research

Sometimes, it takes too much effort to build a component-based model or the necessary data may not be available. An alternative way is to simulate the plant power with one function. This methodology was first advanced by Braun and Klein et al. (1989c) when they developed a system-based optimization based on results from component-based optimization. The method involves correlating overall cooling plant power consumption using a quadratic function form. The inputs are uncontrolled variables and controlled continuous variables while outputs are total cost. A solution for the optimal control vector that minimizes power may be determined analytically by applying the first-order condition for a minimum. The costs associated with the unconstrained control under different mode combinations are compared to identify the minimum.

As discussed before, the uncontrollable variables include ambient dry bulb temperature, wet bulb temperature, and total chilled water load. Separate cost functions are necessary for each operating mode. The individual zone latent-to-sensible load ratios and the ratios of individual sensible zone loads to the total sensible loads for all zones are of secondary importance. The free controlled variables are the flow, pressure, or temperature of the fluid and the number can be reduced significantly by using the simplified strategies (ASHRAE 2003b). Minimizing this function leads to linear control laws for controlled continuous variables in terms of uncontrolled variables. The empirical coefficients of this function depend on the operating modes so that these constants must be determined for each feasible combination of discrete control modes.

The determined controlled variables will be maintained by modulating continuous control variables, such as valve open percentage and motor speed.

For all variable-speed auxiliary equipment (i.e., pumps and fans), the free set-point variables could be reduced to the following: (1) supply air set temperature, (2) chilled water set temperature, (3) tower airflow relative to design capacity, and (4) condenser water flow relative to design capacity (ASHRAE 2003b). All other continuous supervisory controlled variables are dependent on these variables with the simplified strategies. Some dependent but discrete control variables, such as numbers of running pumps, have a relatively small effect on overall power consumption. With all variable-speed pumps and fans, the only significant discrete control variable is the number of operating chillers. Then, optimization involves determining optimal values of only four continuous control variables for each of the feasible chiller modes.

Braun and Mitchell, et al. (1987) correlated the power consumption of the Dallas-Ft. Worth airport chillers, condenser pumps, and cooling tower fans with the quadratic cost function. The discrete control variables associated with the four tower cells with two-speed fans and the three condenser pumps were treated as continuous control variables. In subsequent work, Braun and Klein et al. (1989c) considered complete system simulations (cooling plant and air handlers) to evaluate the performance of the quadratic, system-based approach.

This methodology has been adopted by Ahn and Mitchell (2001) to find the influence of the controlled variables on the total system and component power consumption. A quadratic linear regression equation for predicting the total cooling

system power in terms of the controlled and uncontrolled variables was developed using simulated data collected under different values of controlled and uncontrolled variables. The trade-off among the components of power consumption resulted in the total system power use in that both simulated and predicted systems were minimized at lower supply air, higher chilled water, and lower condenser water temperature conditions.

Bradford (1998) developed linear, neural network, and quadratic type system-based models and a component-based model to predict the system energy consumption including demand side. It has been shown that, for most systems with low outside air requirements, operating the supply air temperature at a lower setpoint and selecting a ChW temperature adequate to meet the supply air setpoint is near optimal. Operations of the cooling tower fans at 100% speed to produce the lowest possible condenser water was often optimal at high load and high outside wet-bulb. The use of component-based models for either on-line or off-line optimal control is viable and robust.

Following are the summary comments for the above studies:

(1) Although the system-based plant model is much simpler than the component-based model, the objective function under each feasible combination of discrete control modes has to be generated, and considerable regression error as well as solution difficulty may exist. The component-based models are more accurate, but it takes a long time to build the model for each project. Iterations are inevitable and convergence could be a problem. Some sophisticated algorithms are also required to optimize such a system.

(2) When plant optimizations are involved in TES optimization, they are conducted simultaneously, i.e. for given external parameters (loop cooling load, WB, tank level, and tank flow rate, etc.) at each time step, the plant internal parameters (such as chiller ChW leaving temperature and cooling tower approach) are optimized to minimize the total power consumption. Such a process is time-consuming and not realistic, either. In practice, these setpoints are fixed for a long time and adjusted seasonally.

2.3 Loop Side Study

Loop side performance places a significant impact on a ChW storage system. This impact is both hydraulic and thermal. The plant and TES need to provide enough cooling to meet the thermal load on the loop side while the SPMP should provide a high enough head to pump the water through the loop. The non-synchronization between flow and load can lead to all kinds of problems, such as low delta-T, excessive flow, and control instability.

Rishel (2002) evaluated the advantages and disadvantages of different building connections. It was shown that a proper connection was essential to ensure that the previous design parameters were maintained with a minimum of energy required by the pumps to move water through the building. Rishel (2003) also studied the sequencing and speed control of a variable speed pump for HVAC water systems. It was pointed out that the pump head curve evolved into a head area when there was a variation in the percentage of the load on cooling coils. The rate of pump speed signal using a remote

differential pressure transmitter should be at least twice a second. The pump can be sequenced properly through the use of wire-to-water efficiency or kW input to the pumping system.

A low delta-T, the difference between return and supply chilled water temperature, exists in almost every real chiller plant, particularly at low loads, resulting in higher pump and chiller energy usage. It will directly reduce the TES capacity and affect its operations. Many papers have discussed how to keep higher delta-T (Kirsner 1995; Hyman and Little 2004; Moe 2005; Taylor 2006). Taylor (2002) also showed why delta-T degradation would almost always occur and how to design around that eventuality to maintain chiller plant efficiency, despite a degrading delta-T. The causes of a degrading delta-T were broken into avoidable causes, causes that can be mitigated or resolved but may not result in overall energy savings, and inevitable causes. Due to a combination of the factors listed above, delta-T can be expected to fall to about one-half to two-thirds of design at low loads. The plant and the TES tank must be operated to accommodate such situations in an efficient manner while still meeting all the coil loads. The focus is to improve chiller low load performance and try to fully load the chiller.

A building side model needs to predict the required total ChW flow rate and corresponding pump head under different operating conditions. Ma and Wang (2009) assumed a fictitious global air handling unit (AHU) to represent all terminal units. An empirical formula was used to predict the total ChW flow as a function of the cooling load, zone air flow rate, and AHU inlet air and water temperatures. This model was verified with a vertical simulation environment. A water network pressure drop model

was developed to calculate the total pump head. The optimal pressure differential set-points under different ChW supply temperature set-points for a given condition were predicted by a pressure differential set-point incremental model. These models are not validated with field tests and their applicability in other systems is not guaranteed.

Moore and Fisher (2003) proposed to continuously optimize the pump differential pressure by striving to keep one valve almost completely open at all times to save pumping energy. They found, although it may cause some valve hunting, the overall performance of the chilled water system remained good. However, it should be noted that, when there is a ChW storage tank, the loop end DP setpoint may be determined to maintain a positive pressure at the highest point.

Lu and Cai et al.(2005c) adopted a fuzzy inference system implemented in the framework of adaptive neural networks to solve the variable DP setpoints of chilled water loops. The inputs are ChW flow rates passing through each AHU and the output is the water head for pipe networks. Good training is needed before using the model. A cooling coil model developed by Wang and Cai et al. (2004) was used to calculate the coil load at given air and water flow rates and temperatures. When there are hundreds or even thousands of cooling coils on the loop, it is impractical to apply this method to analyze the system.

Loop side performance is ignored by most TES system researchers, and it deserves more emphasis in a ChW storage system. The most critical challenge is to simulate the loop supply and return water temperature difference at various operating conditions, particularly part load conditions.

2.4 Equipment Performance Modeling

The equipment models can be divided into physical models, gray-box models, and black-box models. The physical models have high performance in prediction and high control reliabilities within their allowed working conditions and require less training data as well. However, they are rather complicated, and the iteration process is always required in most of these models, which may result in instability and divergence as well as high computational cost and memory demand. Black-box models are simple enough and have manageable computational costs. But they cannot ensure stable performance and are only reliable within the range of the training data covered. Gray-box models are a compromise of the former two. The coefficients have some physical meaning but they have lower complexities and less computational cost. They can be used to extrapolate outside the range of the training data covered. They are preferred in a modular-based optimization study.

Of chiller models, the Gordon-Ng model offers clear superiority (Phelan, Brandemuehl, et al. 1997; Gordon and Ng 2000; Reddy and Andersen 2002a). It was found that the fundamental Gordon-Ng formulation for all types of vapor compression chillers is excellent in terms of its predictive ability, yielding CV values in the range of 2% to 5%, which are comparable to the experimental uncertainty of many chiller performance data sets. Based on these findings as well as the comparison between black-box models and gray-box models, Jiang (2005) and Graves (2003) chose Gordon-Ng chiller models to study the chiller plant optimization.

A forward cooling coil model calculates the coil cooling capacity from entering air and water conditions. But the real control logic is to determine the water flow rate when other conditions are given. The sole ChW leaving temperature will be calculated accordingly from energy conservation principles. Braun (1989) used the basic theory of a counter flow cooling coil, leading to the development of an effectiveness model used for analyzing the performance of cooling coils. Through the introduction of an air saturation specific heat, effectiveness relationships were developed. The air side and water side Number of Transfer Units (NTU) were estimated from the flow rates by regression models. Both the completely dry and wet analyses underpredict the heat transfer where partial dry occurs, but the error is generally less than 5%. The Root mean squared error (RMSE) of the model was approximately 1.4ºF. Overall, the effectiveness model appeared to give satisfactory results for temperature differences up to 50°F between the water inlet temperature and ambient WB temperature. The advantages of this gray-box approach are its simplicity, accuracy and consistency. The accuracy of the effectiveness model is as good (or better) as that associated with standard methods while requiring significantly less computational effort. This model has been used by Jiang (2005), Flake (1998), and Yu (2008) to study the plant optimization. The fan power is calculated from fan laws with 10% minimum flow rate.

The various powers relative to pumps include theoretical power, shaft power, motor power, and electrical power required. The related efficiencies are pump efficiency, mechanical efficiency, and VSD efficiency. Most researchers model pump power as a function of part load ratio (Lu, Cai, et al. 2004; Jiang 2005; Barbosa and

Mendes 2008) or head times flow divided by motor, mechanical, and VSD efficiencies, which are expressed as function of speed ratio (Yao 2004; Lu, Cai, et al. 2005c). Pump laws are used to calculate the power at low speed. When a static head exists, the pump laws can only apply to the hydraulic pressure part.

2.5 Electrical Rate Structure

The electricity rate is the main driving force and the economic incentive for the application of a TES system. There are various kinds of rate structures but most of them can be classified into three types: flat rates, Time of Use (TOU) rates, and Real-Time-Pricing (RTP).

A flat rate structure can be further divided into a declining block rate and an increasing block rate. For the former one, the unit price of each succeeding block of usage is charged at a lower unit rate than the previous blocks. It does not promote conservation and many utilities are moving away from this rate structure. In contrast, for the increasing block rate, the unit price increases with the blocks. The block size can be determined by monthly cumulative energy consumption (kWh) or monthly peak demand (kWh/kW).

Under a RTP rate, a meter is installed to record a customer's electricity consumption at hourly (or sub-hourly) intervals, and a pricing system based on the wholesale cost of electricity during that hour is provided to its customer about 24 hours in advance. Consumers could obtain the maximum financial benefit possible under this system by shifting consumption from hours with high wholesale prices to hours with low wholesale prices (Jiang 2005). Less than 50 electric utilities that offer or will offer this

rate structure have been identified in a field survey, and these utilities predominantly service coastal areas and the South (Henze 2003a). Sun and Temple et al. (2006) generated a RTP rate model that produced a time-varying price for the costs of electricity that depended on time of day and maximum temperature for the day. The effect of the uncertainty of weather prediction and the RTP model on the optimization results deserves serious attention.

A TOU rate defines the cost of energy during specific times of the day and encourages customers to defer energy use until costs are lower. It is fixed in advance usually at the time of signing the contract, and is not subject to variations during the contracted period. TOU utility rates with both energy and demand charges, during the on-peak and off-peak periods, were considered by Morgan (2006). Sometimes, the calculation of monthly billed demand can be very complicated including current month demand, on-peak demand, contract demand, and annual demand (Wei, Liu, et al. 2002).

2.6 Load and Weather Condition Prediction

Plant ChW load prediction is critical for optimal control and optimization of a ChW plant with a TES system. The most popular methods include dynamic load simulation and regression or autoregressive neural network (ANN) models. Considering that long-term forecasts are highly uncertain, a safety factor based on previous forecast errors is appropriate, such as an uncertainty of two or three times the standard deviation of the errors of previous forecasts (ASHRAE 2003b).

Several load prediction models were presented and compared by Henze and Dodier et al. (1997a), such as the unbiased random walk model, bin predictor, harmonic

model, and autoregressive neural network approach. It was found the neural network outperforms other simple methods. There are many other kinds of dynamic or static building load simulation algorithms and programs. The Transfer Function Method (TFM) was used by Hajiah (2000) to calculate the cooling load of the office one-zone and multiple zones building models. Detailed building information was required. Braun (2007a) determined hourly cooling plant load requirements for different buildings and locations with DOE-2 simulations and the coincident TMY2 weather data for DB and WB temperature. Olson simulated the building load with BLAST with a specific weather file (Olson 1993). This method is time-consuming and hardly applies to district cooling, such as a campus or an airport.

An alternative method is to estimate the load with a regression model or an ANN model with time-varying input variables, such as ambient DB temperature, WB temperature, solar radiation, building occupancy, and wind speed. Some variables, such as building occupancy, are not easily measured and variables will need to be forecasted. Massie (2002) claimed that hourly outside air temperature could be estimated sufficiently well using National Weather Service high and low temperature predictions and the ASHRAE model discussed in Chapter 28, Table 2 (ASHRAE 2005). Building loads may be estimated by a variety of methods (Kreider and Haberl 1994). The expected combined error of these estimates will vary by building type and location, and will lead to a loss in optimization accuracy of approximately 10%.

Wei and Liu et al. (2002) developed two cooling load linear regression models based on actual measured cooling energy consumptions at the facility versus the ambient

air DB temperature during fully occupied periods and partially occupied periods. To avoid possible premature depletion of the storage tank due to cooling load prediction error, actual temperatures entered for load forecasting were 1°F to 2°F higher than the forecasted high and low temperatures so that extra capacity was available.

Forrester and Wepfer (1984) presented a forecasting algorithm that used current and previous ambient temperatures and loads to predict future requirements. Trends on an hourly time scale were accounted for with measured inputs for a few hours before the current time. Day-to-day trends were considered by using the value of the load that occurred 24 h earlier as an input. One of the major limitations of this model is its inability to accurately predict loads when an occupied day (e.g., Monday) follows an unoccupied (e.g., Sunday) or when an unoccupied day follows an occupied day (e.g., Saturday). The cooling load for a particular hour of the day on a Monday depends very little on the requirement 24 h earlier on Sunday. They described a number of methods for eliminating this 24 h indicator.

Armstrong and Bechtel et al.(1989) presented a very simple method for forecasting either cooling or electrical requirements that did not use the 24 h regressor; Seem and Braun et al. (1991) further developed and validated this method. The "average" time-of-day and time-of-week trends were modeled using a lookup table with time of day and type of day (e.g., occupied versus unoccupied) as the deterministic input variables. Entries in the table were updated using an exponentially weighted, moving-average model. Short-term trends were modeled using previous hourly measurements of cooling requirements in an autoregressive model. Model parameters adapted to slow

changes in system characteristics. The combination of updating the table and modifying model parameters worked well in adapting the forecasting algorithm to changes in season and occupancy schedule.

Kreider and Wang (1991) used ANNs to predict energy consumptions of various HVAC equipment in a commercial building. The primary purpose in developing these models was to detect changes in equipment and system performance for monitoring purposes. However, the authors suggested that an ANN-based predictor might be valuable when used to predict energy consumption in the future with a network based on recent historical data. Forecasts of all deterministic input variables were necessary to apply this method.

3. METHODOLOGY

The study on optimal operating strategies can be divided into two stages. The first stage is to determine optimal strategies by simulation. During this stage, the loop cooling load, weather conditions, and rate structures are assumed perfectly predicted. Perfect system knowledge is assumed, which means that the system in reality behaves exactly as modeled by a system model. The electricity billing costs under different operating strategies are simulated and compared. The secondary stage is implementation. Appropriate forecasting models are chosen to predict those inputs and a controller is designed to actualize the selected control strategy. The robustness of the control strategy can be tested by conducting a parametric study to identify the most sensitive parameters. More efforts would be paid to these parameters to enhance the accuracy of simulations and predictions.

3.1 Objective Function

3.1.1 System electricity power

Normally, the system power demand recorded by the meter is the kW supplied during a fifteen-minute period. This demand "window" may be a fixed period or a sliding fifteen-minute period in order for the electric utility to record the highest site demand. For a typical ChW storage system, the instantaneous electrical power consists of the following two components:

$$P_{sys} = P_{plant} + P_{non-plant} \quad (1)$$

where P_{sys} is the total power billed by the utility company, and $P_{non-plant}$ covers all other electricity usages excluding ChW production and distribution in the facilities, such as AHUs, terminal boxes, elevators, lighting, office equipment, etc. Models are needed to simulate the second term if it is covered in the bill. P_{plant} is the ChW production-related electricity consumption in the plant and it is sum of the following items:

$$P_{plant} = P_{CT} + P_{CWP} + P_{CHLR} + P_{PPMP} + P_{SPMP} \quad (2)$$

Typically, in a well-maintained chiller plant, more than half of the plant electricity consumption is attributed to chillers, while the other is split between pumps and fans. Miscellaneous power attributed to plant lighting and plug loads is considered to be negligible compared to the major plant loads.

3.1.2 Operating cost function

In most cases, the optimization target of TES system operation is to minimize the operating cost within a billing period, such as a year. Different electricity rate structures lead to different expressions of the operating cost function. For commercial customers with a TOU rate, the billing cost includes two main contributions. One is the cost of the electricity demand (kW) that occurs during the billing period or in any previous month during the ratchet period. The other is the cost of the electricity energy (kWh) consumed over the billing period. For a RTP rate, the demand charge item may disappear but the energy rate varies from hour to hour.

The utility billing cost over the extent of one year can be expressed as (Krarti, Brandemuehl, et al. 1995):

$$C = \sum_{i=1}^{12} \sum_{v=1}^{n} R_{d,i,v} P_{i,v} + \sum_{i=1}^{12} \sum_{i=1}^{N_i} \sum_{k=1}^{24} R_{e,i,k} P_k \Delta t \,, \tag{3}$$

where $R_{d,i,v}$ is the demand charge rate for rate period v and month i, $P_{i,v}$ is the billed demand kW in period v and month i, $R_{e,i,k}$ is the energy charge rate at hour k and month i, P_k is the total power incurred from the system at hour k, N_i is the days in month i, n is the unique demand rate periods, and Δt is a unit time step of one hour. The calculation of $P_{i,v}$ could be complicated when a ratchet is defined. The demand and energy charge rates are fixed when a contract is signed.

For a RTP rate, the demand charge item may disappear and $R_{e,i,k}$ is determined by the utility company reflecting wholesale market prices. The user is notified an hour ahead or one day ahead. For a flat rate, $R_{d,i,v}$ and $R_{e,i,k}$ change for different blocks.

Most utilities have only two distinct rate periods, know as on-peak hours and off-peak hours. The monthly cost function in (3) can be stated as:

$$C_i = \sum_{v=1}^{2} R_{d,i,v} P_{i,v} + \sum_{i=1}^{N_i} \sum_{k=1}^{24} R_{e,i,k} P_k \Delta t \tag{4}$$

3.1.3 Rate structure

The electric utility rate schedule is the main driving force for TES applications. Therefore, the determination of operating strategies and control strategies should be based on the utility's rate structure. Table 1 is a typical TOU energy and demand rate

structure for a TES system. In this table, “R” means electrical rate, subscript e means energy, d means demand, w means winter, s means summer, on means on-peak hours, and off means off-peak hours. In most cases, the definition of winter or summer billing months for the energy rate are the same as that for the demand rate. But it is also possible that the definition of on-peak or off-peak hours for the energy rate is different from that for demand rate.

This rate structure covers most of the rates applied to TES systems. As it is rare to use a RTP or a flat rate structure in a TES system at present, the following study will be based on a TOU rate structure. It is also possible to expand this methodology to the situation with a RTP rate structure.

For a specific control strategy, it is necessary to define an on-peak period and an off-peak period. For summer billing months and winter billing months, such a definition could be different when the electrical rate structure changes. In most cases, this definition matches the definition of on-peak and off-peak hours for energy or demand rates.

Table 1 Typical TOU rate structure

Rate	Winter billing months	Summer billing months
Energy rate		
On-peak	Re_w_on	Re_s_on
Off-peak	Re_w_off	Re_s_off
Demand rate		
On-peak	Rd_w_on	Rd_s_on
Off-peak	Rd_w_off	Rd_s_off

3.1.4 Description of TES control

For a TES system, there has been significant confusion due to a blurring of the terminology. To overcome this problem, Dorgan (2001) developed a multi-dimensional terminology to accurately describe and characterize cool storage operation and control strategies. It ensures consistency of definitions among the various parties involved in the development and implementation of strategies. This dissertation will follow such a framework.

A control sequence is the combination of specific control events that are initiated to properly operate the system components according to the specific operating strategy in place. It must include setpoint values and actions taken upon crossing the set point. The tank operating modes can be charging mode, discharging mode, and match or idle mode. The system operating mode will be more varied, such as charge, charge and load, discharge, discharge and chiller, etc. A control strategy is essentially a tag given to a sequence of operating modes that covers a single cycle of the cool storage system. This cycle is typically a day. An algorithm containing detailed logics will determine the starting and ending time of each operating mode as well as the values of the control variables. The control strategy is an easy way to classify the key strategies available for operating a TES system under various environmental conditions, storage needs, and load conditions. The operating strategy is the overall method of controlling the system in order to achieve the owner's design intent (Morgan 2006).

Therefore, the operating strategy is determined during the design phase but it can be changed if external conditions, such as the rate structure or load profile, are different

from the design. It provides the logic used to determine when each control strategy is selected, as well as what operating mode is implemented within each control strategy. A group of predefined control actions will be performed to actualize each operating mode of the system.

3.2 Optimal Operating Strategy Search Method

3.2.1 Flow chart of strategy search

Figure 2 shows the flow chart of the search procedure for the optimal control strategy for each month. The optimization of TES operations and the optimization of the plant operations are performed alternately. For each month, a search is performed to find a feasible and most cost-effective TES operating strategy. Then, a plant optimization program is launched to find the optimal controlled variables for this month.

An optimal TES control strategy is a trade-off of benefits and risks. The benefit is billing cost savings and the risk is the potential of depleting the tank prematurely, which forces operators to run additional chillers during the on-peak hours. In the simulation, the uncontrolled variables, such as loop total cooling load, loop delta-T, and weather conditions, are assumed perfectly known. However, in practice, these variables will be different from those in simulations. To ensure the selected control strategy is reliable, a minimum tank level setpoint is defined to filter all the combinations. The higher the minimum level setpoint is, the lower the risk of the strategy is.

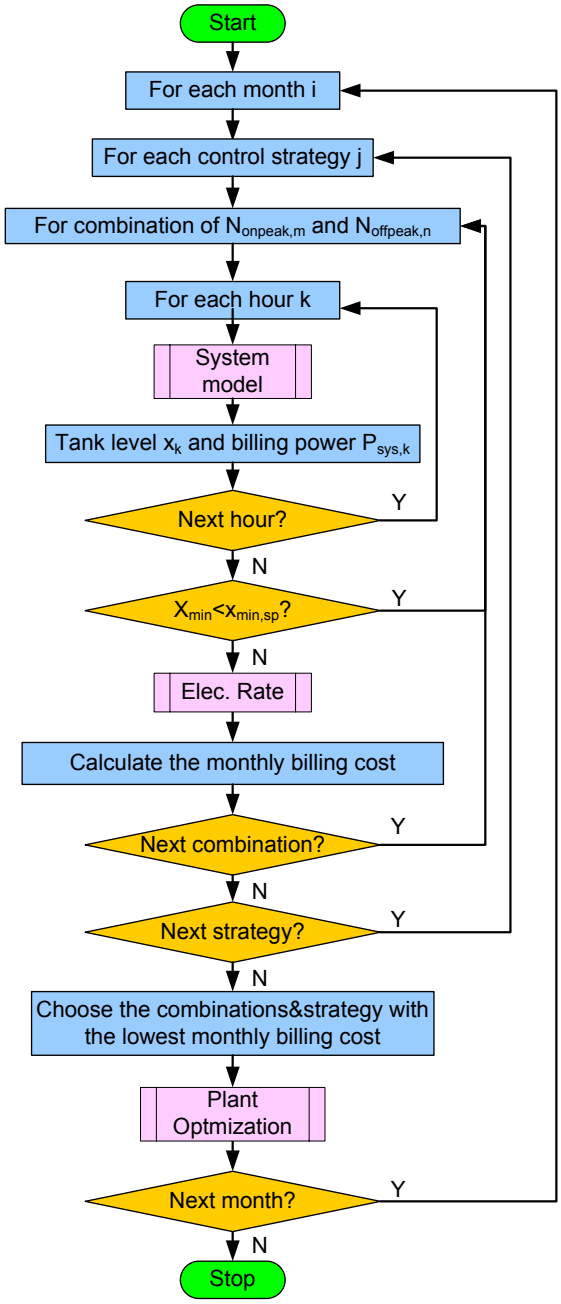

Figure 2 **Flow chart for searching the near-optimal control strategy for each month**

If a demand ratchet is involved, the maximum monthly demand will be determined first by searching the optimal strategy for the month with the highest demand. This normally occurs in the summer months.

3.2.2 Definition of operating strategy

The operating strategy can be described with a control strategy and the maximal numbers of chillers that can be staged on during the off-peak period and on-peak period. This number should be no less than zero and no higher than the number of installed chillers in the plant. The limitation on the number of chillers running is a kind of demand limiting because, for a multi-chiller plant, the ChW-related power is directly proportional to the number of chillers running. Each control strategy consists of a series of control logic, which is used to calculate the plant total ChW flow rate and the number of chillers staged on for each time step.

The traditional control strategies with or without demand limiting are as follows. If there is no demand limiting, the number of chillers running during the charging mode will be the installed chiller number in the plant. During the on-peak period, the maximal number of chillers that can be staged on is zero for full storage control strategy and is equal to or less than the installed chiller number for chiller-priority or storage-priority control.

Within the search loop, all combinations of available control strategies and the maximal chiller number during the off-peak and on-peak periods are explored. The hourly tank water level and system total power are simulated with a model called system model. A minimum tank level setpoint is predefined to prevent premature depletion. The

minimal water level in the current month is compared with the setpoint to determine if the current combination is acceptable. For all acceptable combinations, the scenario with the lowest monthly billing cost will be chosen as the optimal operating strategy for the current month.

The control strategies used include three conventional strategies and one new strategy, which are elaborated in other sections. In addition, the scenario without TES is also simulated as a baseline.

3.2.3 Plant optimization

A plant optimization procedure will be performed right after the TES control strategy optimization procedure. The variables that could be optimized include, but are not limited to, the chiller ChW leaving temperature, CW flow rate of each chiller, and cooling tower approach temperature. Some constraints are applied to these variables, such as the minimal tank water level, the lowest ChW leaving temperature the chiller can produce, and the highest ChW supply temperature the loop can tolerate.

Table 2 Local PID control loop in a chilled water plant

Controlled variables	Continuous control variables
Cooling tower CWLT	Cooling tower fan speed or sequencing
Chiller chilled water leaving temperature	Chiller speed or slide vane
Condenser water flow rate	Condenser water pump speed or valve
Primary chilled water flow rate	Primary chilled water pump speed or valve
Chilled water loop end differential	Secondary pump speed

Table 2 is a list of local PID controls in a chilled water plant. Figure 3 shows the general physical configuration of a chilled water system. All the variables shown are setpoints to be optimized. In practice, these setpoints are maintained by adjusting the equipment speed or control valve position with a PID controller. As mentioned before, except for continuous control variables, discrete control variables will also need to be optimized, such as sequencing of chillers, cooling towers, and pumps. The constraints on the equipment operation, such as maximum and minimum flow rates, limit the possible number of combinations of control variables.

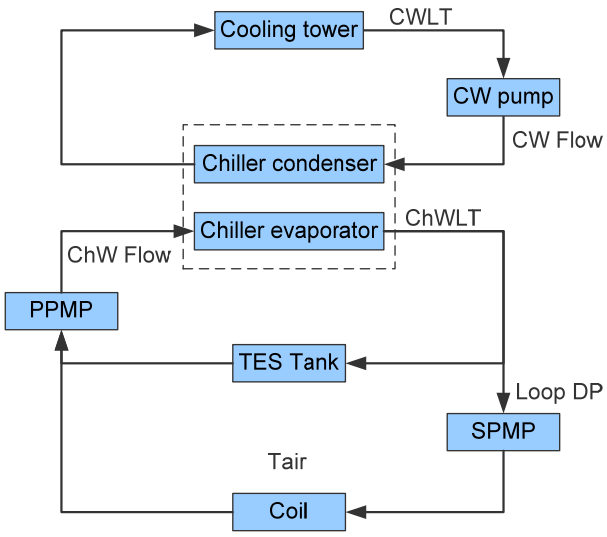

Figure 3 Configuration of a chilled water system with a TES tank

This is a non-linear programming (NLP) problem and it can be solved with the GRG (Generalized Reduced Gradient) Nonlinear Solver in the standard Excel Solver.

This method and specific implementation have been proven in use over many years as one of the most robust and reliable approaches to solving difficult NLP problems.

3.3 System Power Simulation

The flow chart of a System Model is shown in Figure 4. It is used to calculate the hourly tank water level and system total power. This model includes six sub-models and each of them will be introduced in the following sections.

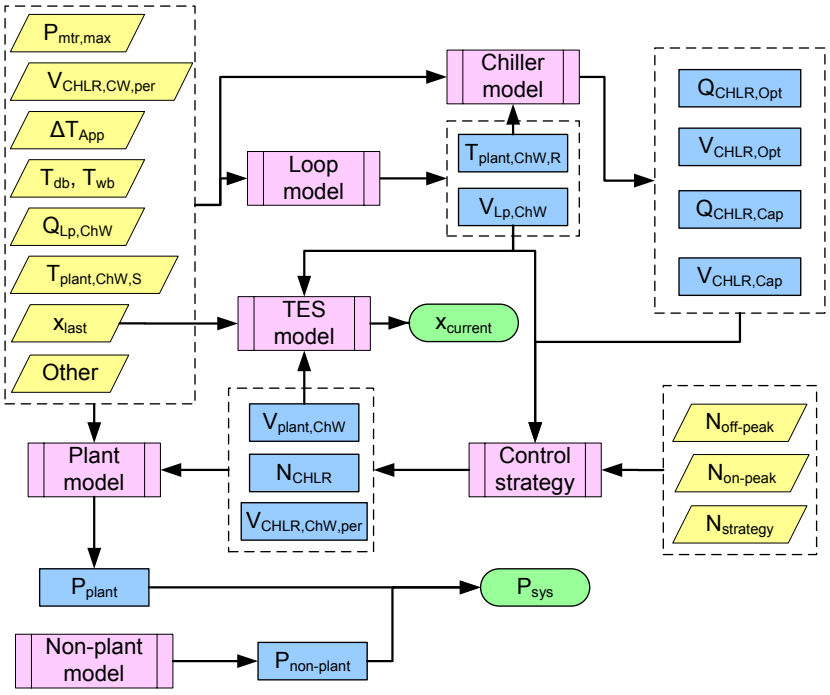

Figure 4 Flow chart of system total power simulation

The control strategy number is $N_{strategy}$ and the maximal numbers of chillers on-stage during the on-peak and off-peak periods are $N_{on-peak}$ and $N_{off-peak}$. In addition,

some other inputs are required, such as tank volume, plant total chiller number, and chiller CWET lower and upper limits.

The advantage of such a system model is that each sub-model is independent and its function is explicitly specified. It also clearly describes the relationships among plant, loop, and TES tank. For different applications, the user may replace them with self-built sub-models or make minor changes on the original ones. In addition, the user can design a new control strategy to maximize the savings based on case by case considerations.

3.4 TES Tank Modeling

3.4.1 Tank state transition equation

In this study, the tank ChW volume ratio and the tank charging or discharging flow rate are utilized to describe the tank state and inventory change rate. In this context, the state-of-charge x is explained as the ChW volume ratio in the tank. The state of a full tank is unity and of an empty one is zero. The primary controlled variable $V_{Tank,ChW}$ is defined as the rate change of the state-of-charge x_k .

$$x = \frac{U_{Tank,ChW}\left(T_{ChW} \le T_{ref}\right)}{U_{Tank}} \tag{5}$$

$$V_{Tank,ChW} = \phi \frac{dU_{Tank,ChW}}{dt} = \phi\left(V_{Plant,ChW} - V_{Lp,ChW}\right) \tag{6}$$

$$x_{k+1} = x_k + \phi(V_{Plant,ChW,k} - V_{Lp,ChW,k})\frac{\Delta t}{U_{Tank}}, \tag{7}$$

subject to the constraints

$$x_{min} \le x_k \le x_{max}$$

$$0 \le V_{Plant,ChW,k} \le V_{Plant,ChW,\max}$$

$$V_{Tank,ChW,\min} \le V_{Tank,ChW,k} \le V_{Tank,ChW,\max}$$

Specifically, U_{Tank} is the tank total volume in gallons, $U_{Tank,ChW}$ is ChW volume in the tank in gallons, $V_{Tank,ChW}$ is tank ChW volume change rate in GPM (positive is charging, negative is discharging, zero is idle), ϕ is a Figure-of-Merit (ϕ is 0.85~0.95 during charging and close to unity during discharging or idle), $V_{Plant,ChW,k}$ is the plant side total ChW flow rate in GPM, $V_{Lp,ChW,k}$ is the loop side total ChW flow rate in GPM, and Δt is the time step, normally one hour.

The terms x_{min} and x_{max} are the upper and lower limits of the tank inventory and are subject to the operating strategy selected. Higher values of x_{min} and x_{max} mean a lower risk of depleting the tank prematurely but lead to higher energy losses due to heat transfer and over charging. If x_{max} is approaching unity, the chiller efficiency could deteriorate dramatically due to low water temperatures in the thermocline. A reference temperature T_{ref} is defined to determine the ChW height in the tank since there is no distinct interface between the chilled water layer and the warm water layer. It is subject to the allowable highest loop ChW supply temperature.

The plant side maximum flow rate $V_{Plant,ChW,max}$ is governed by the PPMP maximum flow rate and chiller ChW flow rate upper limit, whichever is smaller. It is inadmissible if the control action $V_{Plant,ChW,k}$ leads to x_k less than zero or greater than

unity. In addition, due to the limitations in the flow rate into and out of the tank to restrain mixing effects, an additional constraint is applied to the tank maximal charging ($V_{Tank,ChW,max}$) and discharging rate ($V_{Tank,ChW,min}$) based on the tank design parameters.

As the loop side total ChW flow ($V_{Lp,ChW,k}$) is subject to the loop side demand, the tank charging or discharging flow rate is, in fact, controlled by the plant operation ($V_{Plant,ChW,k}$). The tank level change can be calculated from Equation (7). The charge and discharge cycling period is one day or 24 hours.

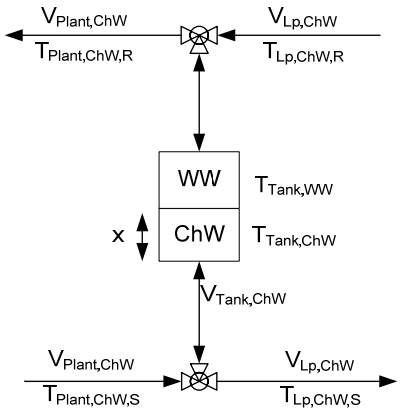

Figure 5 TES parameters relations

3.4.2 Temperature relationship

Figure 5 shows the relationship among flow rates and temperatures related to the tank. The chiller ChW leaving temperature is fixed in one cycling period and could be adjusted month by month. The plant ChW leaving temperature is normally different

from the loop ChW supply temperature. The following assumption is made on the loop supply temperature:

$$T_{Lp,ChW,S} = T_{Plant,ChW,S} + \Delta T_S \quad (8)$$

where ΔT_S is the ChW temperature rise due to pumping, piping heat losses, and tank heat losses. It is around 0.5-1.5 ºF depending on the system characteristics, such as loop DP, piping and tank insulations, and pump efficiencies.

Different from the plant supply temperature, the loop return water temperature may fluctuate diurnally, low at night and high in the daytime. The swing range can be as large as 6.0-8.0 ºF. This could necessitate a more detailed model to define the plant return ChW temperature when there is cooling load on the plant side.

$$T_{Plant,ChW,R} = T_{Lp,ChW,R} + \Delta T_R \text{ during idle or discharging mode} \quad (9)$$

$$T_{Plant,ChW,R} = \frac{\left(V_{Tank,ChW} T_{Tank,WW} + V_{Lp,ChW} T_{Lp,ChW,R}\right)}{V_{Plant,ChW}} + \Delta T_R \text{ during charging mode} \quad (10)$$

Similarly, ΔT_R is the return ChW temperature rise due to pumping, piping heat losses, and tank heat losses. As the return temperature is close to the ambient temperature and PPMP head is much smaller than SPMP head, this item is much smaller than ΔT_S and can be neglected.

$T_{Tank,WW}$ is the bulk temperature of the warm return water stored in the tank. It is assumed that there is no thermal stratification in the warm water layer and it is equal to the average return water temperature during the charging period in the last cycle.

$$T_{Tank,WW} = \frac{\sum_i V_{Tank,ChW,i} T_{Lp,ChW,R,i}}{\sum_i V_{Tank,ChW,i}} \quad \text{when } V_{Tank,ChW,i} > 0 \tag{11}$$

Such a definition may introduce iterations into the whole model. An even simpler way is to assume plant return water temperature is equal to the loop return water temperature since $T_{Tank,WW}$ is close to $T_{Lp,ChW,R}$ for two consecutive days.

3.5 ChW Plant Modeling

3.5.1 Simulation method

In the TES simulation, for each given plant total ChW flow rate and operating chiller number, the ChW plant model will export the total plant power under the given conditions. In this study, an equipment performance-oriented plant model is proposed to calculate the plant power under predefined conditions. This model is based on a Wire-to-Water (WTW) plant efficiency concept. The plant total power can be calculated from the following formula:

$$P_{plant} = (\xi_{CT} + \xi_{CWP} + \xi_{CHLR} + \xi_{PPMP}) Q_{Plant,ChW} + P_{SPMP} \tag{12}$$

As mentioned before, chillers consume the majority of the plant power and chiller performance is the most important factor in plant performance. However, chiller performance may fluctuate heavily under different operating conditions, such as chiller ChW leaving temperature, CW entering temperature, and chiller part load ratio. The scatter plot of a water-cooled centrifugal chiller performance is shown in Figure 6. The rated chiller cooling capacity is 5,500 ton and the rated efficiency is 0.7133 kW per ton

when the ChWLT is 36 ºF and CWET is 85 ºF. The maximum motor power input is 3,933 kW. This plot shows that, when the ChWLT is 36.5±1.0 ºF, the chiller kW per ton can rise to 0.80 or drop to 0.54. For a specific CWET range, the optimal chiller part load is around 4,400 to 4,600 ton or 80% to 84% of the design cooling capacity. The real cooling capacity of the chiller is restricted by the maximum motor power input. A higher CWET leads to a lower chiller capacity.

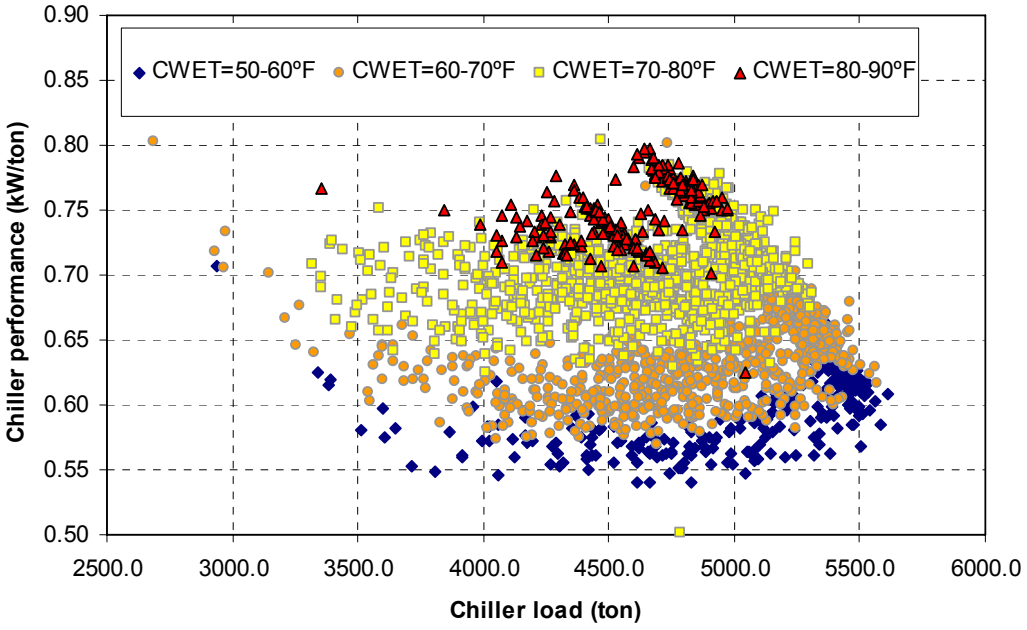

Figure 6 Performance of a centrifugal chiller as a function of chiller load and CWET

Because of its high weight and significant complexity, more effort should be made on chiller performance modeling. In this study, the Gordon-Ng model is chosen to simulate the chiller performance under different conditions. Some regression formulas

together with energy conservation laws are used to simulate the WTW efficiency of pumps and fans.

3.5.2 Plant power modeling

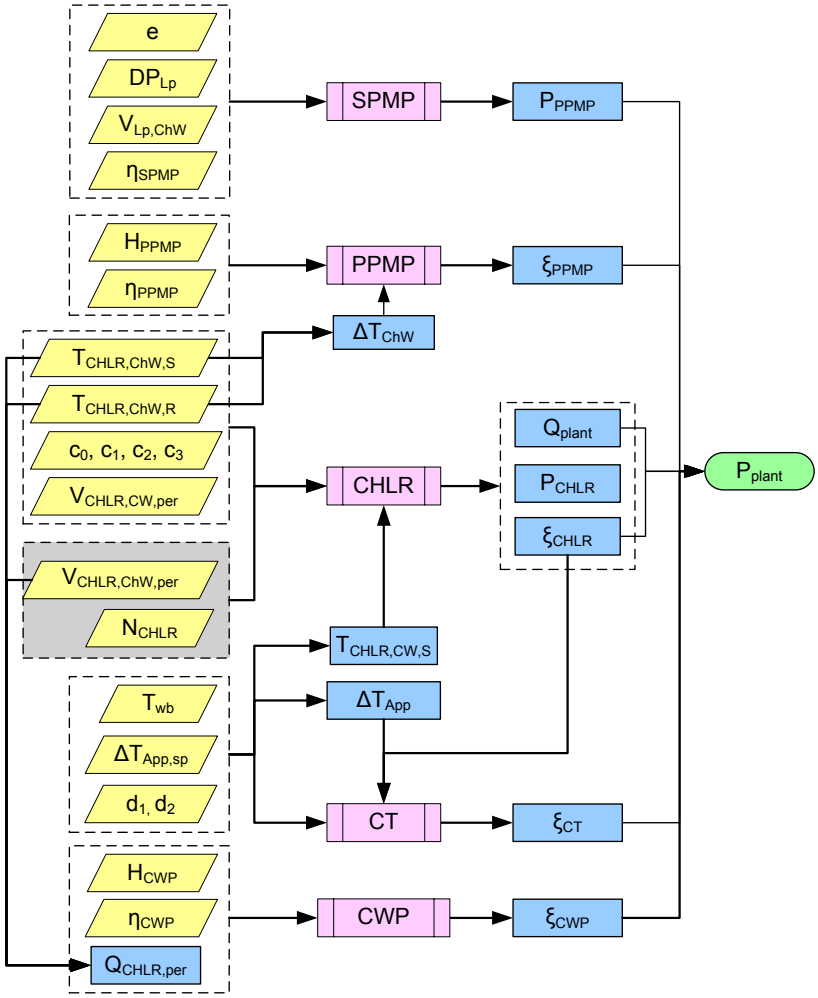

Figure 7 Flow chart of chilled water plant electricity load simulation

Figure 7 is a flow chart of the ChW plant simulation. All the variables on the left are the inputs while the output is the plant total power. The plant model determines the

plant total power consumptions in response to a set of external parameters and a set of plant parameters.

The coefficients e, c0, c1, c2, d1, and d2 can be determined by regression with the trended historical data or equipment performance data. The ChW return temperature $T_{CHLR,ChW,R}$, loop DP setpoint DP_{Lp} and loop total flow rate $V_{Lp,ChW}$ are provided by the loop model. The heads and efficiencies of PPMPs and CWPs, the efficiency of SPMPs, and CW flow rate for each chiller $V_{CHLR,CW,per}$ are assumed constant. The chiller ChW leaving temperature $T_{CHLR,ChW,S}$ and CT approach temperature setpoint $\Delta T_{App,sp}$ are provided by the plant optimization results. The ambient WB temperature T_{wb} is known in the simulations. The running chiller total number N_{CHLR} and the ChW flow rate for each chiller $V_{CHLR,ChW,per}$ are the outputs of the control strategy sub-model.

This forward plant model can be easily set up and used for plant energy simulation. Since it is based on basic physical definitions and conservation laws, it has an explicit physical meaning. Its application is not restricted by the equipment number and sequencing strategies. All calculations are explicit expressions and no iterations are required. One prerequisite is that the pumps are well sequenced and controlled such that the pump head and efficiency are around the normal operation point.

3.5.3 Chiller modeling

A Gordon-Ng model for vapor compression chillers with variable condenser flow is selected in this study. It can apply to unitary and large chillers operating under steady-state variable condenser flow conditions. This model is strictly applicable to inlet guide vane capacity control (as against cylinder unloading for reciprocating chillers, or VFD for centrifugal chillers) (Jiang and Reddy 2003).

The possible independent variables are chiller ChW leaving temperature $T_{CHLR,ChW,S}$, CW entering temperature $T_{CHLR,CW,S}$, chiller production $Q_{CHLR,per}$, and CW flow rate $V_{CHLR,CW,per}$. The model is in the following form:

$$y = c_0 + c_1 x_1 + c_2 x_2 + c_3 x_3 \tag{13}$$

$$x_1 = \frac{T_{cho}}{Q_{ChW}},\ x_2 = \frac{T_{cdi} - T_{cho}}{Q_{ChW} T_{cdi}},\ x_3 = \frac{\left(\frac{1}{COP} + 1\right) Q_{ChW}}{T_{cdi}}$$

$$y = \frac{\left(\frac{1}{COP} + 1\right) T_{cho}}{T_{cdi}} - 1 - \frac{1}{\left(V_{CW,per} \rho_w c_{pw}\right)} \frac{\left(\frac{1}{COP} + 1\right) Q_{ChW}}{T_{cdi}}$$

$$T_{cho} = \left(T_{CHLR,ChW,S} - 32\right) \times 5/9 + 273.15$$

$$T_{cdi} = \left(T_{CHLR,CW,S} - 32\right) \times 5/9 + 273.15$$

$$Q_{ChW} = \frac{12{,}000 Q_{CHLR,per}}{3{,}412},\ COP = \frac{Q_{ChW}}{P_{CHLR}},\ V_{CW} = 0.00006309 V_{CHLR,CW,per}$$

where ρ_w is water density (kg/m^3) and c_{pw} is water heat capacity (kJ/kg·K).

The chiller motor power P_{CHLR} (kW$_e$) can be predicted from:

$$P_{CHLR} = \left[\frac{(c_0 + c_1 x_1 + c_2 x_2 + 1) T_{cdi}}{(-c_3 Q_{ChW} + T_{cho} - \frac{Q_{ChW}}{(V_{CW} \rho_w c_{pw})})} - 1 \right] Q_{ChW} \quad (14)$$

If the motor maximum power input $P_{Mtr,max}$ (kW_e) is given, the chiller maximum cooling capacity under these conditions $Q_{CHLR,Cap}$ (ton) is:

$$Q_{CHLR,Cap} = \frac{3{,}412}{12{,}000} \frac{-b + \sqrt{b^2 - 4ac}}{2a} \quad (15)$$

$$a = c_3 + \frac{1}{(V_{CW} \rho_w c_{pw})}$$

$$b = T_{cdi} - T_{cho} + \left(c_3 + \frac{1}{(V_{CW} \rho_w c_{pw})} \right) P_{Mtr,max} + c_0 T_{cdi}$$

$$c = c_1 T_{cho} T_{cdi} + c_2 (T_{cdi} - T_{cho}) - T_{cho} P_{Mtr,max}$$

The chiller WTW efficiency (kW per ton) is:

$$\xi_{CHLR} = \frac{P_{CHLR}}{Q_{ChW} \frac{3{,}412}{12{,}000}} = 3.517 \left(\frac{(c_0 + c_1 x_1 + c_2 x_2 + 1) T_{cdi}}{(-c_3 Q_{ChW} + T_{cho} - \frac{Q_{ChW}}{(V_{CW} \rho_w c_{pw})})} - 1 \right) \quad (16)$$

Apply the first differential to Q_{ChW} in (14) and the chiller part load ratio $Q_{CHLR,Opt}$ (ton) with the lowest kW per ton is the solution of this equation:

$$\frac{\partial \left(\frac{P}{Q_{ch}} \right)}{\partial Q_{ch}} = 0$$

$$Q_{CHLR,Opt} = \frac{3{,}412}{12{,}000}\frac{-b+\sqrt{b^2-4ac}}{2a} \tag{17}$$

$$a = c_0 + 1,\ b = 2\left(c_1 T_{cho} + c_2 \frac{T_{cdi} - T_{cho}}{T_{cdi}}\right),\ c = -T_{cho}\frac{c_1 T_{cho} + c_2 \dfrac{(T_{cdi} - T_{cho})}{T_{cdi}}}{c_3 + \dfrac{1}{(V_{CW}\rho_w c_{pw})}}$$

It is noted that the actual chiller ChW flow is also limited by the upper and lower limits of evaporator ChW flow rate. The upper limit is intended to prevent erosion and the lower limit is to prevent freezing in the tubes.

3.5.4 Pump modeling

The WTW efficiency of a pump was first introduced by Bernier and Bourret (1999). It was originally used to quantify the whole performance of a ChW plant. In this study, it is used to define the transportation efficiency of plant equipment except for SPMPs.

The general calculation formula of the pump power is:

$$P_{pump} = \frac{0.746V \times H \times SG}{3{,}960\eta_{all}} \tag{18}$$

where P_{pump} is the pump motor power input in kW, V is the volumetric flow rate for each pump in GPM, H is the pump head developed in feet of fluid, SG is the specific gravity of the fluid being pumped (in most cases, the fluid is water and SG=1), and η_{all} is the overall efficiency including pumps, motors, and VSDs.

$$\eta_{all} = \eta_{pump}\eta_{motor}\eta_{VSD} \tag{19}$$

The pump efficiency at full or partial speed η_{pump} is defined by the individual pump efficiency curve. A typical motor efficiency η_{motor} as a function of nameplate loading percentage (x) for large size motors (>25 hp) is given by ASHRAE (1996):

$$\eta_{motor} = 0.94187 \times (1 - e^{-0.0904x}) \tag{20}$$

The efficiency of a typical high-efficiency VSD as a function of percentage of nominal speed (x) is given by:

$$\eta_{VSD} = 50.87 + 1.283x - 0.0142x^2 + 5.834 \times 10^{-5} x^3 \tag{21}$$

The total cooling transported by the pump is:

$$Q_{ChW} = \frac{V_{ChW} \Delta T_{ChW}}{24} \tag{22}$$

where Q_{ChW} is the cooling energy in ton, V_{ChW} is the total ChW volumetric flow rate in GPM, ΔT_{ChW} is the ChW supply and return flow temperature difference in ºF.

The pump WTW efficiency is:

$$\xi_{pump} = \frac{P_{pump}}{Q_{ChW}} = \frac{0.746 N_{pump} \times V \times H}{3{,}960 \eta_{all}} \times \frac{24}{V_{ChW} \Delta T_{ChW}} \tag{23}$$

where N_{pump} is the number of pumps running.

For PPMPs, $N_{pump} \times V = V_{ChW}$. The pump head is relatively constant due to a narrow range of ChW flow rate fluctuation in the evaporator and a flat pump head curve. If η_{PPMP} is the overall efficiency of PPMPs, the WTW efficiency is:

$$\xi_{PPMP} = 0.004521 \frac{H_{PPMP}}{\eta_{PPMP} \Delta T_{ChW}} \tag{24}$$

For CWPs, $N_{pump} \times V = N_{pump} \times V_{CW,per}$. The pump head is relatively constant due to a narrow range of condenser water flow rate in the condenser. Neglecting the heat exhausted by the motor fan and hot surfaces, the energy balance for a chiller is:

$$\frac{V_{CW}\Delta T_{CW}}{24} = \left(1 + \frac{3{,}412\xi_{CHLR}}{12{,}000}\right) Q_{ChW} = \left(1 + \frac{3{,}412\xi_{CHLR}}{12{,}000}\right) \frac{V_{ChW}\Delta T_{ChW}}{24} \tag{25}$$

Consequently, the CW pump WTW efficiency is:

$$\xi_{CWP} = 0.0001884 \frac{H_{CWP}}{\eta_{CWP}} \frac{V_{CW,per}}{Q_{ChW,per}} \tag{26}$$

where H_{CWP} is the pump head in feet, η_{CWP} is the overall efficiency of CW pumps, $V_{CW,per}$ is the CW flow rate for each chiller, and $Q_{ChW,per}$ is the ChW load for each chiller.

For SPMPs, $N_{pump} \times V = V_{Lp,ChW}$, which is different from the total ChW flow in the plant due to the TES tank. The loop total flow rate is determined by loop operations. The pump head can be calculated as:

$$H_{SPMP} = DP_{Lp} + eV^2{}_{Lp\_ChW} \tag{27}$$

where DP_{Lp} is the loop end DP in psid, e is the loop hydraulic performance coefficient. A reset schedule could be applied to DP_{Lp} to save pump energy. The pump power for SPMPs is:

$$P_{SPMP} = \frac{0.746 V_{Lp\_ChW} \times 2.31 \times \left(DP_{Lp} + eV^2_{Lp\_ChW}\right)}{3{,}960\eta_{SPMP}} \tag{28}$$

where η_{SPMP} is the overall SPMP efficiency. Obviously, the energy consumption of SPMPs is subject to the loop side operation and is not determined by plant operations.

3.5.5 Cooling tower modeling

The mass and heat transfer process in a cooling tower is fairly complicated. The effectiveness model is the most popular model in CT simulations but iterations are required to obtain a converged solution. To overcome this obstacle, a simple regression model is proposed in this study.

Practical operating experience shows that the CT performance is directly related to its approach temperature. When a CT fan is speeding up to its full speed to lower the approach temperature, the incremental heat released over the incremental power input declines, or tower WTW performance declines. Conversely, when the fan slows down, the approach temperature rises and tower WTW performance increases. When the fan stops, the WTW efficiency is zero, i.e. no fan power is needed to release the heat to the ambient.

Figure 8 shows the kW per CW tonnage for a CT as a function of the tower approach temperature. A lower approach leads to a higher kW per CW ton. The minimal approach is around 2 ºF. This indicates that, no matter how hard the fan is running, the CT condenser water leaving temperature cannot further approach the entering air WB temperature. When the approach temperature is higher than 20 ºF, the kW per CW ton is approaching 0.016.

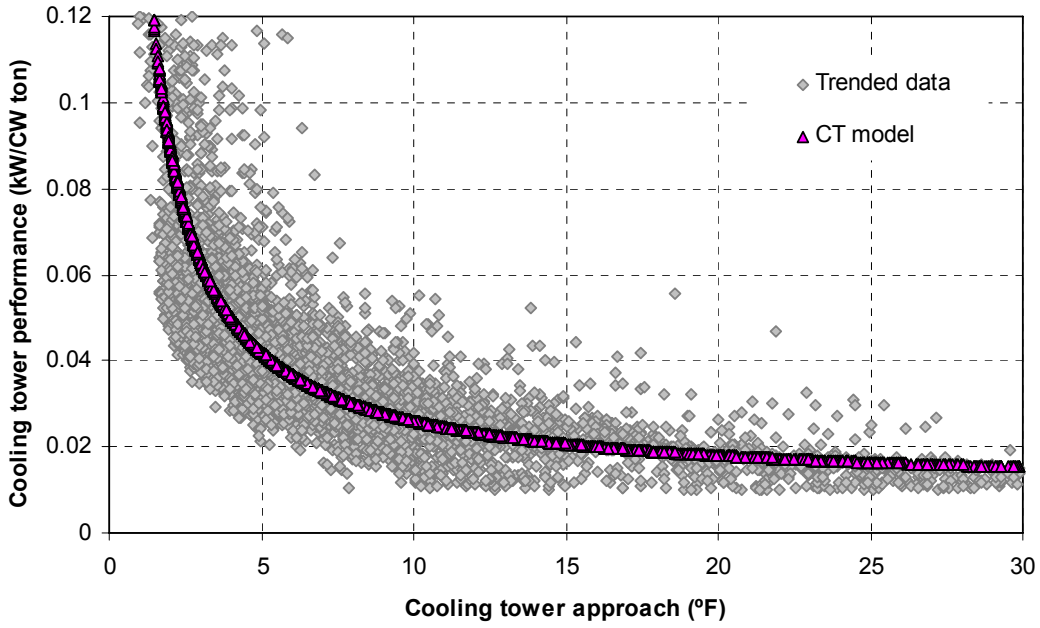

Figure 8 Scatter plot of cooling tower performance as a function of tower approach

Based on these observations, a simple CT fan power model is proposed to calculate the tower WTW performance:

$$\frac{P_{CT}}{Q_{CW}} = d_1 + \frac{d_2}{\Delta T_{app}} = \frac{P_{CT}}{(1+0.2843\xi_{CHLR})Q_{ChW}}$$

$$\xi_{CT} = \frac{P_{CT}}{Q_{ChW}} = \left(d_1 + \frac{d_2}{\Delta T_{App}}\right)(1+0.2843\xi_{CHLR}) \quad (29)$$

where ΔT_{App} is the actual CT approach temperature, which is obtained from the following formula:

$$\Delta T_{App} = T_{CT,CW,R} - T_{wb} \quad (30)$$

where $T_{CT,CW,R}$ is the CT leaving temperature, which should be higher than the ambient WB temperature. In addition, coefficients d_1 and d_2 are regressed from the trended data, and ΔT_{App} is maintained by sequencing the cooling towers or modulating fan speed.

3.6 Loop Side Simulation

As mentioned before, the loop side performance plays an important role in the ChW water storage tank operation. The parameters of most concern are the loop total cooling load, loop water return and supply delta-T (or loop average return temperature or total ChW flow rate), and SPMP head. The loop total cooling load is given in the control strategies simulation study but the cooling load prediction model is needed in the controller design.

3.6.1 Loop delta-T characteristics

The loop ChW delta-T is subject to many factors, such as chiller ChW leaving temperature, cooling coil air leaving temperature, type of flow control valves, coil design parameters and degrading due to fouling, tertiary connection types, coil cooling load, air economizers, etc. Moreover, there may be tens of buildings and hundreds of AHUs tied to the loop, and it is impossible to study all coils one by one to obtain the loop average return water temperature. However, it does not mean that nothing can be done with it. We can first get some hints from a typical profile of the loop delta-T.

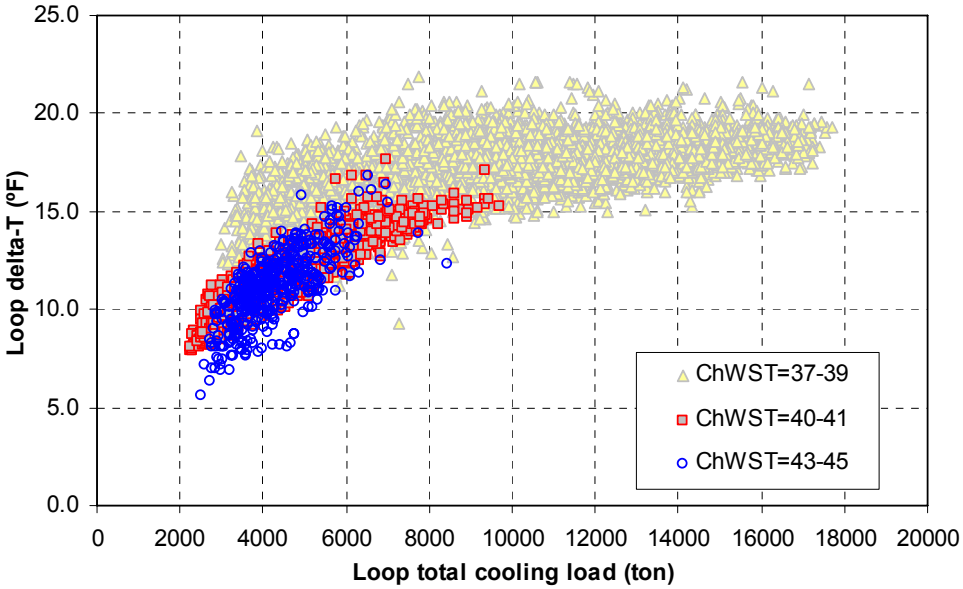

Figure 9 Loop DT as a function of the loop cooling load and supply temperature

Two quantifiable and measureable parameters are loop ChW supply temperature and loop total cooling load. Figure 9 shows a scatter plot of the loop delta-T as a function of these two parameters. A higher cooling load induces a higher delta-T while a higher ChW supply temperature leads to a lower delta-T. At the high load end, the delta-T approaches a steady value (in most cases, it is the coil design delta-T). When the ChW supply temperature is higher than 40 °F, there is no obvious difference in the delta-T.

The coil part load performance is one of the main contributors to the quick drop of the delta-T at the low cooling load end. The rising ChW supply temperature during the winter time is another one. When air side parameters are unchanged, increasing the coil ChW entering temperature results in a lower return temperature and an even higher loop ChW flow rate. During the swing season or winter season, the load of the coils in

the exterior zone of the building may drop to an extremely low level, leading to laminar flow in the water tubes and a low delta-T. The water film heat transfer resistance inside the tube is only a small portion of the overall air-to-water heat transfer resistance at the design flow rate, but as the water velocity falls, this resistance rises until, at laminar flow conditions, it accounts for almost 90% of the overall resistance (Taylor 2002). According to ARI Standard 410 (ARI 2001), for coils with smooth tubes, turbulent flow occurs when Re is higher than 10,000. But such a high number seldom occurs in a typical HVAC cooling coil. The laminar flow occurs when Re is less than 2,100. Contrary to conventional thinking, delta-T below the onset of a laminar flow increases rather than decreases. If an AHU is running under an economizer mode, the coil entering air temperature is low causing correspondingly low return water temperatures. As a result, low delta-T is a complex phenomenon, and it is hard to describe it with a simple formula.

3.6.2 Loop delta-T regression model

Considering the difficulties in developing a physical model to simulate the loop delta-T, a linear model regressed from the trended data is used in this study.

$$\Delta T_{Lp} = \sum_{i=1}^{n} h_i x_i + h_0 \tag{31}$$

$$V_{Lp,ChW} = \frac{24 Q_{Lp,ChW}}{\Delta T_{Lp}} \tag{32}$$

where x_i are the variables that could be the dominant factors of the loop delta-T model, such as ChW supply temperature, loop total cooling load, ambient DB and WB

temperature, hour of the day, weekday or weekends, and month. The air system side parameters, such as coil air leaving temperature, total air flow rate, coil design delta-T, and sensible load ratio, are not included due to the diversity or unpredictability.

A statistics program SAS is utilized to help select an appropriate set of regressors from the candidates. The model should perform satisfactorily but be simple enough. This compromise can be based on the adjusted R^2 or R^2_{adj}. Usually, the model that maximizes R^2_{adj} is considered to be a good candidate as the regression equation. Another criterion is the Cp statistics, which is a measure of the total mean square error for the regression model. A "best" regression equation either has a minimum Cp or a slightly larger Cp, which does not contain as much bias. An all-possible regression method is used and minimum RMSE and Cp evaluation criteria are used in conjunction with this procedure since the candidate pool is not too large. It can find the "best" regression equation, and is not distorted by dependencies among the regressors, as stepwise-type methods are (Montgomery and Runger 2002).

The Ordinary Least Squares (OLS) linear regression method is adopted to indentify the model coefficients from the trended data. To calculate the error of the calibrated model, the well-known coefficient of determination R^2 and Coefficient of Variation of the Root Mean Squared Error (CVRMSE) are introduced. An alternative definition is CV*. If CV and CV* indices differ appreciably for a particular model, this would reveal that the model may be inadequate at the extremities of the range of variation of the response variable (Jiang and Reddy 2003).

Sometimes, even if the model accurately fits the data on which it was trained (this type of evaluation is referred to as "internal predictive ability"), it may not necessarily be robust enough to guarantee accurate predictions under different sets of operating conditions. This is the major drawback in black box models, such as a regression model, but less so in physical models (Reddy and Andersen 2002a). The well-accepted approach to evaluate the "external predictive ability" of a model is to use a portion of the available data set for model calibration while the remaining data are used to evaluate the predictive accuracy. Two-thirds of the trended data are for model calibrations while the remainders are used for model evaluations.

The exact form of the regression model may vary for different projects. It could be necessary to build different models to accommodate air-conditioning system operation changes at different seasons. A constant delta-T can be used in a rough, first order simulation.

3.6.3 Loop DP setpoint

Figure 10 shows a general control method of a variable speed SPMP. If only one building is serviced, the user will be cooling coils. If several buildings are tied in on a loop, each building will be considered as an artificial coil and the Flow Control Valve (FCV) is removed. A PSV is necessary to avoid a vacuum at the highest point in the system.

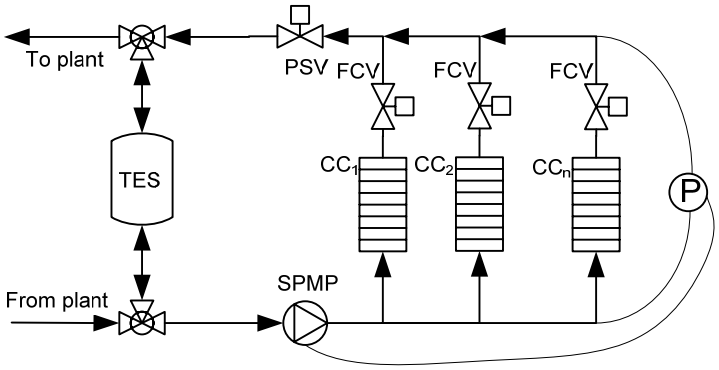

Figure 10 Principle of SPMP speed control

A DP sensor is installed at the loop hydraulic end (normally the farthest end) and the SPMPs are sequenced and the pump speed is modulated to maintain the predefined DP setpoint. Theoretically, the optimal DP is to maintain all discharge air temperatures with at least one control valve in a saturated (fully open) condition. In practice, such logic is rarely used. The reset schedule is defined for the DP setpoint according to the maximal design hydraulic head requirement for all users or operating experiences. As a result, a formula can be used to state the secondary pump head.

$$H_{SPMP} = DP_{Lp} + eV_{Lp,ChW}^2 \tag{33}$$

where e is the coefficient of a system hydraulic performance curve and $eV^2_{Lp,ChW}$ is the water pressure drop on the main supply and return pipes as well as in the tank. This coefficient can be derived from hydraulic calculations or regressed from trended historical data. It may vary with the flow distribution change among the coils. For the same total flow rate $V_{Lp,ChW}$, the more water flowing through the coil close to the pump, the lower this parameter is. For a typical system, this distribution is relatively stable and

its effect can be ignored. The number of SPMPs staged on can also contribute to the change of the coefficient when most of the SPMP head drop is attributed to the fittings before and after the SPMPs.

3.6.4 Loop side modeling

Figure 11 is the flow chart of modeling loop total flow rate as well as the plant chilled water return temperature. The outputs are the loop ChW flow demand and the plant ChW return temperature.

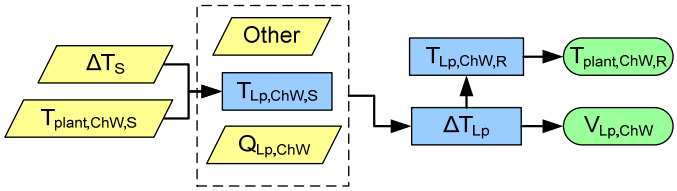

Figure 11 Flow chart of loop side modeling

3.7 TES Control Strategy Study

3.7.1 Control strategies design

According to the definition of a control strategy, it is essentially a tag given to a sequence of operating modes that covers a single cycle of the cool storage system. This cycle is one day in this study. The objective is to reduce the electricity consumption while avoiding prematurely depleting the tank. Different control strategies are defined in advance. The inputs of the sub-model are the combination of control strategy type and

chiller number limiting, while the output is the plant ChW total flow rate and staging of chillers.

To make full use of the TES system, a new control strategy will be proposed in this study. This strategy determines the number of chillers running and the ChW flow rate for each chiller in the next 24 hours right before the end of the last on-peak period. It treats summer season and winter season similarly. The following is the background of this new control strategy.

During the summer time, the on-peak energy and demand rates are much higher than off-peak rates. The diurnal WB temperature fluctuation is small and the benefits of running chillers during the low WB hours are small. To fully charge the tank before the start of the on-peak period, the plant cannot wait until after midnight when the ambient WB temperature is usually the lowest. Therefore, the high priority is to move the ChW production from the on-peak period to the off-peak period. The medium priority is to load the chiller at the optimal part load ratio. A low priority is to run the chiller during the low WB hours.

During the winter time, the utility rate activation of load shifting does not exist. The diurnal WB fluctuation could bring obvious improvements for chiller and tower total performance. This improvement is most effective during the swing season when chiller condenser water entering temperature can drop from 80-85 °F to 55-60 °F. As a result, the high priority is optimally loading the chillers and the medium priority is to run the chillers during the low wet-bulb hours to further improve the chiller performance.

3.7.2 Conventional control strategies

Generally speaking, conventional control strategies for a chilled water TES system can be divided into full storage, partial storage with chiller-priority, and partial storage with storage-priority. Demand limiting control can also be applied to the on-peak period or off-peak period or both to keep the total system electric demand from exceeding a predetermined facility demand limit.

The chiller-priority is easy to implement and does not require the cooling load forecast. For the storage-priority, an easily applied control is, during the on-peak period, the plant is operated as a constant flow while discharging the tank such that the tank is completely depleted at the end of the on-peak period. This is termed load-limiting storage priority control by Braun (1992). This tends to minimize the cooling plant peak electrical power use, and is nearly optimal in terms of energy costs with the presence of TOU electric rates.

For a TOU rate, the full storage control strategy can be stated as:

$$V_{Plant,ChW} = \begin{cases} V_{Plant,ChW,max} & x \le x_{max} \quad off-peak \\ V_{Lp,ChW} & x = x_{max} \quad off-peak \\ 0 & x \ge x_{min} \quad on-peak \end{cases} \tag{34}$$

The chiller-priority control can be stated as:

$$V_{Plant,ChW} = \begin{cases} V_{Plant,ChW,max} & x \le x_{max} \quad off-peak \\ V_{Lp,ChW} & x = x_{max} \quad off-peak \\ min\left(V_{Plant,ChW,max}, V_{Lp,ChW}\right) & x \ge x_{min} \quad on-peak \end{cases} \tag{35}$$

The storage-priority control strategy can be stated as:

$$V_{Plant,ChW} = \begin{cases} V_{Plant,ChW,max} & x \le x_{max} \quad off-peak \\ V_{Lp,ChW} & x = x_{max} \quad off-peak \\ \left[\sum_{on-peak} V_{Lp,ChW,k} - U_{Tank}\left(x_s - x_{min}\right) \right] \Big/ 60 t_{on-peak} & x \ge x_{min} \quad on-peak \end{cases} \tag{36}$$

where x_{max} is the charging cycle tank upper limit, x_{min} is the discharging cycle tank lower limit, x_s is the tank level at the beginning of the on-peak period, and $t_{on-peak}$ is the number of total on-peak hours. The tank can be charged until it is full ($x_{max} = 1$) or charged to the state-of-charge ($x_{max} < 1$) with which the cumulative load during the next on-peak period can be met. At the end of the on-peak period, the tank level should be higher than the predefined lower limit (x_{min}).

It is shown that, during the off-peak period, three control strategies have the same control logic. The chillers are running under maximal capacity before charging cycle is finished. When the tank is in an idle mode, the plant flow rate follows the loop demand and the chiller load could be between maximal and minimal load ratio. During the on-peak period, the full storage avoids running chillers while the chiller-priority makes full use of chiller capacity.

In short, conventional control strategies only make use of the load shifting function of the TES system and neglect the function of optimally loading chillers and running chillers during low WB hours. During the winter time when the demand rates (penalties) do not exist, the TES could cost more money considering the pumping energy and tank energy losses. That is why it is recommended the TES tank be shut down during the winter time for some facilities.

3.7.3 New operating strategy

To make full use of the TES system, a new control strategy is proposed in this study. This strategy determines the number of chillers running and the ChW flow rate for each chiller in the next 24 hours right before the end of the last on-peak period. To distinguish this new strategy from others, it is called optimal control strategy.

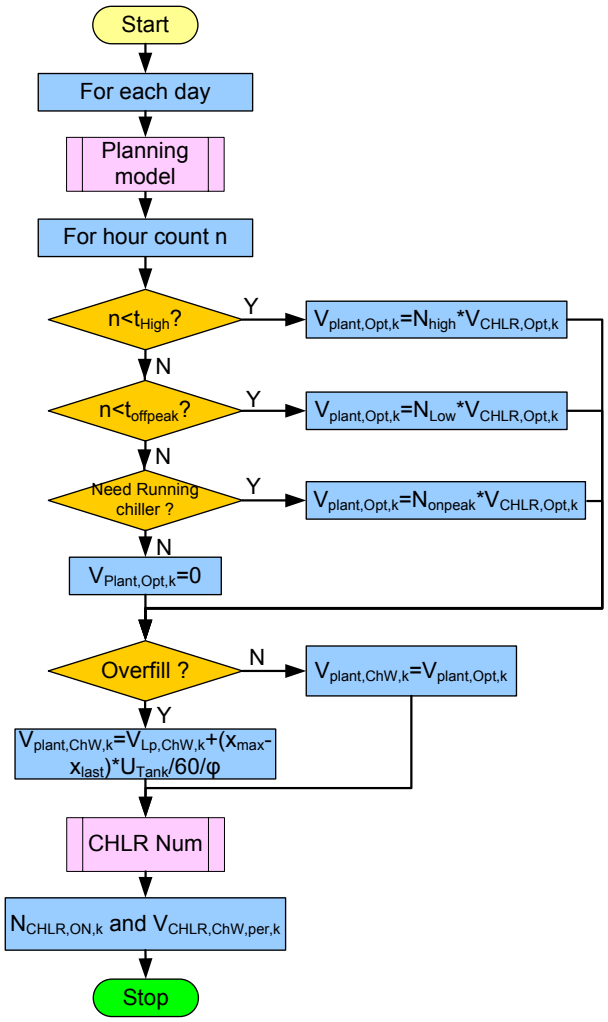

Figure 12 Flow chart of a new control strategy algorithm

Figure 12 shows the algorithm of the new control strategy. Two subroutines are involved in the flow chart. The Planning Model provides the number profile of chillers running during the next cycle. The Chiller Num calculates the real on-stage chiller number as well as the ChW flow rate per chiller.

It is noted that "optimal" does not mean the globally best option but rather means the best one among the options available. During the winter months when there is no definition for on-peak period in the utility rate structure, the high WB hours in a day can be artificially defined as the on-peak period and the possibility of running chillers during this period should be reduced.

Based on the loop total ChW flow demand in the next 24 hours ($U_{Plant,ChW,Daily}$), the Planning Model shown in Figure 13 calculates the necessary running chiller number N_{Low} and N_{High} as well as the corresponding duration (CT_{Low} and CT_{High}). The daily average optimal chiller flow ($V_{CHLR,Opt,avg}$) is used to calculate the sum of the running chiller numbers in each hour during the off-peak period (N_{Tot}). The average number of the chillers running during the off-peak period is N_{Avg}.

$$U_{Plant,ChW,Daily} = U_{Lp,ChW,Daily} + U_{Tank} \times \left(x_{\min} - x_{init}\right) \tag{37}$$

$$N_{Tot} = Roundup(U_{plant,ChW,Daily} / 60 / V_{CHLR,Opt,avg}, 0)$$

$$N_{Avg} = N_{Tot} / t_{off-peak}$$

$$N_{Low} = min(Rounddown(N_{avg}, 0), N_{off-peak})$$

$$N_{High} = max(Roundup(N_{avg}, 0), N_{off-peak})$$

$$CT_{Low} = min((1 + N_{Low}) \times t_{offpeak} - N_{Tot}, t_{of-fpeak})$$

$$CT_{High} = min(N_{Tot} - N_{Low} \times t_{offpeak}, t_{off-peak})$$

As a result, during the off-peak period, N_{High} chillers will run for CT_{High} hours, and then N_{Low} chillers will run for CT_{Low} hours.

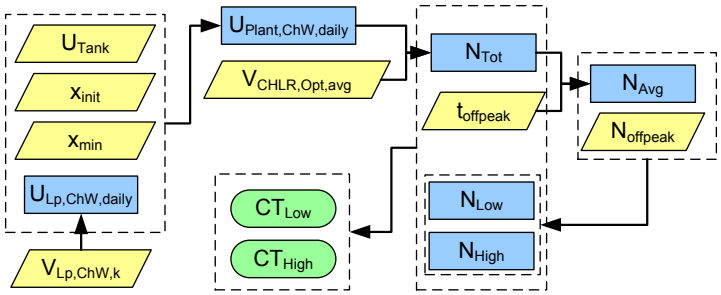

Figure 13 Flow chart of planning model during the summer time

The function of the CHLR Num subroutine is to determine the actual on-stage chiller number and the ChW flow rate per chiller. The inputs are the plant total ChW flow rate and the chiller optimal or maximal cooling load. The maximal and minimal ChW flow rate in evaporators and the maximal numbers of chillers staged on are taken into account in calculating the practical number of chillers staged on.

3.8 Implementation of Control Strategies

3.8.1 Procedure of implementation

The procedure of implementing the optimal operating strategy can be found in Figure 14. First of all, the historical data, such as profiles of loop cooling load and

weather conditions, are prepared as the simulation baseline conditions. The utility rate structure and system information are summarized to build the rate model, plant model, TES model, loop model, non-plant power model, and chiller model. The complexity of the models is dependent on the availability of the information and the precision requirements. Different control strategies can be added to realize specific purposes. The plant variables to be optimized are selected according to system controls. After that, the program is run to determine the monthly operating strategies and optimal setpoints.

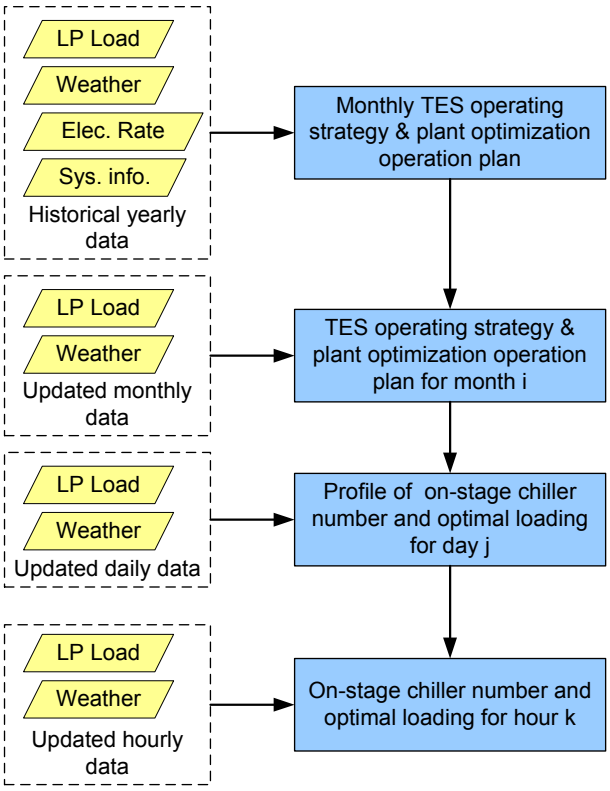

Figure 14 Flow chart of optimal operating strategy implementation

For each month i, the predictions of loop load and weather conditions will be updated based on the prediction deviations in previous months and rerun the updated operating strategy. The optimal plant setpoints can also be adjusted if necessary. For each day j, right before the start of the off-peak period, the control strategy will generate a profile of on-stage chiller number and optimal loading for the next 24 hours. The loop cooling load and weather conditions are updated from the model and weather service, which should be much more accurate than monthly predictions. For each hour k, the load and weather can be further updated and the on-stage chiller number and optimal loading can be adjusted accordingly.

3.8.2 Chiller control logic

As there is no control device on the tank, the control logic is, in fact, the logic of the chiller sequencing and modulating. Figure 15 shows the flow chart of the chiller on-stage number and flow rate setpoint determination. For each time step (for example 5 minutes), the chiller optimal load ratio is updated based on measured actual chiller ChW leaving temperature, CW entering temperature, and CW flow rate. It is compared with the current chiller load calculated from the current chiller ChW flow rate. If the difference is within a predefined low limit, the ChW flow is kept unchanged. Otherwise, a new flow rate setpoint is calculated and the chiller ChW flow rate is modulated to maintain the setpoint. The hourly on-stage chiller number follows the output of the control strategy.

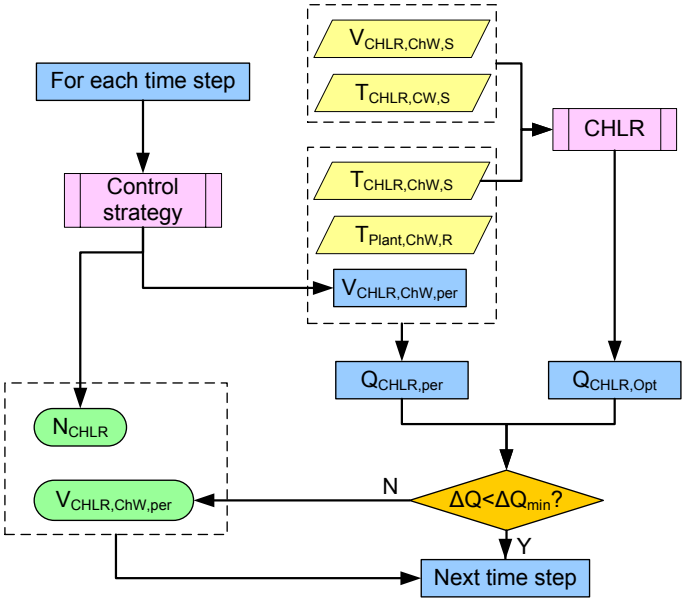

Figure 15 Chiller sequencing and flow control logic

In practice, the ChWLT and CWET can affect the chiller optimal flow rate, but such effects are small. The optimal ChW flow rate is mainly subject to the fluctuation of plant delta-T. The change rate of plant delta-T is slow, in the order of 0.5°F per hour. Therefore, under most conditions, it is acceptable to adjust the chiller flow rate every 5-10 minutes. Such an adjustment is a feed-forward control and will not lead to oscillations.

If the tank is fully charged before the start of the on-peak period, the plant enters the match operating mode. The total chilled water flow rate will be controlled by maintaining zero charging or discharging flow in the tank.

3.8.3 Weather and load predictions

For each day right after the end of the on-peak period, the controller will determine the profile of the on-stage chiller number and each chiller ChW flow rate in the next 24 hours based on the predicted weather conditions, loop cooling load and loop delta-T.

Different prediction approaches or information sources provide different degrees of accuracy for a specific project. For example, the cooling load prediction models range from the very simple (such as, unbiased random walk model) through the less simple (such as, bin predictor, multiple regression models, and harmonic models) to the complex (such as, autoregressive neural network). Due to its greater complexity and additional input variables, one might expect the neural network to outperform the simpler models (Henze 1995). Some websites (such as www.weather.com) provide local hour-by-hour or 15 min weather service. They can also provide severe weather alerts, such as a heat wave or a freezing rain. All these can be a good source of weather forecasting.

The decision of model and source selection is up to the controller designer but the reliability of the controller could be different. A more precise model can enhance the robustness of the control strategy and reduce the risk of loss of cooling.

3.9 Uncertainty Analysis

The simulation results are based on the assumption of perfect knowledge of the system. In practice, the validation of the conclusions needs to be investigated due to all

kinds of disturbances and errors coming from operating conditions prediction, improper model parameters, and model identifications. The purpose of uncertainty analysis is to study the robustness of the identified optimal operating strategy when subject to various sources of uncertainties and evaluate the relative importance of different sources of uncertainties (this is called a sensitivity study). It is also used to evaluate the trade-off between savings and increased probability of prematurely depleting the tank (this is called a risk study).

Basically, there are three distinct phases when developing schemes for the uncertainty analysis: definition of various sources of uncertainties, statistical methods for simulating their effects, and analysis of results in terms of different risk attitudes (low or high risk) (Jiang 2005).

3.9.1 Uncertainty source

The uncertainty sources can be divided into three types (Jiang 2005):

(1) Model-inherent uncertainty, such as imperfect plant component models or plant parameters and imperfect regression fit in model calibrations. Any mathematical model can only reduce but not eliminate the differences between simulated and actual performance. An error can also occur from the regression fit when the data points used to identify the model coefficients do not cover the whole operating region of the equipment. Severe deviations could occur when extrapolation is used.

(2) Process-inherent uncertainty, such as ChWLT deviation from the setpoint due to the dead-band or system error of the controller. A dead-band is needed in a feedback controller to avoid oscillations. Actuator constraints, un-modeled dynamic system

behavior, nonlinearities (such as valve sticking), and environmental disturbances can also bring about imperfect deviations and uncertainties (Ma, Chung, et al. 1999). Based on the typical actuator constraints for these two variables, we would expect the accuracy of the temperature control to be in the range of 0.5-1.5 °C and 2-5% of RPM for accuracy of the fan speed control.

(3) External prediction uncertainty, such as loop ChW load and delta-T predictions, non-ChW production electricity consumption, and weather condition forecasting. Such information is needed in daily plant planning.

3.9.2 Uncertainty definition

The variations and disturbances in a model can be dealt with by adding an error term in the model. A general form of a multivariable Ordinary Least Squares (OLS) regression model with one response variable y and p regressor variables x can be expressed as (Reddy and Andersen 2002a):

$$y = x_{(1,p)}\beta_{(p,1)} + \varepsilon(0,\sigma_y^2) \tag{38}$$

The random error term ε is assumed to have a normal distribution with variance σ^2 (square of the model Root Mean Square (RMS)) and no bias (zero mean). It can be expressed as the sum of the errors of each regressor.

$$\varepsilon(0,\sigma_y^2) = \varepsilon_{x_1}(0,\sigma_{x_1}^2) + \varepsilon_{x_2}(0,\sigma_{x_2}^2) + ... + \varepsilon_{x_p}(0,\sigma_{x_p}^2) \tag{39}$$

$$\sigma_{y_1}^2 = \sigma_{x_1}^2 + \sigma_{x_2}^2 + ... + \sigma_{x_p}^2 \tag{40}$$

For the optimal control strategy, the main input is the daily total ChW volume demand ($U_{Lp,ChW,Daily}$), which is equal to the sum of hourly ChW flow demand in the

next 24 hours. If it is assumed that the loop total load and loop delta-T are independent and have a normal distribution and zero mean, their ratio is a Cauchy distribution. But in practice, they are correlated and their means are not zero. Their ratio becomes even more complicated. Here it is assumed that the hourly ChW flow rates ($V_{Lp,ChW,k}$) are not correlated, and their error is a normal distribution.

$$V_{Lp,ChW,k} = f_k(x_1, x_2, ...) + \varepsilon(0, {\sigma_{Lp,ChW,k}}^2) \tag{41}$$

The daily total loop ChW volume demand will be in the following form:

$$U_{Lp,ChW,tot} = 60 \times \left(\sum_{k=0}^{23} f_k(x_1, x_2, ...) + \varepsilon(0, \sum_{k=0}^{23} {\sigma_{Lp,ChW,k}}^2) \right) \tag{42}$$

If the variances of hourly ChW flow rates ($\sigma_{Lp,ChW,k}$) are assumed equal, the variance of $U_{Lp,ChW,tot}$ will be $86400\,{\sigma_{Lp,ChW}}^2$ or $\sigma_{U_{Lp,ChW,tot}} = \sqrt{86400}\sigma_{Lp,ChW}$. A 100(1-α)% confidence interval formula for this normal distribution is given by:

$$\sum_{k=0}^{23} f_k(x_1, x_2, ...) \pm Z_{\alpha/2}\sigma_{U_{Lp,ChW,tot}} \tag{43}$$

Some of the popular values of Z_α are shown in Table 3.

Table 3 Table of confidence interval for a normal distribution

α	0.1	0.05	0.025	0.01	0.005	0.001
Z_α	1.282	1.645	1.96	2.326	2.576	3.09

Therefore, there is a 100(1-α)% chance that the tank will not be depleted if the following inequality is valid:

$$U_{\tan k} x_{\min} \geq Z_{\alpha/2} \sigma_{U_{Lp,ChW,tot}} = Z_{\alpha/2} \sqrt{86400} \sigma_{Lp,ChW} \quad (44)$$

A higher confidence interval (a smaller α) leads to a higher $Z_{\alpha/2}$ and a higher $x_{\min}$. This is consistent with observations. This inequality can be used to estimate the tank water level lower limit according to the RMSE of ChW flow rate predictions.

3.9.3 Sensitivity analysis

Conventional methods for sensitivity analysis and uncertainty propagation can be classified into four categories: sensitivity testing, analytical methods, sampling based methods, and computer algebra based methods. Sensitivity testing involves studying model response for a set of changes in the model formulation, and for a selected model parameter combination. Analytical methods involve either the differentiation of model equations and subsequent solution of a set of auxiliary sensitivity equations, or the reformulation of the original model using stochastic algebraic or differential equations. On the other hand, the sampling based methods involve running the original model for a set of input and parameter combinations (sample points) and estimating the sensitivity and uncertainty using the model outputs at those points. Yet another sensitivity analysis method is based on direct manipulation of the computer code of the model, and is termed automatic differentiation (Isukapalli 1999).

Sensitivity testing is often used to evaluate the robustness of the model, by testing whether the model response changes significantly in relation to changes in model

parameters and structural formulation of the model. The application of this approach is straightforward, and it has been widely employed. The primary advantage of this approach is that it accommodates both qualitative and quantitative information regarding variation in the model. However, the main disadvantage of this approach is that detailed information about the uncertainties is difficult to obtain using this approach. Further, the sensitivity information obtained depends to a great extent on the choice of the sample points, especially when only a small number of simulations can be performed.

In this study, inputs are subject to all kinds of uncertainties. A sensitivity testing can be performed to filter the factors which are the most critical to the optimization objective function. A more accurate model or more realistic values can be applied to reduce the uncertainty of the simulation results. The effect of external prediction model uncertainty (such as cooling load, weather, and delta-T) can also be tested by this method.

3.9.4 Risk analysis

The utility billing cost is the most essential but not the only factor in decision-making for operators. Lowering the risk of prematurely depleting the tank by running additional chillers than those projected should also be emphasized. Maximizing the savings and minimizing risk exposure are two conflicting objectives. Therefore, it should be based on the same risk level when comparing the operating cost of different operating strategies.

In this methodology, all operating strategies are compared based on the same tank level minimal limit (x_{min}). A lower limit can increase the effective tank cooling storage capacity and reduce operating cost but results in a higher risk. The decision maker may adjust this value to accommodate different risk attitudes. This value can also be reset month by month. For example, during the summer months when the penalty is high for running additional chillers, a higher limit can be selected to prepare for an unexpected heat wave. During the winter months when the plant demand peak is much less than the peak set in summer, running additional chillers has little penalty. It is more cost-effective to lower the limit so as to reduce heat loss through the tank wall.

To test the robustness of the selected optimal operating strategy, some scenarios can be designed by scaling up or down cooling load or delta-T. They are used to test if the superiority of operating strategies changes significantly or if there is a risk of prematurely depleting the tank. It can also test if the savings of the selected operating strategy shrink or expand remarkably.

4. APPLICATIONS

Two practical applications of this methodology are introduced in this section. The first one is an existing TES system with a state-of-the-art control and metering system at the DFW International Airport Energy Plaza. The optimal operating strategies are determined by comparing different scenarios to achieve significant utility billing cost savings. A plant optimization procedure is performed for the optimal control strategy to further improve the plant performance.

The other case study is an old chilled water system without thermal storage located within the Capital Complex in Austin and operated by the Texas Facilities Commission (TFC). It consists of four independent chilled water plants, which serve nineteen buildings. TFC proposed an energy retrofit project to construct a TES system and connect the four plants into one ChW loop intended to substantially reduce the state's utility billing cost of plants. The purpose of the study is to perform an economic assessment on this proposed energy retrofit project and determine an optimal tank size. This problem can be solved with a simplified plant and loop model. The simple payback periods with different tank sizes are presented when all known costs are considered, and an optimal tank size is recommended.

4.1 DFW: System Introduction

4.1.1 System configuration

This system is located in the Dallas-Fort Worth (DFW) metropolitan area, and it is a central utility plant serving the DFW International Airport. The Energy Plaza (EP) consists of six steam boilers with a total capacity of 260,300 pounds per hour, six 5,500 ton constant-speed centrifugal chillers, called OM chillers, one 90,000 ton-hr naturally stratified ChW storage tank, five 1,350 ton glycol-solution chillers, called PCA chillers, and eight two-speed cooling towers. This plant is designed with six 150 hp constant speed primary pumps and four 450 hp variable-speed secondary pumps. This study only deals with the ChW system. The heating hot water system and glycol system are treated in the non-plant part. The chilled water produced in the EP is distributed to eight "vaults" beneath each terminal through underground piping in tunnels. The chilled water is then branched off to the end users. Figure 16 shows a schematic diagram of this chilled water system.

The EP condenser water system consists of eight identical cooling towers, each of which is equipped with a 150 hp two-speed fan and a 400 hp CW pump. These eight cooling towers are divided into two groups. Each group has four cooling towers located on one side of the EP, i.e. east and west, with a separate basin. The CW pumps are automatically staged on or off to provide condenser water for all running OM and PCA chillers. Figure 17 is a simplified diagram of the EP CW system. In order to keep water surfaces in the two basins at the same level, a basin equalizer with an automatic control valve is installed.

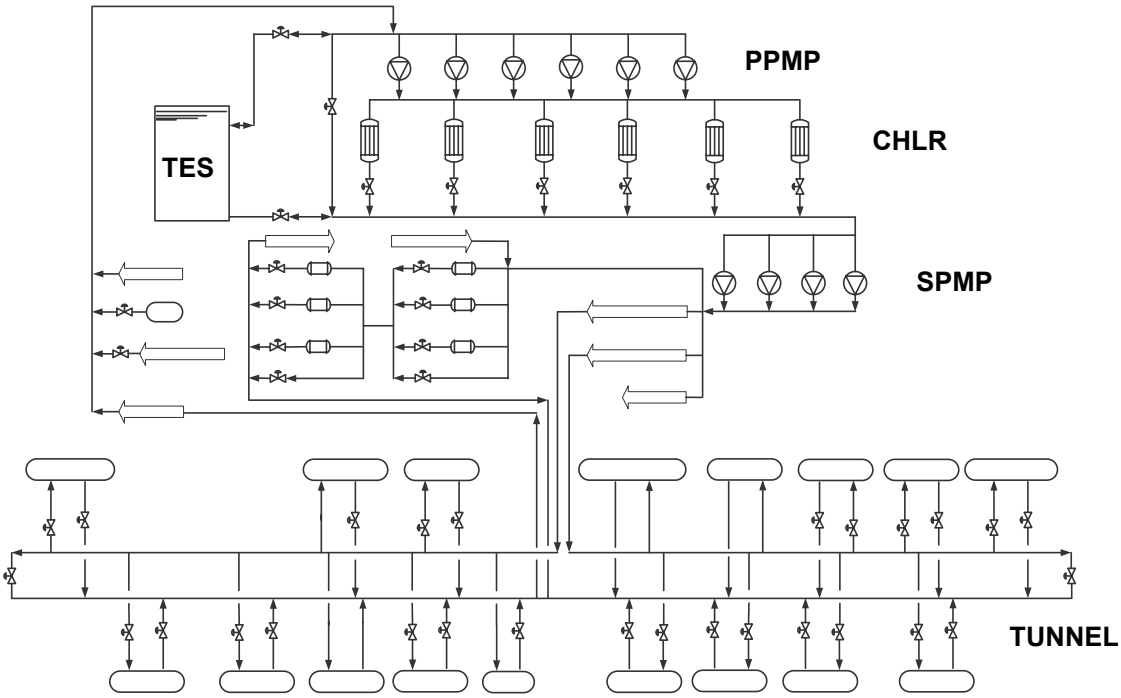

Figure 16 Schematic diagram of the ChW system

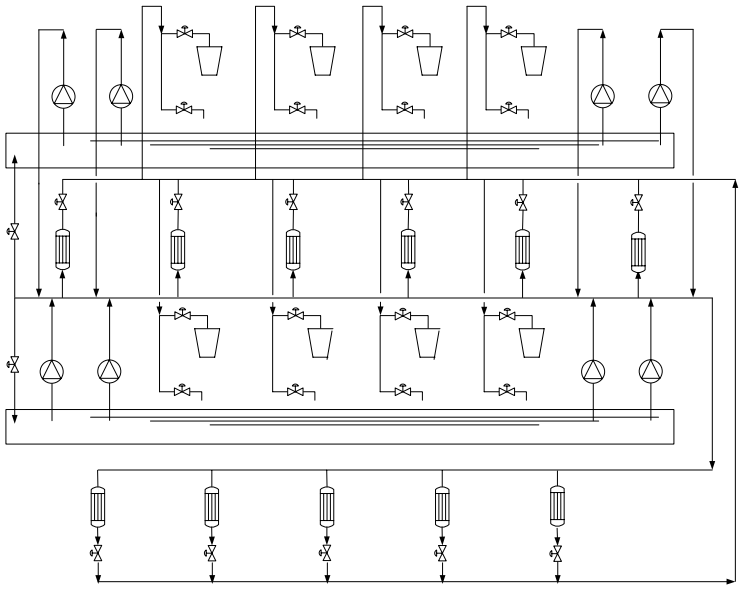

Figure 17 Schematic diagram of the CW system

A naturally stratified, column-shape, ChW storage tank is erected between the PPMP suction side header and the chiller discharge side header. It is 138 ft in diameter and 57 ft in height. Since the TES tank was installed and is used as the "expansion tank," the existing expansion tank has been disabled. The top of the TES tank is open to the atmosphere and the tank level is maintained at 54.3 - 54.9 feet. The design cooling storage capacity is 90,000 ton-hr when the chilled water supply temperature is 36 °F and the return temperature is 60 °F. The effective storage volume is around 5,400,000 gallons.

The direct digital control (DDC) system utilized on site is Emerson Process Management's Delta-V digital automation system. All the chillers, boilers, heat exchangers, cooling towers, TES tank, various pumps, and automatic control valves are monitored and controlled by this system. It also monitors and controls the chilled water, steam, hot water, and PCA distribution systems in the tunnel and some of the air-handler units in the EP and the terminals.

4.1.2 Electricity rate structure

The monthly electricity billing cost consists of a meter charge, current month non-coincident peak (NCP) demand charge, four coincident peak (4CP) demand charge, and energy consumption charge. The total monthly electricity billing charge (C_{Total}) is:

$$C_{Total} = C_{delivery\_point} + R_{4CP} D_{4CP} + R_{NCP} D_{NCP} + R_{energy} E_{consumption} \quad (45)$$

The rates R_{4CP}, R_{NCP}, and R_{energy} for each month are subject to minor adjustments, and rates from March 2007 to February 2008 are used in the simulation.

The meter charge $C_{delivery\_point}$ is constant for each month. All demand kWs used have been adjusted to 95% power factor. The monthly average power factors during this period will be used in the power factor correction.

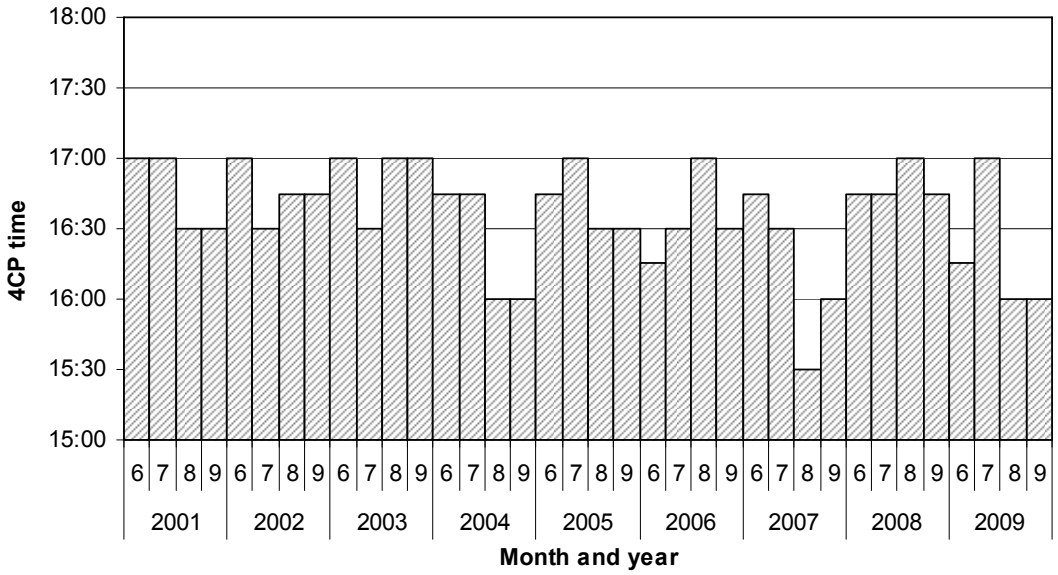

Figure 18 The 4CP time recorded by the ERCOT in the last nine years

The 4CP demand kW is the average of the plant's integrated 15 minute demands at the time of the monthly Electric Reliability Council of Texas (ERCOT) system 15 minute peak demand for the months of June, July, August and September (called summer months) of the previous calendar year. The exact time will be announced by ERCOT. The plant's average 4CP demand will be updated effective on January 1 of each calendar year and remain fixed throughout the calendar year. It is impossible to precisely predict the time of the ERCOT system 15 minute peak demand. There is no

definition on the period of the 4CP demand. However, based on analyzing the historic 4CP events shown in Figure 18 (Data come from www.ERCOT.com), it is found that the 4CP event always occurs between 15:30 and 17:00 on week days. Half hour and one hour allowances are made before and after this period to avoid hitting the 4CP peak time. Therefore, in this study, the highest kWs during 15:00 to 18:00 in the summer months are used to calculate the 4CP demand.

The NCP kW applicable shall be the kW supplied during the 15 minute period of maximum use during the billing month. The current month NCP demand kW shall be the higher of the NCP kW for the current billing month or 80% of the highest monthly NCP kW established in the eleven months preceding the current billing month.

For this facility, everyday including weekends and holidays is treated as a working day. The 4CP demand can be regarded as on-peak demand while NCP demand is the all day demand.

When it comes to calculating electricity billing cost savings for each operating strategy, the scenario without TES is used as a baseline. Since there is no special thermal energy storage rate structure in Texas's deregulated electricity market, the same rate structure will be applied in calculating the baseline cost.

When calculating the current month utility billing cost, it is necessary to determine the plant's 4CP demand and the highest monthly NCP kW established in the previous eleven months. Consequently, a preliminary run of the program will be conducted to find these two numbers for each control strategy.

4.1.3 Current system operation

At present, the chillers and TES tank are manually operated and at most four OM chillers are allowed to run when EP operators are charging the TES tank. EP operators have been trying to charge and discharge the TES tank according to a predetermined schedule to minimize demand related charges.

Figure 19 shows the electricity consumption daily profiles on four consecutive summer days. The demand kWs have been converted to 95% power factor. During the charging period, the maximal number of chillers running was four. From 18:00 - 18:30, OM chillers were staged on gradually to fully charge the tank and provide cooling to the loop side. One chiller was staged off at around 6:30. The tank entered the match mode when the tank level reached a predetermined height. Around 15:00 or 15:30, all OM chillers were staged off and the TES tank took over the cooling load. The charged NCP demand exceeded 23,000 kW in the summer months. The power for each OM chiller and associated pumps and cooling towers is around 4,400 kW at full load. When all OM chillers are off, the plant demand drops to around 3,600 kW in the summer months, which is the baseline demand contributed by the PCA chillers, secondary pumps, plant HVAC, lighting, boilers, etc.

Figure 20 is an illustration of the tank charging and discharging on a summer day (08/12/2007). As the EP operators did not follow a strict time schedule to stage off and stage on chillers, three chillers were still running at 15:00. All chillers were staged of at 15:30 and one chiller was brought on at 19:00. Figure 19 and Figure 20 reflect the typical operation of the TES system on a summer day.

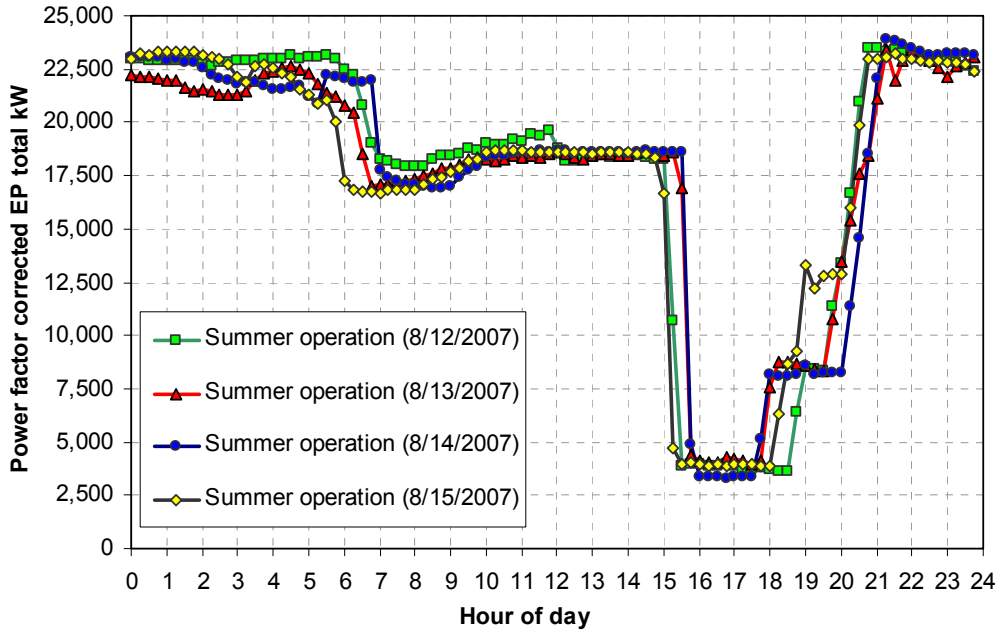

Figure 19 **Power factor corrected EP total kW profiles on selected summer days**

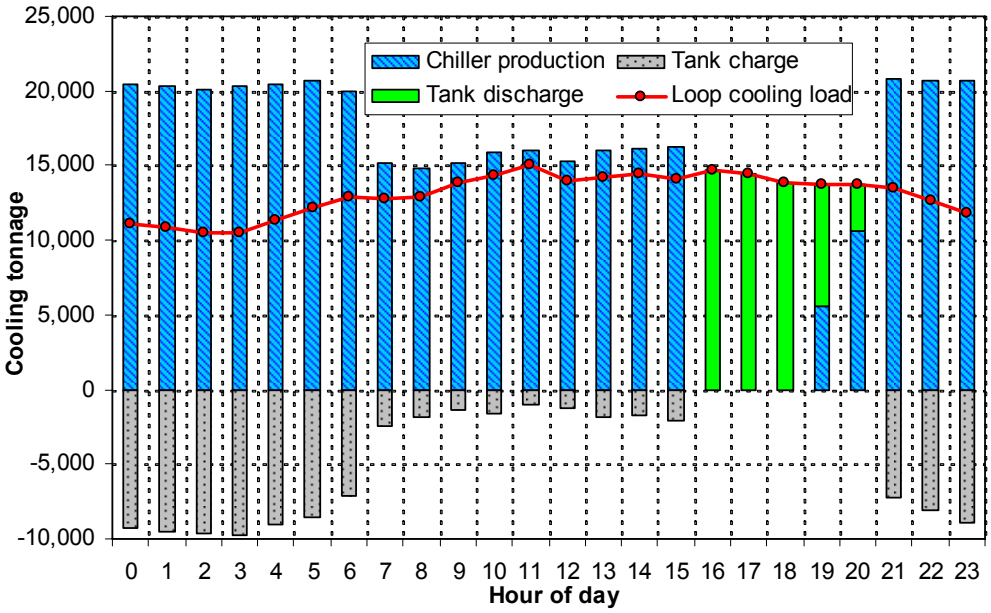

Figure 20 **OM chiller and TES tank charge/discharge operation on a summer day**

Table 4 shows the calculation of the 4CP demand for the 2008 calendar year. The metered demand kWs are corrected to 95% power factor before calculating the average of the four coincident peaks. On August 13, 2007, a 4CP peak demand of 16,904 kW was hit by the EP on 15:30, which led to a 3,664 kW increase in the 4CP demand kW in 2008 compared with the 4CP demand in 2007. If the coincident peak in August was assumed to be 3,800 kW, the 4CP demand kW in 2008 would be 3,850 kW, which is 3,276 kW lower than the current value of 7,126 kW. If the annual average transition charge rate is $2.00/kW, the plant would have paid $78,624 more in 2008 due to this high 4CP value.

Table 4 4CP demand calculation for 2008 calendar year

Year	Month	4CP time	Week day	Power (kW)	Power factor	kW after correction
2007	June	6/19/2007 16:45	2	3,347	84.5%	3,762
	July	7/12/2007 16:30	4	3,427	84.9%	3,835
	August	8/13/2007 15:30	1	15,160	85.2%	16,904
	September	9/7/2007 16:00	5	3,571	84.8%	4,001
				Average (4CP demand kW in 2008)		7,126

The charging start time was determined by operators according to their experiences and judgment. No predefined operating strategy was followed for TES operations, except that the TES was to be used during the 4CP period, and the TES was full prior to the start of the discharging period. When EP operators charged the TES tank over night, they tended to fully load all four OM chillers, so that they could fully charge

the TES tank as quickly as possible. The operating strategy in the summer months is to minimize the EP monthly electricity billing cost by avoiding OM chillers running during the on-peak hours. During the off-peak period, the maximum number of chillers running is no larger than four to limit the plant NCP demand.

The chiller chilled water leaving temperature setpoint is manually set at 36 ºF and is fixed all year round. The ChW flow through the chiller evaporator is controlled by modulating flow control valves on the leaving side of the evaporator. The ChW flow rate setpoint can be manually overridden, so that the TES tank could be charged faster. The sequencing of the constant speed PPMPs is dedicated to the corresponding chillers. The VFD speed of the SPMPs is modulated to maintain the average of differential pressures at the loop ends in the tunnels at a given setpoint. This setpoint is manually adjusted to be between 25 psid and 48 psid all year round to ensure there are no hot complaints from terminals.

The cooling tower staging control in place is a very complicated algorithm. The existing control intends to stage the number of fans and select high and low speed of fans to minimize the chiller compressor electricity consumption. Six stages are defined in the controllers. The CW pumps are automatically sequenced to provide CW for the OM chillers and the PCA chillers. In order to maintain the CW flow set point through the condensers of the PCA chillers, the number of CW pumps in operation is always one more than the number of OM chillers in operation.

4.2 DFW: System Modeling

4.2.1 System power

The trended historical data from March 1, 2007 to February 29, 2008 are used for system modeling and TES operating strategies simulations. The electricity consumed by OM chillers, CT fans, CW pumps, PPMPs and SPMPs is considered as plant chilled water electricity load while all other electricity consumptions are non-plant electricity loads. According to trended historical data, 84.2% of EP total electricity consumption is contributed to the chilled water system, 8.4% is consumed by the PCA system, and 7.4% is consumed by miscellaneous equipment, such as EP air-conditioning, air compressors, lighting, and plug loads. Therefore, the power consumed by the plant covers the majority of the total EP power consumption.

$$P_{sys} = P_{plant} + P_{non-plant} \tag{46}$$

$$P_{plant} = P_{CHLR} + P_{CT} + P_{CWP} + P_{PPMP} + P_{SPMP} \tag{47}$$

Figure 21 shows the monthly profiles of billed and simulated EP electricity consumption. The billed profile is from EP monthly utility bills, and the simulated profile comes from the simulation results of the full storage scenario. A good match is found although some differences exist in several months. This could be attributed to imperfection of models, inaccurate parameter inputs, or operations different from actual situations. The purpose of the baseline scenario is not to mimic the actual situation but to provide a cost baseline for economic study on other optional scenarios. The present system power model can reasonably predict the monthly electricity consumption.

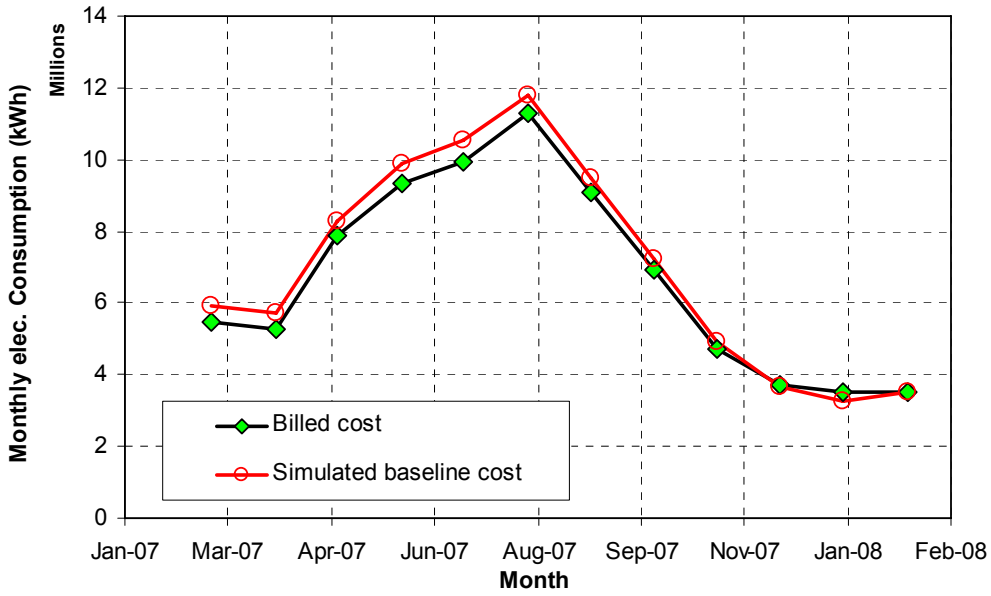

Figure 21 Profiles of billed and simulated EP monthly electricity consumption

Table 5 Parameters of TES system loop side

Loop Hydraulic	LP end DP upper setpoint	DP_h	28.0	psid
	LP end DP lower setpoint	DP_l	22.0	psid
	LP end DP upper shift flow	V_{upper}	16,000	GPM
	LP end DP lower shift flow	V_{lower}	10,000	GPM
	LP hydraulic coef.1	e_1	1.00E-07	
	LP hydraulic coef.2	e_2	5.00E-08	
	LP hydraulic coef.3	e_3	3.00E-08	
	LP load factor	f_{load}	1.00	
Loop DT	LP supply temperature rise	ΔT_s	1.0	ºF
	LP DT coef.0	h_0	32.1898	
	LP DT coef.1 ($T_{LP,ChW,S}$)	h_1	-0.5439	
	LP DT coef.2 ($Q_{LP,ChW}$)	h_2	6.86E-05	
	LP DT coef.3 (T_{wb})	h_3	6.34E-02	
	LP max DT	$\Delta T_{Lp,max}$	22.0	ºF
	LP min DT	$\Delta T_{Lp,min}$	12.0	ºF
	LP DT system error	$\Delta T_{Lp,error}$	0.0	ºF

4.2.2 Loop side modeling

The parameters and inputs for the TES system loop side are shown in

Table 5. The upper and lower limits of the loop end DP as well as the loop flow rate change points are subject to hydraulic requirements and operating experiences. If the loop total ChW flow rate is equal to or lower than 10,000 GPM, the DP setpoint is 22.0 psid. If the rate is equal to or higher than 16,000 GPM, the DP setpoint is 28.0 psid. The ChW secondary DP setpoint be reset linearly from 22 psi to 28 psi, when the secondary ChW flow is between 10,000 GPM and 16,000 GPM. Three hydraulic coefficients are regressed from trended data corresponding to one, two, or three SPMPs running scenarios. These coefficients are used to calculate the hydraulic differential pressure drop on the pipes between the SPMPS and the tunnel end of loop. A loop load factor is defined to test the reliability of operating strategies when the actual load profile is different from the one used in the simulation.

A temperature rise exists between the loop supply temperature and the chiller chilled water leaving temperature, which is due to tank heat losses, pumping heat gain, and piping heat losses. Figure 22 shows an annual profile of the trended temperature rise, which fluctuates between 0.0 ºF and 2.0 ºF most of time. The temperature rise higher than 4.0 º in the last three months is due to chiller ChW leaving temperature reset tests. When these points are excluded, the annual average temperature rise is 1.0 ºF. For purposes of this simulation, these points are excluded, because they represent results of commissioning studies implemented by the Energy Systems Laboratory.

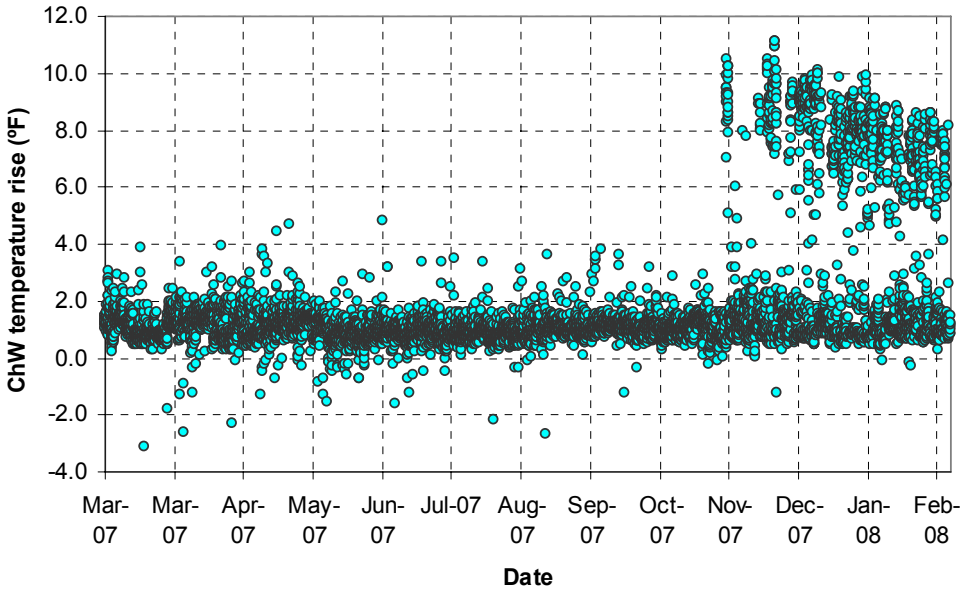

Figure 22 ChW temperature rise before and after the TES tank

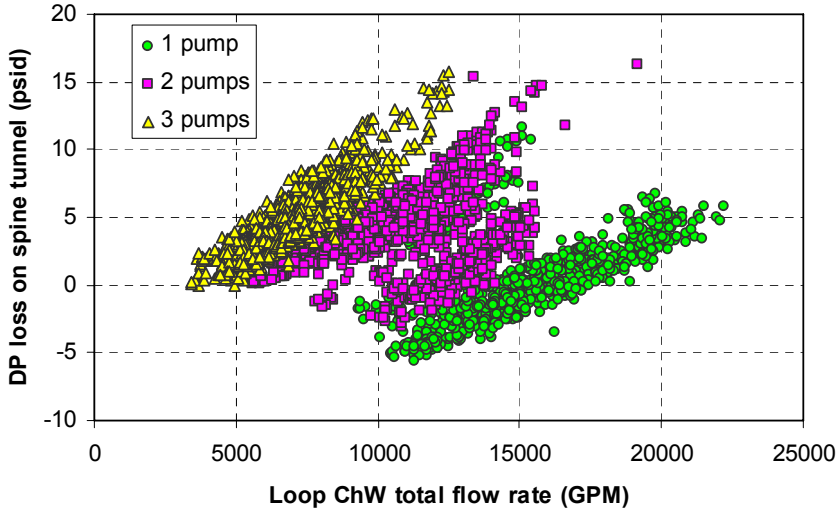

Figure 23 DP losses on spine tunnel piping as a function of total ChW flow rate

When the tunnel end DP setpoints are determined, a loop hydraulic coefficient is required to calculate the differential pressure before and after the SPMPs. This coefficient can be regressed from a plot of tunnel piping DP losses versus tunnel total flow rate, which is shown in Figure 23. It is shown that three groups of points are displayed, which are corresponding to one, two, and three pumps running. A negative DP loss could be explained by the inaccuracy of pressure sensors. Three different coefficients can be regressed from those three groups of points.

$$H_{loss} = eV^2{}_{Lp\_ChW} \tag{48}$$

Equation (49) is a linear regression model developed to simulate the loop delta-T as a function of ChW loop supply temperature (x_1), loop total cooling load (x_2), and ambient WB temperature (x_3). A higher loop supply temperature, a lower WB temperature, and a lower loop total ChW load lead to a lower loop delta-T, which is consistent with the observations. An upper and a lower limit are defined to avoid unreasonable regression results when an extrapolation is applied. The system error of the loop delta-T can be used to check the effect of loop delta-T prediction deviations on the system total energy and costs.

$$\Delta T_{Lp} = h_0 + h_1 x_1 + h_2 x_2 + h_3 x_3 \tag{49}$$

Figure 24 is a comparison of the measured and predicted ChW supply and return temperatures. If the model accurately fits the data on which it was trained, this type of evaluation is referred to as “internal predictive ability”. The external predictive ability of a model is to use a portion of the available data set for model calibration, while the remaining data are used to evaluate the predictive accuracy. The RMSEs of the internal

and external predictions are 1.13 ºF and 1.14 ºF, respectively. The CVs of the internal and external predictions are 6.86% and 6.93%, respectively.

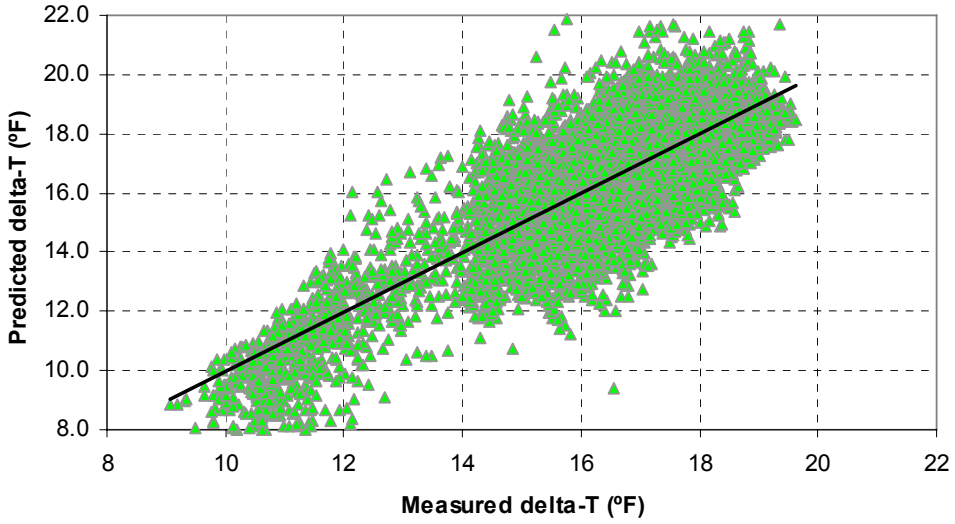

Figure 24 Comparison of measured and predicted loop temperature differences

4.2.3 Plant side modeling

Table 6 shows the main parameters and inputs for the plant side. The efficiencies of all pumps are assumed constant and determined from pump efficiency curves and design flow rates. The overall efficiency is a product of motor efficiency, shaft efficiency, and pump efficiency (and VSD efficiency for SPMPs). The pump heads are determined from pump head curves. It is assumed that all pumps are sequenced reasonably to ensure that the running pumps are operated around the design points.

Table 6 Parameters of TES system plant side

SPMP	SPMP overall efficiency	η_{spmp}	75%	
	SPMP design flow rate	V_{spmp}	8,000	GPM
PPMP	PPMP overall efficiency	η_{ppmp}	80%	
	PPMP head	H_{ppmp}	80	ft
CHLR	CHLR Coefficient 0	c_0	-2.81E-01	
	CHLR Coefficient 1	c_1	1.02E+01	
	CHLR Coefficient 2	c_2	1.74E+03	
	CHLR Coefficient 3	c_3	2.71E-03	
	CHLR Cond. water flow	V_{cw}	10,300	GPM
	Total CHLR number	N_{CHLR}	5	
	ChW leaving temperature	$T_{ChW,S}$	36	ºF
	CHLR ChW low limit	$V_{chw,min}$	4,000	GPM
	CHLR ChW high limit	$V_{chw,max}$	7,400	GPM
	Motor max power input	$P_{mtr,max}$	3,933	kW
	Max CW enter temp	$T_{CW,max}$	83.0	ºF
	Min CW enter temp	$T_{CW,min}$	60.0	ºF
CT	CT Coefficient 1	d_1	0.01	
	CT Coefficient 2	d_2	0.16	
	Approach setpoint	$\Delta T_{app,sp}$	6.0	ºF
CWP	Pump head	H_{cwp}	92	Ft
	Pump overall efficiency	η_{cwp}	82%	

The CT coefficients are obtained from the regression results of the historical data. The cooling tower model fitting curve is shown in Figure 25 and the WTW efficiency is shown in Equation (50). It should be noted that the coefficients obtained from the trended historical data are only applicable to the current cooling tower operation strategy. If a new CT operation strategy is used, the coefficients are subject to adjustment. A physical CT model, such as an Effectiveness-NTU model, is used to simulate the cooling tower fan power under all operating conditions. Then, the simulation data are used to obtain the coefficients of the new CT model.

$$\xi_{CT} = \frac{P_{CT}}{Q_{ChW}} = \left(d_1 + \frac{d_2}{\Delta T_{app}} \right)\left(1 + 0.2843\xi_{CHLR}\right) \tag{50}$$

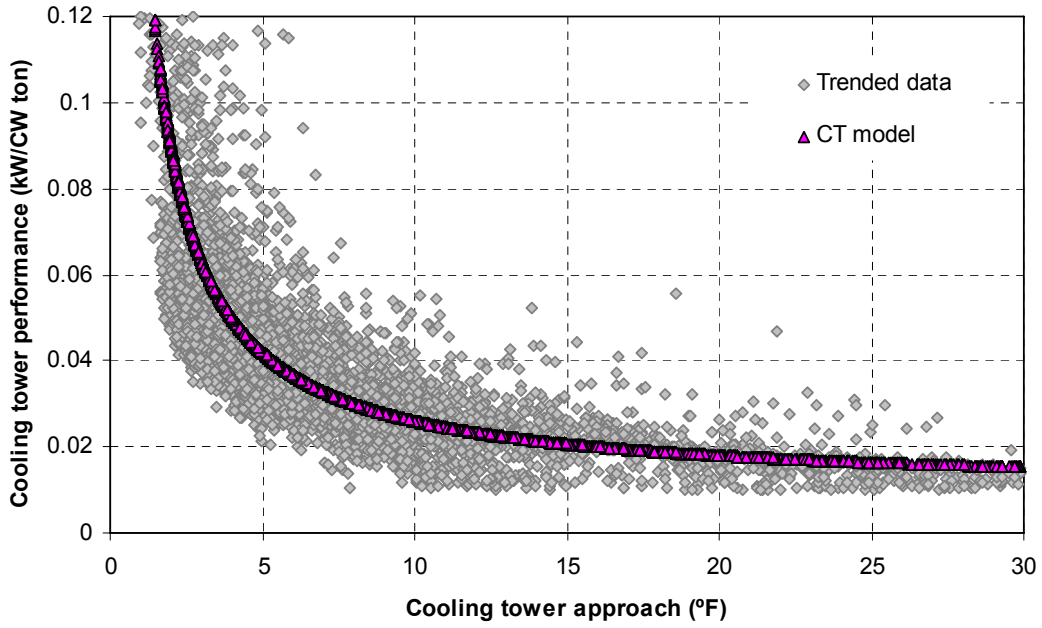

Figure 25 Cooling tower regression model

The simulation can only be as accurate as the model. The accuracy of the model determines the reliability of the simulation results. OM chillers consume about 65% of the total electricity in the EP. The accuracy of the chiller model plays an critial role in system modeling. A physical model will lead to a high computational cost, and an emperical model or black-box model is not reliable out of the range of the trainning data. As a result, a semi-emperical model called Gordon-Ng model is selected to simulate the chiller performance.

The coefficients of the Gordon-Ng chiller model are obtained by regressing with the trended historical data of the OM chillers. The chiller WTW efficiency is shown in Equation (51). The rated CW flow rate is equal to the average of the trended data. In this study, the total available chiller number is limited to four. The chiller ChW leaving temperature default setpoint is 36 ºF. The ChW flow rate limits and CW entering temperature limits are based on the chiller design specifications.

$$\xi_{CHLR} = 3.517\left(\frac{(c_0 + c_1 x_1 + c_2 x_2 + 1)T_{cdi}}{(-c_3 Q_{ChW} + T_{cho} - \frac{Q_{ChW}}{(V_{CW}\rho_w c_{pw})})} - 1\right) \tag{51}$$

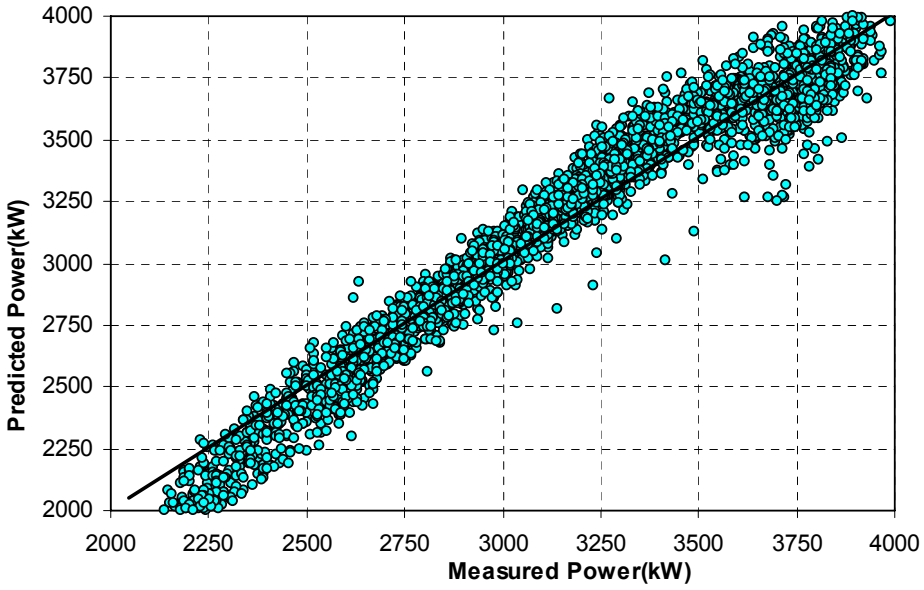

Figure 26 Comparison of OM chiller measured and predicted motor power

Figure 26 is a comparison between measured and predicted motor power using the Gordon-Ng model. Statistical analysis shows that the RSME of the internal predictions is 102.5 kW, CV is 2.96%, and CV* is 3.02%. To test the external prediction performance of the calibrated OM chiller model, the trended data from March 2008 to January 2009 are selected and a good match is also observed. The RSME is 104.3 kW, CV is 3.14%, and CV* is 3.12%. Specifically, the accuracy is obviously high between 2,500 kW and 3,000 kW, which corresponds to the part load range of the OM chillers with the highest efficiency.

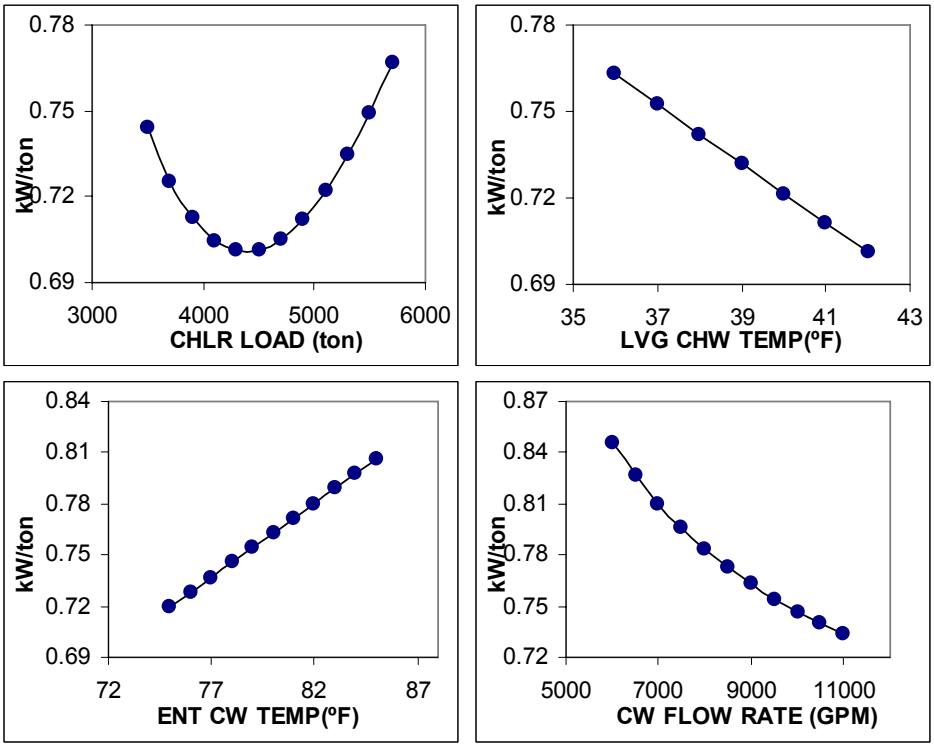

Figure 27 OM chiller model parametric studies

Figure 27 shows the results of OM chiller parametric studies. A higher ChW leaving temperature, a lower CW entering temperature, and a higher CW flow rate lead to a lower kW per ton value. It is found that the optimal chiller PLR occurs at around 4,400 ton or 80% of chiller rated capacity.

In this study, a month by month plant optimization will be performed to optimize chiller ChW leaving temperature and CT approach setpoint. They are assumed constant within each month and can be adjusted month by month.

4.2.4 Tank and non-plant power modeling

Table 7 Parameters of TES system tank and non-plant power

TES	Tank volume	U_{tank}	5,400,000	gal
	Tank initial height	x_{initi}	0.20	
	Tank ChW low limit	x_{min}	0.20	
	Tank ChW high limit	x_{max}	1.00	
	Tank charging high limit	$V_{tank,max}$	22,958	GPM
	Tank discharging high limit	$V_{tank,min}$	-22,958	GPM
	Tank Figure of Merit	Φ	0.95	
Non-plant power	Coefficient 1	g_1	1266.3	
	Coefficient 2	g_2	-4.4327	
	Coefficient 3	g_3	0.1983	
	Winter shift DB	$T_{wb,shift}$	60	ºF
	Winter base power	$P_{w,base}$	750	kW

The tank parameters and non-plant power model are listed in Table 7. The tank water level lower and upper limits are set 0.2 and 1.0, respectively. They can be adjusted to accommodate a conservative or an aggressive operating strategy. The tank Figure-of-Merit is based on the statistic analysis of tank inventory change. Mild mixing is observed

in this tank and 0.95 is selected. A high limit of charging and discharging rate is imposed to avoid intense turbulence around the dispensers.

The non-plant power is composed of two segments. When the ambient DB temperature is lower than 60 ºF, the non-plant power is 750 kW constant. Otherwise, a second-order polynomial is used to calculate the total non-plant power contributed by plant HVAC, glycol production, air compressors, etc. Figure 28 shows the fitting curve of electricity consumption on non-ChW production and Equation (52) shows the mathematical form of the regression model.

$$P_{non-plant} = \begin{cases} 750 & when DB < 60^{\circ}F \\ g_1 + g_2 T_{DB} + g_3 T_{DB}^2 & when DB \geq 60^{\circ}F \end{cases} \quad (52)$$

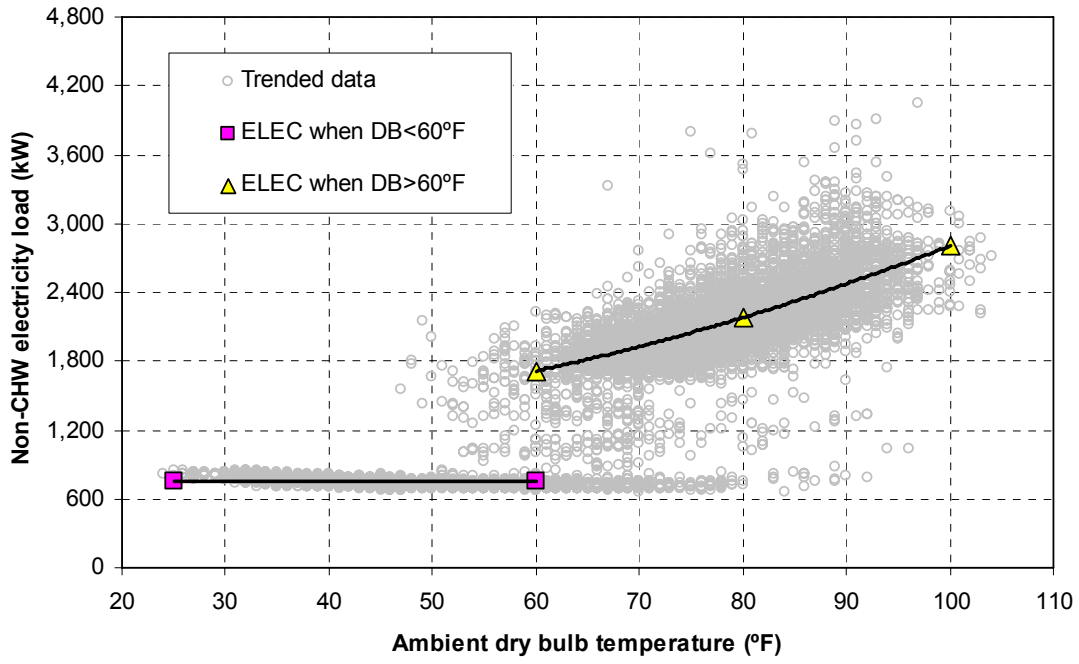

Figure 28 Modeling of electricity consumption on non-ChW Production

4.3 DFW: Operating Strategy Simulation

4.3.1 Simulation settings

Several points deserve more attention for this specfic project before the simulation:

There are six scenarios defined in the simulations, which are shown in Table 8. The first and the second scenarios are the optimal control strategy proposed in this paper, the next three ones are conventional strategies, and the last one is the scenario without TES as the baseline. The plant optimization is only applied to the first scenario. The existing operation is very close to Scenario 3. The current rate structure will be applied to all scenarios. The scenario without the TES tank is only used to compare the operating cost change with different control strategies and the effect of plant optimization improvement. A baseline 4CP demand and a highest monthly NCP demand will be calculated for each scenario by performing a preliminary simulation.

Table 8 Simulation scenario definition

Scenario No.	Control strategy	Plant optimization
1	Optimal	Yes
2	Optimal	No
3	Full storage	No
4	Chiller-priority	No
5	Storage-priority	No
6	Without TES	No

For each control strategy, an on-peak period and an off-peak period are defined for both the summer months and winter months. In the summer months, the on-peak period is defined as 15:00 to 18:00 and other hours are defined as the off-peak period. In the winter months, the on-peak period is defined as 14:00 to 17:00 when the ambient WB is high in a day. Running chillers during this period should be minimized since the plant performance is low when the ambient WB temperature is high. However, if the gains by shifting cooling load from the high WB hours to the low WB hours are less than the losses through the tank heat losses and mixing effects, it is preferred to run chillers during the on-peak period.

As the 4CP demand power is based on the metered data in the previous year, a baseline 4CP demand $D_{4CP,baseline}$ is determined for each control strategy by running simulations for the summer months. The 4CP demand cost for the current month is calculated with the following formulas:

$$C_{4CP} = R_{4CP} D_{4CP,baseline} + 12 R_{4CP} (D_{4CP,current} - D_{4CP,baseline})/4 \quad \text{for the summer months} \quad (53)$$

$$C_{4CP} = R_{4CP} D_{4CP,baseline} \quad \text{for the winter months} \quad (54)$$

These formulas indicate that, in the summer months, if the current month 4CP demand is higher than the baseline demand, a quarter of the difference (the 4CP demand is the average of CP demands in the four summer months) will be charged for 12 months in the next year. In winter months, the 4CP demand charge is calculated with the baseline demand.

An 80% ratchet of the highest monthly NCP kW established in the 11 months proceeding the current billing month is defined for the current month NCP demand.

Historic data show that the peak NCP demand normally occurs in the summer months. In this study, a preliminary simulation is conducted first for the summer months to establish the annual peak NCP demand for each control strategy. The NCP demand costs in each month can be calculated as follows:

$$C_{NCP} = R_{NCP} Max(D_{NCP,current}, 0.8 * D_{NCP,peak}) \quad (55)$$

During the winter months, an artificial on-peak period is also defined. Running chillers during this period should be minimized since the ambient WB temperature is high and overall plant performance is low.

When it comes to choosing the acceptable operating strategies for each month, the minimal tank water level for each month is set to 0.01. A larger number shows a more conservative strategy.

There are six scenarios in the simulations. The first and second ones are the optimal ones proposed in this dissertation. A plant optimization procedure is applied in the first one. The next three ones are the conventional strategies and the last one is the scenario without TES as a baseline. As the rate structure for this facility without TES is unknown, the current rate structure will be applied to the reference case.

It is noted that, as the rate structure without TES is unknown, the savings in this study are different from the real savings of erecting a TES tank. It is only used to compare the operating cost change with different control strategies and plant optimization improvement.

The plant variables to be optimized are chiller ChWLT and CT approach temperature setpoint. The default values of 36 ºF and 6.0 ºF are applied to all operating

strategies during the search process. When the simulation is finished, a plant optimization is conducted to find the optimal setpoints for Scenario 1. The upper and lower limits of the ChW leaving temperature are 44 ºF and 36 ºF, respectively. The upper and lower limits of the CT approach temperature setpoint are 10 ºF and 2 ºF, respectively. The GRG algorithm in the Excel Solver tool is used to find the solution.

4.3.2 Simulation results

Figure 29 shows the monthly savings plots for the different scenarios. The simulated monthly costs for each scenario are also shown in Table 9. It is obvious that the optimal control strategy outperforms others in each month. The optimal control strategy with plant optimization (Scenario 1) is the one with the lowest electricity billing cost for every month. If Scenario 6 is used as the baseline, the annual electricity total billing cost savings for full storage, chiller-priority, and storage-priority are 2.6%, 1.0%, and 2.6%, respectively. The annual savings due to implementing the TES tank are $199,185. There is no obvious difference in monthly billing costs between the full storage (Scenario 3) and the storage-priority (Scenario 5) because the tank is so large that it is not necessary to run chillers during the on-peak period in the summer months. For Scenario 2, the annual saving is 6.8%, which is 4.2% or $330,079 more than that of Scenario 3 (close to current operations). This could be regarded as the savings due to TES operation optimization. Compared to Scenario 3, Scenario 1 can reduce operating costs by 7.3% or $565,815 per year. Therefore, the annual savings due to plant optimization are $235,736. The analysis above shows that the savings due to TES and plant operation optimization can be very significant.

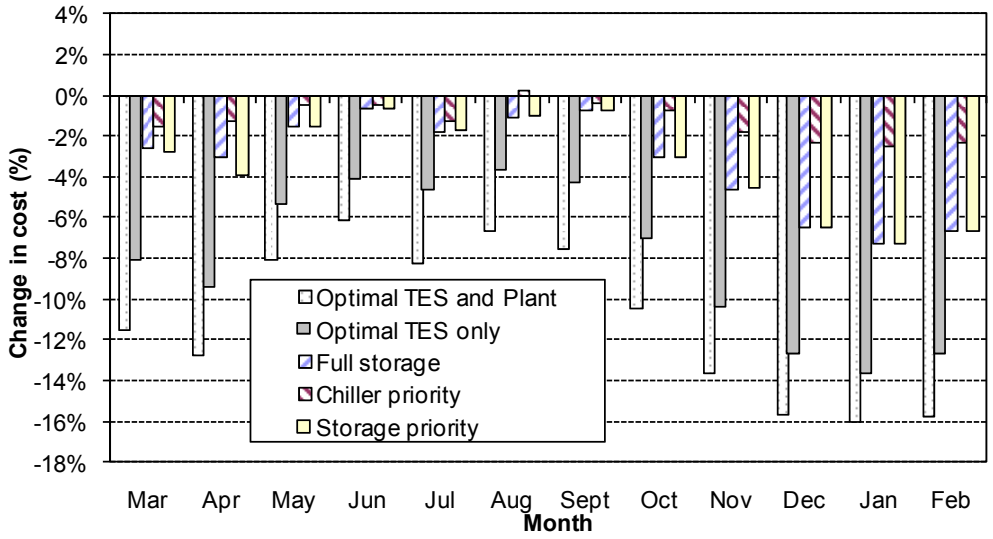

Figure 29 Simulation results of different control strategies

Table 9 Comparison of simulated monthly costs for DFW

	Optimal control strategy			Conventional control strategies			Baseline
Scenario	1		2	3	4	5	6
Month	Optimal control strategy with plant optimization		Opt. w/o plant opt.	Full storage	Chiller priority	Storage priority	Monthly bill without TES
	Monthly bill	Saving %					
Mar	$ 507,562	-11.5%	-8.1%	-2.6%	-1.5%	-2.8%	$ 573,506
Apr	$ 472,123	-12.7%	-9.4%	-3.0%	-1.3%	-3.9%	$ 540,835
May	$ 678,620	-8.1%	-5.4%	-1.5%	-0.5%	-1.5%	$ 738,075
Jun	$ 816,189	-6.1%	-4.1%	-0.6%	-0.4%	-0.6%	$ 869,079
Jul	$ 858,703	-8.2%	-4.6%	-1.8%	-1.2%	-1.8%	$ 935,384
Aug	$ 961,067	-6.6%	-3.7%	-1.1%	0.2%	-1.1%	$ 1,029,173
Sept	$ 774,267	-7.5%	-4.3%	-0.7%	-0.4%	-0.7%	$ 837,365
Oct	$ 592,072	-10.5%	-7.0%	-3.1%	-0.7%	-3.1%	$ 661,379
Nov	$ 416,077	-13.6%	-10.3%	-4.6%	-1.8%	-4.6%	$ 481,615
Dec	$ 323,240	-15.7%	-12.7%	-6.5%	-2.3%	-6.5%	$ 383,306
Jan	$ 297,200	-16.0%	-13.6%	-7.3%	-2.5%	-7.3%	$ 353,690
Feb	$ 313,320	-15.8%	-12.6%	-6.6%	-2.3%	-6.6%	$ 372,033
Total	**$ 7,010,439**	**-9.8%**	**-6.8%**	**-2.6%**	**-1.0%**	**-2.6%**	**$ 7,775,439**
	Absolute saving	-$765,000	-$529,264	-$199,185	-$75,181	-$204,766	

The savings percentage of Scenario 1 is high in the winter months and low in the summer months. This can be explained by the larger difference of the chiller kW per ton for the optimal part loads and the maximum capacity when the chiller CW entering temperature is low. The savings for Scenario 4 are negligible because the demand savings are small. If the tank size is much smaller than the current size, the full storage strategy may not be applicable, and the savings for Scenario 5 are close to that for Scenario 4.

Table 10 and Table 11 detail the simulation results of Scenario 1. The completed simulation results of all scenarios can be found in Appendix A. The annual billing cost is $7,010,439, which is $765,000 less than that of the baseline. The billing cost savings consist of $384,395 per year from the energy costs reduction and $380,605 per year from the demand costs reduction. The highest monthly NCP demand in this year is 20,653 kW and 4CP demand is 3,744 kW. The annual electricity energy reduction is 4,830,190 kWh. However, the annual total cooling production increases 1,056,533 ton-hr due to tank heat losses and mixing effects.

In the summer months, no chiller is staged on during the on-peak period for Scenario 1 and the maximum number of running chillers is four during the off-peak period. In the winter months, the maximum number of chillers running is two to four during the off-peak period. Sometimes, it is even more cost effective if chillers are running during the on-peak period. This is explained where the energy savings by reducing tank losses are higher than the energy savings due to improvements in the plant performance.

Table 10 Monthly consumptions and productions for Scenario 1

	Optimal control strategy with plant optimization (Scenario 1)							
Month	On-peak energy (kWh)	Off-peak energy (kWh)	Charged 4CP kW	Charged NCP kW	Current month 4CP kW	Current month NCP kW	On-peak ChW production (ton-hr)	Off-peak ChW production (ton-hr)
3	210,513	5,207,181	3,744	16,523	2,908	13,082	6,343,352	0
4	193,983	4,987,660	3,744	16,523	3,135	14,552	6,195,198	0
5	559,494	7,251,778	3,744	16,523	15,912	16,379	8,007,623	427,326
6	257,960	9,164,301	3,744	20,449	3,584	20,449	9,817,257	0
7	280,923	9,679,940	3,744	20,266	3,745	20,266	10,452,526	0
8	303,185	10,926,673	3,744	20,653	4,006	20,653	11,588,419	0
9	265,707	8,654,059	3,744	19,895	3,642	19,895	9,446,183	0
10	241,315	6,376,364	3,744	19,309	3,638	19,309	7,416,188	0
11	185,397	4,311,455	3,744	16,523	3,060	13,601	5,303,138	0
12	224,638	3,079,563	3,744	16,764	16,764	16,764	3,986,745	149,818
1	115,851	2,867,172	3,744	16,523	2,858	10,425	3,630,117	0
2	196,780	2,991,516	3,744	16,523	9,695	9,695	3,796,718	85,416
Total	**3,035,747**	**75,497,661**			**3,744**	**20,653**	**85,983,464**	**662,559**
Diff.	8,886,173	-4,055,983					-12,526,689	11,470,155

Table 11 Monthly costs and operations for Scenario 1

	Optimal control strategy with plant optimization (Scenario 1)						
Month	Monthly electricity billing cost ($)	Demand cost ($)	Energy cost ($)	$N_{offpeak}$	N_{onpeak}	ChW leaving temperature (ºF)	ΔT approach (ºF)
3	$ 507,562	$ 65,224	$ 442,338	3	0	43.5	4.6
4	$ 472,123	$ 65,224	$ 406,899	3	0	42.8	4.7
5	$ 678,620	$ 65,224	$ 613,396	3	3	40.3	4.8
6	$ 816,189	$ 76,287	$ 739,902	4	0	39.3	4.7
7	$ 858,703	$ 76,506	$ 782,197	4	0	42.0	4.7
8	$ 961,067	$ 79,220	$ 881,847	4	0	40.7	4.8
9	$ 774,267	$ 73,825	$ 700,443	4	0	41.1	4.8
10	$ 592,072	$ 72,405	$ 519,666	4	0	42.2	4.6
11	$ 416,077	$ 62,952	$ 353,124	3	0	43.0	4.8
12	$ 323,240	$ 63,771	$ 259,469	3	4	44.0	4.6
1	$ 297,200	$ 62,952	$ 234,248	2	0	41.0	4.6
2	$ 313,320	$ 62,952	$ 250,367	2	2	43.3	4.6
Total	**$ 7,010,439**	**$ 826,543**	**$ 6,183,896**				
Diff.	$ 765,000	$ 380,605	$ 384,395				

The optimal chilled water supply temperature is 39-42 ºF from June to October and it is 40-44 ºF from November to May. This indicates that a higher ChW supply temperature is preferred in the winter months because the energy savings from chiller performance improvements outperform the pump energy increase due to a lower loop delta-T. The optimal cooling tower approach setpoint is 4.6-4.8 ºF all year round, which is lower than the current setpoint. This indicates that the energy savings from chiller performance improvements are more than the fan energy increase due to a lower cooling tower CW leaving temperature.

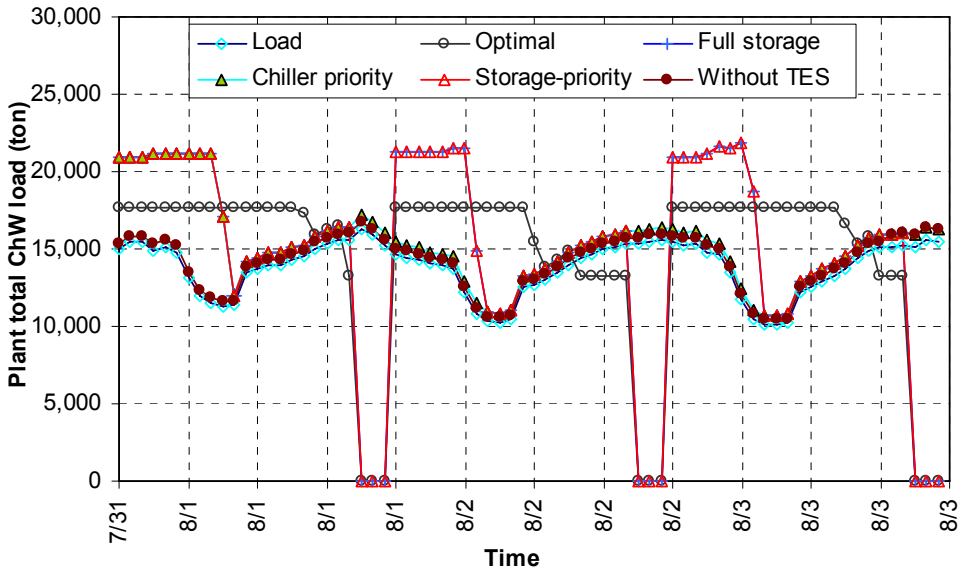

Figure 30 Comparison of plant ChW load profiles for different strategies

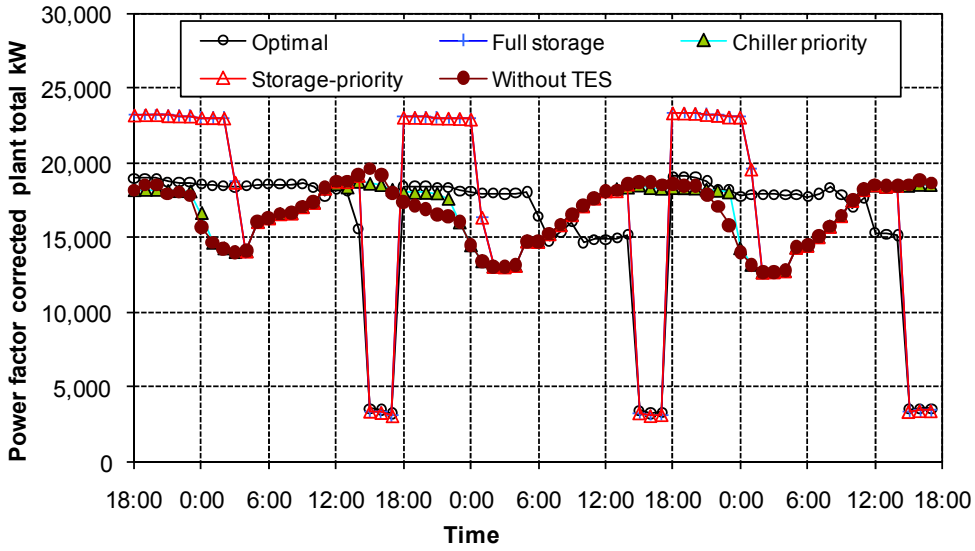

Figure 31 Comparison of plant total kW profiles for different strategies

To help understand the plant operations under different strategies, Figure 30 shows the plant and loop ChW load profiles during three consecutive days in August. Figure 31 shows the plant total demand hourly profiles after power factor correction in the same three days. As expected, the load of the plant without TES closely follows the loop load but it is a little higher because of loop supply temperature increases. When the tank is fully charged, the profile of the chiller-priority strategy almost overlaps the load profile because there is enough cooling capacity in the plant and the tank is in an idle mode. The profiles of the full storage and the storage-priority match with each other because there is no need to run chillers during the on-peak period. These two strategies both charge the tank at the maximal capacity since the start of the off-peak period and then enter the idle mode before 6:00 am. Different from others, the optimal control strategy maintains a constant plant chilled water production for a long time. One chiller

is shed several hours before 15:00 to ensure the tank is fully charged right before 15:00. During most hours, all chillers staged on are loaded at the part load with the highest efficiency. The off-peak demand for the optimal control strategy is around 4,500 kW less than that for the full storage and the storage-priority. The on-peak demand for the optimal control strategy is around 16,000 kW less than that for the chiller-priority and scenario without TES.

4.3.3 Sensitivity study

To study the sensitivity of plant parameters on the monthly operating cost of the optimal control strategy without plant optimization, a series of sensitivity studies are performed using August as an example. Table 12 lists the selected parameters, the default values, and minimum and maximum limits of the fluctuation range. Five points are selected for each parameter.

Table 12 Parameter range of sensitivity study for DFW

Variables	Default	Min	Max	Unit
Tank FOM	0.9	0.810	0.990	-
CHLR ChW LT	38.0	36.0	40.0	ºF
CT APP SP	6.0	4.0	8.0	ºF
CW FLOW	10,000	8,000	12,000	GPM
LP DP SP	28	24	36	psid
LP ST rise	1.0	0.70	1.30	ºF

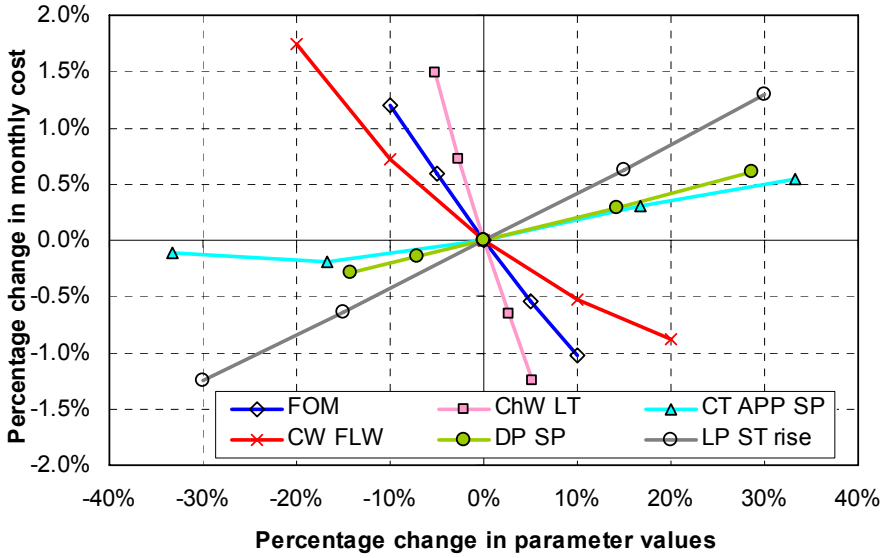

Figure 32 Monthly operating costs sensitivity to variants of plant parameters

The simulation and analysis results are shown in Figure 32. The most sensitive parameter is the chiller chilled water leaving temperature. For a 1.0 ºF increase in the chiller chilled water leaving temperature, the monthly electricity billing cost decreases 0.6% or $6,220. This includes both chiller efficiency improvement due to a lower chiller ChWLT and SPMP energy increases due to a lower loop delta-T. The next most important one is the FOM of the tank. A higher FOM leads to a lower monthly cost. For the normal range of 0.85 to 0.95, the corresponding change in monthly cost is 1.1% or $10,816. This is followed by the CW flow rate per chiller. When the efficiency and pump head are assumed constant, a higher flow rate leads to a lower monthly cost.

The three parameters left have a positive correlation with the monthly electricity billing cost. If the loop supply temperature rise increases 0.3 ºF for any reason, such as bad tank wall insulation, the monthly electricity billing cost could increase 1.3% or

$12,270. A higher loop end DP setpoint will consume more SPMP pump power. If the loop DP setpoint is reset from 32 psid to 28 psid, the monthly billing cost savings are $3,064. It is noted that an optimal CT approach setpoint exists for this case, at around 5.0 ºF, which is consistent with the results of the system monthly simulation.

4.4 DFW: Controller Design

A general supervisory control is applied in this TES system. The following are some additional aspects that need more detailed explanation.

4.4.1 Load prediction model

A multiple linear regression model is built to predict the loop side total ChW demand (y) as a function of the ambient DB temperature (x_1), WB temperature(x_2), hour(x_3), month(x_4), and ChW supply temperature (x_5). The regression model is shown as follows:

$$y = h_0 + h_1x_1 + h_2x_2 + h_3x_3 + h_4x_4 + h_5x_5 + h_6x_1x_2 + \cdots + h_{19}x_3x_5 + h_{20}x_4x_5 \quad (56)$$

The method of least squares is adopted to estimate the coefficients (h_0 to h_{20}), which are shown in Table 13. Figure 33 shows a comparison between the predicted and measured loop cooling loads. The dots on the black diagonal mean a perfect match. A good match is observed at both the high load end and the low load end. The RMSE is 699 ton, adjusted R^2 is 0.967, and CV is 7.59%. The two-week hourly profiles of measured and predicted loads are shown in Figure 34.

Table 13 Coefficients of load prediction model for DFW

h_0	8635.789	h_7	6.97084	h_{14}	-0.25236
h_1	72.13634	h_8	-9.1161	h_{15}	-0.89142
h_2	-526.24	h_9	-62.2157	h_{16}	0.62022
h_3	72.27549	h_{10}	-3.6092	h_{17}	2.0874
h_4	831.4887	h_{11}	-2.93946	h_{18}	-0.48663
h_5	138.2628	h_{12}	2.42504	h_{19}	2.53542
h_6	1.11588	h_{13}	-0.22857	h_{20}	0.33879

It should be noted that the coefficients of this model are regressed from the historical data. Since some commissioning and retrofitting projects have been conducted and will continue to be conducted on the loop side, the loop total cooling load is subject to change. The coefficients should be updated periodically to reflect this change.

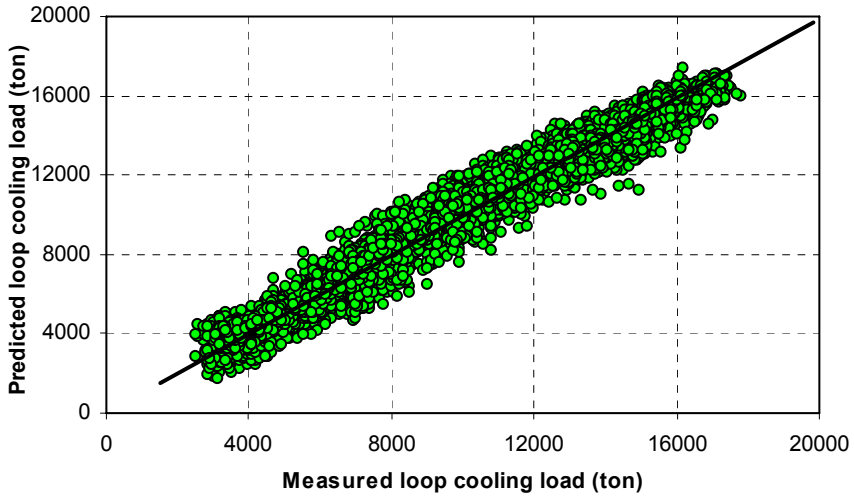

Figure 33 Comparison between predicted and measured loop cooling loads

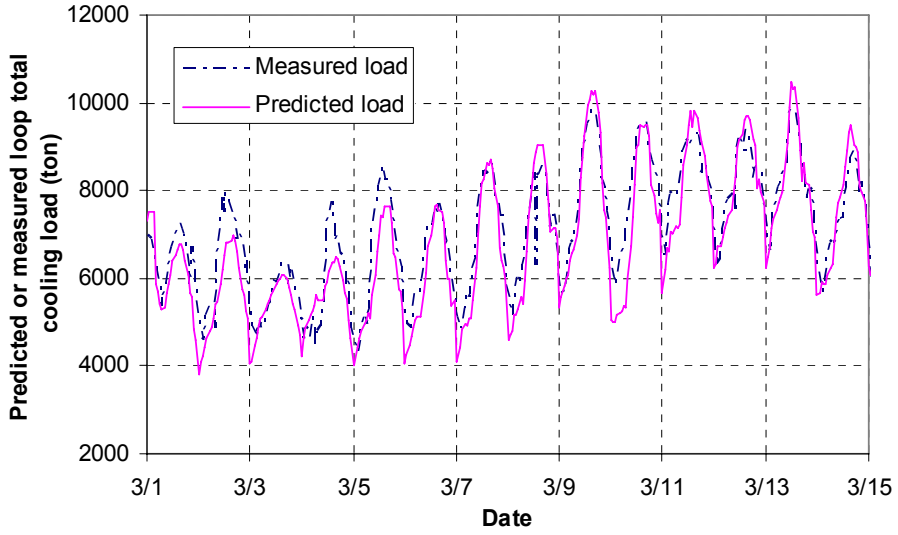

Figure 34 Profiles of measured and predicted loop cooling load

4.4.2 Weather condition prediction model

Generally speaking, weather condition prediction in the next 24 hours is much more reliable than the long-term prediction. A good source of future weather prediction comes from The Weather Channel. Its unique TruPoint^{SM} technology delivers the most accurate weather reports and forecasts for more locations than any other weather provider. The TruPoint uses weather radar, satellite, a lightning detection network, weather prediction models, surface sensors and other available observation data to derive the current weather conditions for 1,000 more observation points than standard national weather station sites. Temperature, wind, humidity, precipitation, visibility, and cloud cover are updated several times each hour for points every 1.5 miles across the country. This same technology is used to extend existing weather conditions six hours into the future at 15-minute intervals. This enables TruPoint to provide a highly specific and

localized short-term forecast that will help the operators stay one step ahead of the weather (www.weather.com). Local hourly weather conditions in the next 48 hours are provided on this website.

Figure 35 shows a comparison of two hourly dry bulb temperature profiles for 48 hours. One profile comes from NCDC data recorded at the College Station Easterwood Airport and the other one from Weather Channel predictions. It is observed that a good match is found in the first 24 hours, while obvious differences start showing up in the next 24 hours.

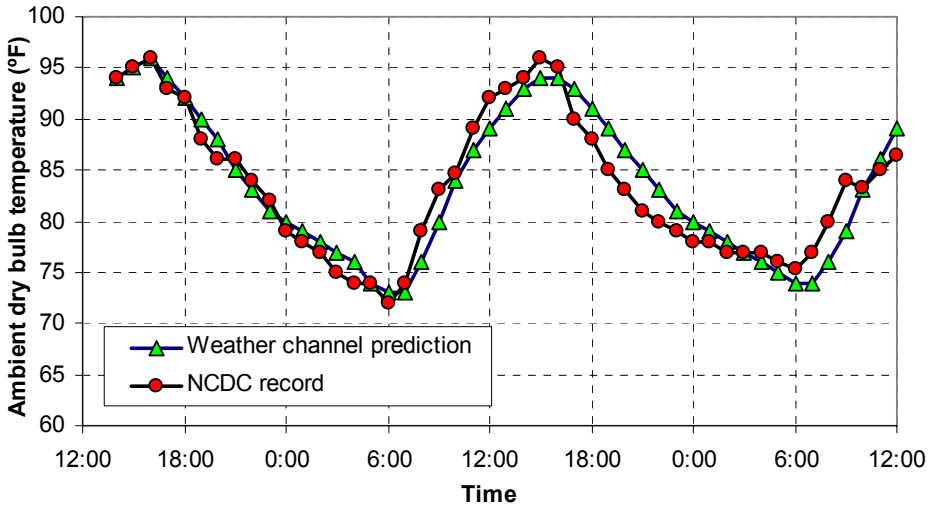

Figure 35 Comparison between Weather Channel predicted and NCDC recorded dry bulb temperature profiles

4.4.3 TES control

Along the vertical direction of the tank, temperature sensors are fixed in an interval of around one foot to measure the temperature profile in the tank. The tank

inventory or the ChW level can be monitored to provide inputs to other controllers. There is no control equipment on the tank.

4.4.4 OM chiller control

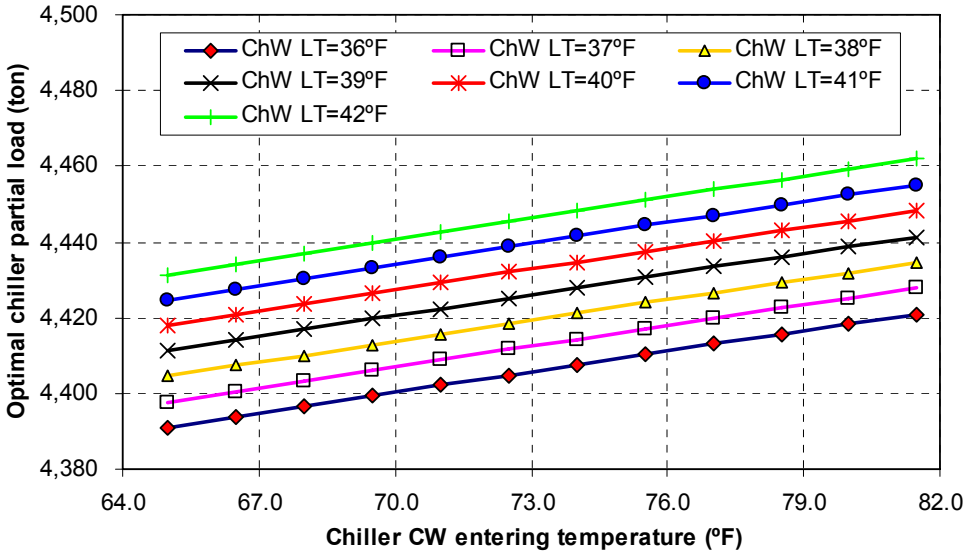

Figure 36 Chiller optimal part loads as a function of ChW leaving and CW entering temperature

The control of OM chillers includes chiller sequencing and chiller part load control. The maximum numbers of chillers running during the off-peak period and on-peak period are restricted by the current month optimal operating strategy. The hourly profile of the number of chillers running since the start of the off-peak period is predicted by the optimal control strategy. In practice, the tank inventory or the tank ChW level is monitored by the temperature sensors located along the vertical direction of the tank wall. It is possible to adjust the number of chillers running to accelerate or

decelerate charging speed but the maximum numbers of chillers on stage should not be overridden. The chiller ChW leaving temperature setpoint can be maintained through the chiller internal controller.

The part load of the chiller is determined by the ChW entering and leaving temperatures as well as the ChW flow rate through the evaporator. Since the entering temperature cannot be controlled by the chiller and the leaving temperature is maintained at a predefined setpoint, the ChW flow rate will be modulated to keep the chiller part load at an optimal value when the entering ChW temperature fluctuates from time to time. As introduced previously, the range of OM chiller optimal part load is very narrow, which is shown in Figure 36. These profiles are simulated with the calibrated Gordon-Ng model. When the CW entering temperature varies from 65 ºF to 81.5 ºF and ChW leaving temperature varies from 36 ºF to 42 ºF, the range of the optimal part load is between 4,390 ton and 4,462 ton. As a result, the ChW flow rate through the chiller evaporator is modulated to accommodate the fluctuation of ChW entering temperature.

Figure 37 shows the statistic analysis on the distribution of loop ChW delta-T change. The absolute values of the loop ChW delta-T change from March 2007 to February 2008 are divided into 12 bins with an interval of 0.5 ºF. The frequency column chart shows that the highest frequency is 0.5 ºF. The possibility that the change is larger than 3.0 ºF is very low. The cumulative profile shows that the probability of the change equal or less than 3.0 ºF is 97.8%. Consequently, during most of the time, the modulation of the chiller flow control valve will be very slow. Since the region of the optimal part load is flat, a relative wide control band can be defined to avoid valve

hunting. A long time step, for example 5 minutes, can be defined to adjust the valve position. Such a slow control will not play a significant impact on the chiller internal control.

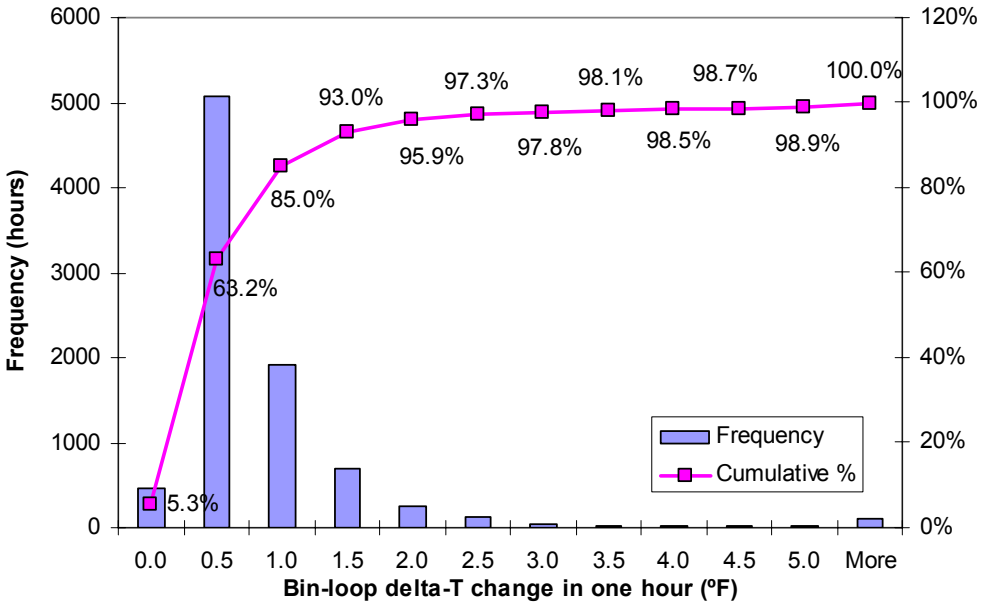

Figure 37 Distribution of loop delta-T change in one hour

4.4.5 Cooling tower control

The control of a cooling tower consists of CT sequencing and CT condenser water leaving temperature control. A popular CW leaving temperature control method is to maintain a constant CT approach temperature. This objective can be achieved by staging on or off cooling towers and modulating fan speed. The strategies of sequencing cooling towers are various, but some general guidelines are summarized to improve the cooling tower performance. For example, for all variable-speed fans, it is more efficient

to operate all fans at the same speed. For multi-speed fans, it is efficient to activate lowest-speed fans first when adding the tower capacity and reverse for removing the capacity. Keep more towers online but prevent the flow rate lower than the minimal flow rate for the tower. It should be noted that a group of CT model coefficients corresponds to a specific CT control method. If the control method is changed, the coefficients should be updated accordingly.

4.4.6 Pump control

The original control logic of CW pumps, ChW primary and secondary pumps is still followed. However, the ChW primary flow rate is varied by modulating the flow control valves.

4.5 DFW: Summary and Conclusions

The DFW Energy Plaza is a large-scale chilled water system with a water storage tank and an advanced control system. The methodology proposed in this dissertation is successfully applied in this system to optimize the operation of the TES and chiller plant. The system is modeled and simulated based on the trended data. The utility rate structure is introduced and analyzed to define the off-peak and on-peak periods. Six scenarios are defined and simulated based on the cooling loads and weather conditions between March 2007 and February 2008. Following are some conclusions drawn based on the monthly comparison among the six scenarios.

(1) The annual utility billing cost savings due to implementing a TES tank is $199,185 when a full storage strategy is adopted.

(2) If an optimal TES operation strategy is used, it can result in additional savings of $330,079 per year. This strategy includes avoiding running chillers during 15:00 and 18:00 in the summer months, optimally allocating cooling load to each chiller, and leveling the demand profile by optimally sequencing the chiller.

(3) If suggested plant optimization measures are implemented, it may bring additional savings of $235,736 per year. These measures are resetting chiller ChW leaving temperature and CW entering temperature monthly.

(4) Many of these optimal control strategies were implemented in the actual optimization performed on the EP by Energy Systems Laboratory engineers.

4.6 TFC: System Introduction

4.6.1 Background

Texas Facility Commission (TFC) facilities division oversees the building maintenance and construction activities of state-owned office buildings and facilities. In the downtown area of Austin, the chilled water for nineteen buildings supervised by the TFC is supplied by four individual ChW plants. TFC proposed an energy retrofit project to establish a chilled water storage system and connect the four individual ChW plants into one ChW loop to substantially reduce the state's utility billing costs of the plants. The purpose of this study is to preliminarily assess the economic feasibility of connecting these plants with underground piping and erecting a new chilled water TES tank for the new ChW loop.

4.6.2 Site description

The four plants studied are Sam Houston Central Plant (CPP), Stephen F. Austin Plant (SFA), Robert E. Johnson Plant (REJ), and William P. Clements Plant (WPC). The CPP supplies steam and chilled water to various buildings within and surrounding the State Capitol Complex. Part of the electric power fed to the CPP from Austin Energy is distributed to Lorenzo de Zavala Archives & Library (ARC), Sam Houston Building (SHB), and John H. Reagan Building (JHR). The SFA plant supplies chilled water and heating hot water (HHW) to Lyndon B. Johnson Building (LBJ), William B. Travis Building (WBT), and itself. Part of the electric power fed to the SFA plant from Austin Energy is distributed to the SFA building. The REJ plant services the REJ building with ChW, HHW, and electricity. The WPC plant services the WPC building with ChW, HHW, and electricity.

Since the existing underground ChW piping diagram could not be obtained during the assessment phase, a schematic diagram of the existing ChW systems based on the walk-through is shown in Figure 38. The TES tank is initially planned to be in the SHB. According to TFC, it could also be installed in the SFA. At this level of assessment, the location of the TES tank does not affect the calculation results. However, during the design phase, the location of the TES tank as well as the piping arrangement should be carefully selected.

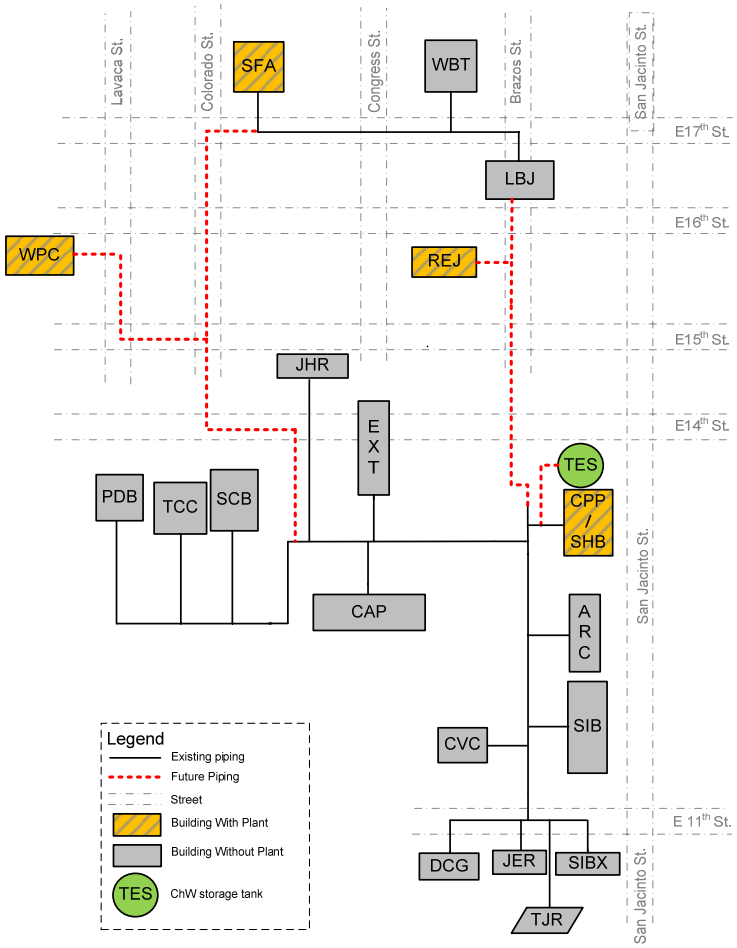

Figure 38 Schematic of ChW piping structure for TFC Capital Complex

The SFA and WPC plants tie in on the CPP loop at the JHR building so as to ease the ChW drought on the CPP west loop. The REJ plant can tie in on the CPP loop at the SHB building. The assumed new piping layout is shown in Figure 38. The goal was to connect the four plants into a loop intended to share the TES tank and take advantage of redundant cooling capacity in each plant. A ring-loop is constructed to provide a higher safety factor for system operations. The total length of the new pipes is estimated to be 3,096 ft. The final piping arrangement will be subject to further adjustment when

existing piping size, future tank location, construction cost, and other factors are considered.

The summary of the chiller information for each plant is show in Table 14. According to ASHRAE standards, centrifugal chillers have a service life of 23 years. This means that the chillers in the CPP plant, in order of oldest to youngest, are or were due for replacement in 2005, 2013, 2017, and 2024. CH#2 in the CPP plant is being replaced with a new 1,450 ton chiller. CH#1 and #3 in the SFA plant are being replaced with two 1,550 ton chillers. In the REJ plant, all of the chillers are relatively new and there is no replacement plan at present.

Table 14 Chiller information summary in four plants for TFC

Plant	Chiller #	Manufacturer	Refrigerant	Capacity (ton)	Year
CPP (SHB)	1	Trane	123	1470	2001
	2(Being replaced)	Trane	123	1,450	2009
	3	Trane	123	1250	1990
	4	Trane	123	1280	1994
SFA	1(Being Replaced)	Trane	R11	1550	2009
	2	Trane	123	1470	2003
	3(Just Replaced)	Trane	R11	1550	2009
REJ	1	Trane	123	555	1998
	2	Trane	123	555	1998
	3	Trane	123		
	4	Trane	123	70	1998
WPC	1			800	1985
	2			800	1985
	3	YORK(Not running)	R11		

The two 800 ton chillers in the WPC plant are scheduled to be replaced in 4 to 5 years. However, the installation of a new TES tank could make these retrofits less urgent and the cost to replace these two chillers will be considered as a potential avoided cost in the economic analysis.

The total cooling capacity is 5,450 ton for the CPP plant, 4,570 ton for the SFA plant, 1,180 ton for the REJ plant, and 1,600 ton for the WPC plant. Since the CPP and SFA plants are newer than the REJ and WPC plants, they are assumed to have a higher performance. In this context, the chillers installed after 2000 are called new chillers and the chillers installed before 2000 are called old chillers.

Table 15 Rate structure for all plants after TES installation for TFC

	Nov-Apr	May-Oct
Energy Rate		
On-Peak	1.67 ¢ per kWh	2.37 ¢ per kWh
Off-Peak	-0.33 ¢ per kWh	0.52 ¢ per kWh
Demand Rate		
On-Peak	$ 10.94 per kW	$ 11.64 per kW
Off-Peak	$ 0.00 per kW	$ 0.00 per kW

4.6.3 Rate structure

Austin Energy is the electricity provider for each of the four plants. Currently, the CPP plant is charged with the State Large Primary Service (E16) utility rate. The SFA plant is charged with the State Large Primary Service Rate (E15) rate. The REJ and WPC plants are charged with the State General Service - Demand Rate (E14) rate. A Rider clause (Rider time-of-use (TOU)-Thermal Energy Storage) may be applicable to

the four plants when a TES tank is erected and four plants are connected together with underground piping. Details on these three rate structures as well as the Rider TOU-Thermal Storage System can be found in Appendix B. The structure of the E16 rate structure is shown in Table 15.

An additional fuel charge will be added to the energy rate and the fuel charge is updated by Austin Energy regularly. In 2008, the fuel charge rate was $0.03544 per kWh for the E15 and E16 rates and was $0.03653 for the E14 rate. According to the information from the TFC, the fuel charge will be increased by 5% in 2010, 6.5% in 2011, and 11.5% in 2012. The average fuel rate in the next three year will be $0.03816 per kWh for the E15 and E16 rates and is $0.03933 per kWh for the E14 rate, which will be used in the following simulation and analysis. The new transmission charge, beginning in 2009, will be applied to all rate structures, and the price is $0.21207 per monthly peak kW. The transmission demand is the highest kW in each month.

According to the utility rate policy, when the power factor during the interval of greatest use is less than 85%, billing demand shall be determined by multiplying the indicated demand by 85% and dividing by the lower peak power factor. The monthly average power factors for each plant in 2008 are used in the simulation. The off-peak demand, on-peak demand, and transmission demand are all corrected to 85% in the following simulations.

According to the policy of Austin Energy Rider TOU-Thermal Energy Storage, the summer (May 1 through October 31) demand on-peak hours are from 4:00 p.m. to 8:00 p.m., Monday through Friday (except for Memorial Day, Independence Day, and

Labor Day). The remaining summer hours are considered off-peak hours (It is 1:00 pm to 9:00 pm if this Rider clause is not applied). The winter billing demand on-peak is all hours (It is 8:00 am to 10:00 pm if this Rider clause is not applied). The winter billed demand shall be the highest fifteen-minute demand recorded during the month, or 90% of the summer billed demand set in the previous summer; whichever is less (This clause does not exist if the Rider clause is not applied). The summer energy on-peak hours are from 1:00 p.m. to 9:00 p.m., Monday through Friday, and the winter energy on-peak hours are from 8:00 a.m. to 10:00 p.m., Monday through Sunday. The remaining summer hours are considered off-peak (This clause is the same as those without the Rider clause).

In order to qualify for the Rider clause, the demand shifted to the off-peak period with a TES tank should be no less than the lesser of 2,500 kW or 20% of the customer's normal on-peak summer billed demand.

4.6.4 Baseline development

The available data from Austin Energy are the hourly plant total electricity profile and plant monthly utility bills for each plant. Considering that some new chillers were installed in the CPP and SFA plant in 2009, the fuel charge rate will be updated, and a transmission charge will be added to the utility rates, it is not appropriate to use the utility bills in 2008 as the utility energy consumption and cost baselines. The utility energy and cost baselines used in the savings calculations are simulated from the baselines of the cooling load and electricity fed to buildings for each plant.

As the cooling energy produced at each plant is not metered, the baseline cooling load profile for each plant is estimated based on the hourly electricity consumption profile for each plant. The electricity distributed from the plants to the buildings was estimated using the building electricity usage indexes and the building gross square footage, which is shown in Appendix C. The electricity used for chilled water production is equal to the metered total electricity consumption minus the electricity distributed to the buildings. The hourly ChW load baseline profile can be obtained by dividing the electricity consumption for ChW production (kWh) with the estimated overall plant performance (kW per ton).

The following assumptions are made to develop the cooling load baseline, electricity fed to buildings, and utility billing cost baseline:

1. The selected baseline period is from Jan 01, 2008 to December 31, 2008.
2. According to the chiller log provided by SHB plant personel and the new chiller specifications, the efficiency of the new chillers is estimated to be 0.6 kW per ton and the efficiency of the old chillers is 0.9 kW per ton. The efficiency of auxiliary power is estimated to be 0.2 kW per ton. Chiller #2 was replaced in 2009. In 2008, there were three old chillers (#2, #3, and #4) and one new chiller (#1) in the CPP plant, but at most two old chillers and one new chiller were staged on. As a result, it is esimtated that the overall average performance of the CPP plant was 1.0 kW per ton in 2008.
3. In 2008, the overall average performance was 1.0 kW per ton for the SFA plant and was 1.1 kW per ton for the REJ and WPC plants.

4. The CPP plant is charged with the E16 rate. The SFA plant is charged with the E15 rate. The REJ and WPC plants are charged with the E14 rate. The Rider clause is not applied for any plant.
5. The updated fuel charge rate and the transmission charge are applied in the utility billing cost simulation.
6. In the CPP plant, the new chiller (#2) is on line. The old chillers (#3 and #4) will not be staged on until the new chillers (#1 and #2) cannot meet the cooling load.
7. In the SFA plant, the new chillers (#1 and #3) are on line.
8. In the baseline simulation, the TES tank is not built and there are no Continuous Commissioning® measures implemented in the CPP plant and loop.

The monthly electricity energy and demand prices updated for each plant are shown in Appendix C. The baselines of utility billing cost, plant demand, building electricity energy, and plant total cooling load for each plant can be found in Appendix D.

4.7 TFC: System Modeling and Simulation

4.7.1 Simulation settings

Based on the chiller logs recorded by the plant operators and field investigations, following are some assumptions made in the TES simulation:

1. The changes of loop side cooling load and electricity fed to buildings from the four plants due to weather adjustments and the proposed building retrofits and commissioning are not considered in the analysis.
2. The ambient hourly dry bulb temperature and wet bulb temperature hourly profiles trended by NCDC are used in the simulation. The weather station is located at the Austin-Bergstrom International Airport.
3. When a TES tank is installed and new ChW piping is buried, all plants are charged under the E16 with the Rider clause. The updated fuel charge rate and the transmission charge are applied in the simulation.
4. Three conventional control strategies (full storage, chiller priority, and storage priority) with limiting on the maximum number of chillers running during the off-peak and on-peak periods are simulated to find the optimal operation strategy for each month.
5. For each control strategy, the on-peak control period during the summer months is from 4:00pm to 8:00 pm when the demand cost is high. During the winter months, the on-peak control period is defined as 8:00 am to 10:00 pm, which matches the energy on-peak hours in the winter months.
6. A 10 ºF constant ChW supply and return temperature difference is assumed for the whole year. The chiller chilled water leaving temperature is 40 ºF and the condenser water entering temperature is 81 ºF.
7. The figure of merit of the storage tank is 0.98. The tank water minimum level is 0.2 and the maximum level is 1.0.

8. The electricity energy and cost baselines generated in the previous section are used when calculating the savings for different size tanks.
9. The efficiency is 0.6 kW per ton for the new chillers and is 0.9 kW per ton for the old chillers. The auxiliary power for each plant is 0.2 kW per ton.
10. The new chillers in the CPP plant will be staged on first, followed by the new chillers in the SFA plant. The old chillers in the CPP, REJ, and WPC plants will be staged on when all new chillers have been staged on. The maximum load for each chiller is equal to its nameplate capacity.
11. The summer on-peak demand savings (kW) for each tank size is equal to the average of the monthly on-peak demand reductions (kW) from May to October.
12. The rebate from Austin Energy and maintenance & operation cost change are not considered in the economic analysis.

As a result, the operating strategy of the tank is to shave the on-peak demand during the summer months and is to decrease the energy consumption by reducing chiller run time during the on-peak period of the winter months. For each month, the operating strategy with the lowest monthly billing cost is selected as the optimal one.

4.7.2 Simulation procedure

The model was used to simulate the following TES tank sizes: 1 million (M) gallon, 2M gallon, 3M gallon, 3.5M gallon, 4M gallon, 5M gallon, 6M gallon, and 7M gallon. For each tank size scenario, the monthly savings were summed to obtain the total annual savings.

The estimation of the tank cost is based on the information provided by a TES tank manufacture. The piping cost including design, material, construction, and installation is estimated to be $8,854,560 according to the information provided by the TFC. The estimated avoided chiller cost at the WPC plant is $1,881,344 based on the RSMeans cost data books. The breakdown of all cost estimations can be found in Appendix E. Based on all these considerations, a simple payback in years was calculated for each option.

Table 16 Billing costs and energy simulation results summary for TFC

Tank size (Million gal)	Annual billing cost savings ($)	Annual cost savings percentage	Annual energy cost savings ($)	Annual demand cost savings ($)	Total elec. consumption reduction (kWh)	Demand reduction (kW)	Annual cooling production increase (ton-hr)
1.0	$ 471,298	10.1%	$ 223,536	$ 247,762	2,863,909	2,059	6,007,818
2.0	$ 627,097	13.5%	$ 240,909	$ 386,188	2,688,822	3,127	6,051,099
3.0	$ 798,285	17.1%	$ 256,078	$ 542,207	2,478,769	4,345	6,094,219
3.5	$ 907,231	19.5%	$ 264,109	$ 643,121	2,377,427	5,036	6,114,129
4.0	$ 912,437	19.6%	$ 269,598	$ 642,838	2,326,156	5,036	6,123,930
5.0	$ 922,487	19.8%	$ 280,153	$ 642,335	2,211,959	5,036	6,144,385
6.0	$ 932,876	20.0%	$ 290,422	$ 642,454	2,095,404	5,036	6,164,696
7.0	$ 940,319	20.2%	$ 297,746	$ 642,573	2,008,835	5,036	6,180,300

4.7.3 Simulation results

The simulation results for eight tank size options are summarized in Table 16 and Table 17. The details for the monthly results of different tank size scenarios can be found in Appendix F. As expected, a larger size tank can shift more electricity load during the on-peak period to the off-peak period and lead to a higher on-peak demand

reduction and annual total billing cost savings. When the tank size is larger than 3.5 M gal, the total demand cost savings tend to approach a constant value. The summer on-peak demand reduction also remains 5,036 kW. More than half of the cost savings come from demand cost reductions. The total energy reductions are over 2.0 million kWh, which is explained by plant performance improvement and cooling load shifting from low performance plants (REJ and WPC) to high performance plants (CPP and SFA). The tank heat loss also leads to extra cooling production. A larger tank leads to a higher cooling production.

Table 17 Simulation results of eight tank size options for TFC

Tank size (Million gal)	Annual billing cost savings ($/year)	Avoided CHLR cost in WPC ($)	Tank cost ($)	Piping cost ($)	Total capital cost ($)	Simple payback (years)	Qualified for Rider TOU-TES?
1.0	$ 471,298	$1,881,344	1,841,448	8,854,560	10,695,982	18.7	N
2.0	$ 627,097	$1,881,344	2,859,573	8,854,560	11,714,082	15.7	Y
3.0	$ 798,285	$1,881,344	3,877,698	8,854,560	12,732,182	13.6	Y
3.5	$ 907,231	$1,881,344	4,386,760	8,854,560	13,241,232	12.5	Y
4.0	$ 912,437	$1,881,344	4,895,823	8,854,560	13,750,282	13.0	Y
5.0	$ 922,487	$1,881,344	5,913,948	8,854,560	14,768,382	14.0	Y
6.0	$ 932,876	$1,881,344	6,932,073	8,854,560	15,786,482	14.9	Y
7.0	$ 940,319	$1,881,344	7,950,198	8,854,560	16,804,582	15.9	Y

When the new piping cost, tank cost, and avoided chiller cost are accounted for, the simple paybacks are calculated, which are shown in Table 17. All options except for the 1.0 M gallon tank option qualify for the Rider clause. The tank size will also be limited by the available lot size and available project budget. A very large or very small

tank makes the payback longer. Since the option with a 3.5 M gallon tank has the shortest payback time, it is recommended as the optimal option. The total capital cost is $13,241,232 and the annual billing cost savings are $907,231. The summer on-peak demand total reduction for four plants is 5,036 kW or 45.9% of the total summer on-peak billing demand in 2008. It is noted from Table 17 that no rebate from Austin Energy is assumed. The utility will provide a rebate for TES, but the exact amount is not known at this point. The simple paybacks will be significantly less when the Austin Energy rebates are included.

Table 18 Monthly simulation results for a 3.5 M gallon tank for TFC

Month	Elec. Energy savings (kWh)	Energy cost savings ($)	Demand cost savings ($)	Control strategy	off-peak num	on-peak num
1	172,807	$ 24,619	$ 47,278	Storage-priority	4	3
2	155,522	$ 23,248	$ 48,383	Storage-priority	5	2
3	167,428	$ 24,631	$ 50,178	Storage-priority	4	3
4	170,318	$ 23,811	$ 51,736	Storage-priority	4	3
5	199,848	$ 18,692	$ 58,747	Full storage	5	0
6	239,460	$ 21,032	$ 60,030	Full storage	5	0
7	259,450	$ 21,919	$ 62,638	Full storage	5	0
8	258,152	$ 22,736	$ 62,176	Full storage	5	0
9	231,960	$ 19,127	$ 58,275	Full storage	5	0
10	193,506	$ 16,715	$ 50,138	Full storage	4	0
11	171,877	$ 23,764	$ 44,533	Storage-priority	4	2
12	157,098	$ 23,816	$ 49,010	Storage-priority	4	2
Total	2,377,427	$ 264,109	$ 643,121			

The monthly results for a 3.5M gallon tank option are shown in Table 18. The total electrical energy reduction is 2,377,427 kWh per year. The total billing cost savings ($907,231 per year) come from the energy cost savings ($264,109 per year) and demand

cost savings ($643,121 per year). Storage priority control strategy is used during the winter months, while full-storage control strategy is preferred during the summer months. During the winter months, the maximum number of chillers on-stage during the on-peak period is limited to 2 or 3 to reduce on-peak electricity consumption. During the summer months, the maximum number of chillers staged on during the on-peak period is zero, which means no chiller is staged on and the TES tank can meet the chilled water demand during the on-peak period. The maximum number of chillers staged on during the off-peak period is 4 or 5 to fully charge the tank. This also indicates that only the new chillers in the CPP and SFA plants will be staged on, while the older ones will be on standby.

This is only a simulation based on the information available at the present time. An in-depth engineering study is needed to determine more details when additional information and data are available, such as average plant performance, piping costs, loop load changes due to building commissioning and weather, TES storage plant placement, and other data. However, this study provided a preliminary feasibility study for TFC to determine whether or not to move forward with a LOANSTAR loan application from the State Energy Conservation Office.

4.7.4 Sensitivity study

In this study, some important parameters use estimated values and are assumed constant all year around. It is necessary to test if the uncertainties of these parameters can significantly change the payback time. The selected parameters are FOM, loop ChW delta-T, cooling load factor, and tank minimal ChW water level setpoint. Seven

scenarios are designed for each parameter. A 3.5 M gallon tank is used for the sensitivity study. The annual savings and payback time are calculated for all scenarios shown in Table 19. For each parameter, the scenario shaded is the default value used in the previous simulations.

Table 19 Parameter range of sensitivity study for TFC

Variables	Unit	1	2	3	4	5	6	7
Tank FOM	-	1.00	0.98	0.96	0.94	0.92	0.90	0.88
ChW DT	ºF	11.5	11.0	10.5	10.0	9.5	9.0	8.5
Load Factor	-	1.08	1.04	1.00	0.96	0.92	0.88	0.84
Tank min level	-	0.35	0.30	0.25	0.20	0.15	0.10	0.05

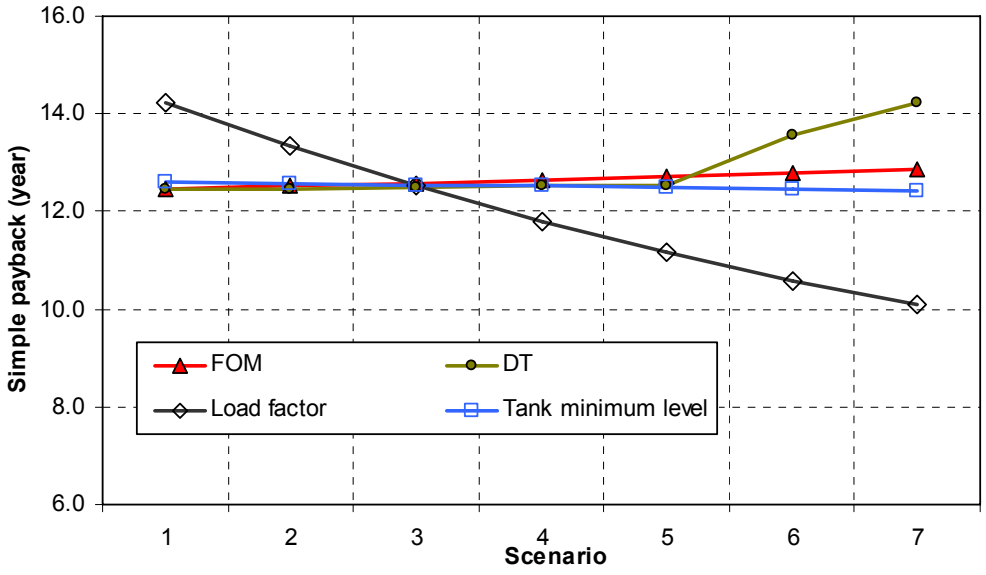

Figure 39 TFC TES tank payback sensitivity to variants of plant parameters

The sensitivity of the TES system simple payback to different parameters is shown in Figure 39. It is noted that the most sensitive parameter is load factor, while the least sensitive one is the tank minimum ChW level. Even as the tank minimum level changes from 0.35 to 0.05, the payback shortens only 0.2 years. The payback time will increase only 0.4 years even if the tank FOM drops from 1.00 to 0.88. However, if the plant load factor decreases from 1.08 to 0.84, the payback time reduces 3.1 years. As the Continuous Commissioning® is conducted on the building side, an obvious ChW consumption reduction is expected in the future and a shorter payback time will be expected, accordingly. The loop delta-T has no obvious effect on the payback until it is less than 9.5 ºF when one chiller has to be staged on during the on-peak period. This is due to a reduced tank capacity because of a lower loop ChW delta-T.

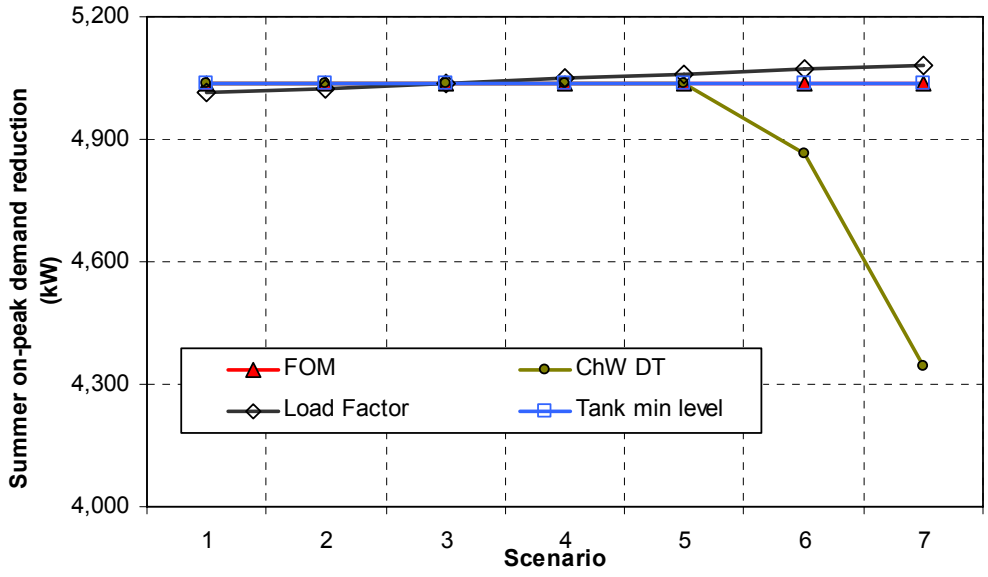

Figure 40 TFC TES tank on-peak demand reduction sensitivity to variants of plant parameters

As an important factor, the summer on-peak demand reduction is also calculated for each scenario, which is shown in Figure 40. The effect of tank FOM, ChW delta-T, and load factor on the demand reduction is negligible. However, the demand reduction drops 692 kW if the loop delta-T is reduced to 8.5 °F. A higher delta-T leads to a higher tank inventory and more electricity load can be shifted from the on-peak hours to the off-peak hours. Finally, the actual cooling profile is important to determine the demand. Even if the cooling load increases by 8% compared to the baseline, the on-peak demand reduction does not change due to sufficient tank capacity.

4.8 TFC: Summary and Conclusions

The TFC chilled water system in the downtown area of Austin is an aged system and it consists of four standalone loops. An underground piping system is to be established to connect the four loops together, and a chilled water storage tank is to be erected and shared among the four plants. Based on the analysis on the historical data, utility rate structures, and equipment information, the electricity energy and billing cost baselines are generated. A simplified TES plus four plants model is built based on some assumptions. To find the optimal tank size and operation strategy, eight scenarios are designed and simulated. Following are some conclusions:

(1) A 3.5 million gallon tank is recommended as the optimal option since this scenario has the shortest payback time and the project total cost is within the budget.

(2) Full storage strategy is selected for the summer months and storage-priority strategy is selected for the winter months. Only the new chillers in the CPP and SFA plants will be staged on, while all other chillers will be on standby.

(3) The total cost of the project is $13,241,232, and it can bring annual billing cost savings of $907,231 and avoided chiller cost of $1,881,344. The annual electrical energy reduction is 2,377,427 kWh and the simple payback is 12.5 years.

(4) The new system will qualify for the Rider TOU-TES clause.

5. SUMMARY

5.1 Summary of Present Work

A thermal energy storage tank provides great opportunities to reduce the operating costs of a cooling system. Different from other studies on an ice storage tank, a naturally stratified chilled water storage system is the focus of this study. Driven by the needs for making full utilization of a chilled water TES system, a generic methodology for determining the optimal operating strategies for a chilled water storage system under a Time-of-Use electricity rate structure has been developed. It allows the investigation of a wide range of key parameters influencing the system's behaviors and the operating costs. This work can be summarized into a theoretical section and application section.

5.1.1 Theoretical work

This methodology is based on a new classification of operating strategies and a comprehensive search path. Each operating strategy consists of a type of control strategy and the maximum numbers of chillers on-stage during the off-peak and on-peak periods. These two numbers should be no less than zero and no higher than the maximum number of chillers available in the plant. For each month, a search is performed for all possible operating strategies, and the hourly profiles of the tank chilled water level and system total power are simulated by a System Model. The operating strategies with the lowest tank water level lower than a predefined limit are removed. An Electricity Rate Model is

run to calculate the monthly billing cost of each remaining operating strategy. The operating strategy with the lowest billing cost is selected as the optimal strategy for the current month. Plant optimization with a GRG nonlinear solver is followed for the selected optimal operating strategy to further improve the whole system performance. The most popular plant variables to be optimized are chiller ChW leaving temperature, CT approach temperature, and CW flow rate per chiller.

In this study, a TES system is composed of three parts: TES tank, plant, and loop. A System Model is used to calculate the hourly tank chilled water level and the whole system power at given inputs. It defines the relations among sub-models built for the above three parts as well as for control strategies, non-plant power, and the chiller model. As each sub-model is self-contained, it is possible to simplify or complicate each sub-model to accommodate various prerequisites of precision and limitation of time and resources. It is also possible to place new control strategies into the System Model to explore its savings potential.

In the TES sub-model, the ChW volume is used to describe the tank inventory, and the ChW flow rate is selected to quantify the inventory change. The tank operating mode is controlled by modulating the plant total ChW flow rate. The operating strategy is, in fact, to define a profile of the plant total ChW flow. A FOM is used to quantify the capacity loss due to mixing effects in the thermocline. The loss due to tank wall heat transfer, together with pumping and piping heat loss is accounted for by the temperature rise between the chiller ChW leaving temperature and the loop ChW supply temperature.

A forward plant sub-model is built to calculate the plant power at a given total plant flow rate. Considering the fact that it is most complex and most important in a plant, the chiller is modeled with a semi-physical model called the Gordon-Ng model to accommodate extrapolation. A wire-to-water efficiency in kW per ton is used to define the pump and fan performance. The plant power is the product of total plant ChW production and the sum of kW per ton for CTs, CWPs, CHLRs, and PPMPs plus the SPMP power. Specifically, a new regression model is proposed to calculate the cooling tower fan power as a function of the cooling tower approach temperature. This model eliminates iterations required in an effectiveness model. This plant sub-model can also be used to study plant optimizations and estimate the savings potential of various commissioning measures or retrofitting options.

The purpose of the loop side sub-model is to simulate the loop ChW return temperature, which is critical to a ChW storage system. A regression model is suggested and the standard least-squares linear regression method is adopted to indentify the model coefficients from the trended data. The internal and external predictive abilities are both tested to ensure a high reliability. The SPMP power is calculated from the loop ChW total flow rate, loop hydraulic coefficients, and loop end DP setpoints.

Four control strategies are built into the Control Strategy sub-model: full storage, chiller-priority, storage-priority, and a new optimal strategy. The scenario without TES can also be simulated and used as the baseline when calculating the savings. The function of the Control Strategy sub-model is to determine the hourly profile of the on-stage chiller number and plant total ChW flow rate based on certain algorithms. For the

new optimal strategy, the billing costs are reduced by shifting electricity load during the on-peak hours to the off-peak hours and leveling the peak demand or reducing the on-peak demand. It can further booster the plant efficiency by optimally loading the chiller and avoiding running chillers during the high ambient WB hours.

In addition, a non-plant power sub model is required to simulate the power which is billed along with, but not covered in above models. Its form could be different case by case. The chiller model is also used to calculate the chiller part load with the lowest kW per ton and load capacity at different conditions.

5.1.2 Applications

This methodology was used in two projects to illustrate its applicability under two widely-different scenarios. Every project is a one-of-a-kind, and it is not anticipated that this methodology can be applied to all applications without special considerations and modifications. Such considerations and modifications are also illustrated in the two applications.

The first project is the DFW International Airport Energy Plaza. This is a state-of-the-art energy system with a comprehensive control, metering and trending system. A 90,000 ton-hr naturally stratified ChW storage tank was erected to eliminate running chillers during the on-peak period in the summer months. The electricity for this facility is charged under a special TOU rate structure and two demand charges are defined. The purpose of the simulations is to find optimal operating strategies and plant operating setpoints to minimize the annual total electricity billing cost.

The other project is a feasibility and preliminary design study for the installation of a TES system in downtown Austin for the Texas Facilities Commission. The purpose of this study is to evaluate the economic feasibility of connecting four stand-alone plants, together with underground piping, and erecting a new ChW TES tank for the system. As this is an old system and little trended data is available, a constant loop delta-T and a constant chiller supply temperature are assumed. Eight scenarios with different tank size were evaluated and the annual energy and dollar savings are obtained. Based on the estimation of tank costs, the simple paybacks of the eight options are presented.

5.1.3 Original contributions

The original and major contributions of this research are summarized as follows:

(1) Proposed a generic methodology to determine the optimal control strategies for a chilled water storage system. This method is easy to follow and has great flexibility. Its practicability is illustrated with two project applications.

(2) Built a new classification of various operating strategies. It consists of a control strategy and the maximum number of chillers running during the off-peak and on-peak periods, which is like demand limiting. This classification clarifies and refines the conventional definitions. It is also easy to implement in practice.

(3) Introduced a new tank state transition equation with chilled water volume in the tank and ChW flow rate entering or leaving the tank. Different from the equation with chilled water tonnage, this equation eliminates the effect of

chilled water delta-T on the tank inventory and makes tank inventory consistent.

(4) Built a new forward plant model to simulate the chilled water plant power and no iterations are involved. In this model, the chiller is modeled with a semi-physical model to accommodate extrapolation. A wire-to-water efficiency in kW per ton is used to define the pump and fan performance. Especially, a new regression model is proposed to calculate the cooling tower fan power as a function of the cooling tower approach temperature.

(5) Proposed a new control strategy to make full use of the energy savings potential of a TES system. Except for shifting ChW production from high cost hours to low cost hours, this strategy will load the chiller optimally and avoid running the chiller during the high WB hours. It may further increase the annual billing cost savings for the DFW project. The tank operation during the winter months can be justified.

5.2 Future Work

Some of research activities which can be conducted to complement and enhance this work are as follows:

(1) Study the characteristics of the loop delta-T profile and investigate a more accurate method to predict it. This may improve the reliability and precision of this methodology.

(2) The operating strategies generated by this method will depend on the quality of the underlying assumptions and models. The studies introduced in the

dissertation are still based on simulations. The next required step is the development of a real controller for a practical system and implement the control strategy to prove its effectiveness, especially in comparison with conventional strategies. An accurate load prediction model and weather information source will be needed.

(3) Study the interactions between AHU air side and water side and optimize the operations of the whole HVAC system including plant, tank, loop, AHUs, and terminal boxes.

(4) In the process of the deregulation of public utilities, RTP rates will be more popular in the future. Proposing a new operating strategy to minimize the billing cost under an RTP rate structure will be a new task. It is necessary to build a model to predict the electricity price and a model to predict the cooling load in the next 24 hours. For each day, the definitions of the off-peak and on-peak hours can be determined according to the following principle. The volume of the ChW shifted from the on-peak hours to off-peak hours will be equal to the tank volume. If not shifted, the cost of this part of ChW production is maximized. An accurate weather data source or weather condition prediction model is a critical step for this study.

(5) Study the effect of loss of cooling capacity on the facility operation. To avoid hitting an on-peak high demand when the tank is unexpectedly depleted before the end of on-peak hours, a short time loss of cooling or supplying an unusual high temperature chilled water could be an emergency measurement.

Its negative effect on the building thermal comfort can be mitigated by the thermal inertia of the facility.

(6) Study the life-cycle economic effectiveness of a TES project. In most cases, a TES project is a big long-term investment. Simple payback methods cannot reflect the effects of various factors, such as loan interest, electricity rate fluctuation, taxes, and equipment depreciation. Using a system without TES as a reference, a life-cycle economic analysis can be performed to study the advantages and disadvantages of a TES system.

(7) Conduct the risk analysis of the TES system operations. In the simulation study, scenarios can be designed to investigate the results under different weather conditions, load profiles, and system performances. Compare the possibilities of prematurely depleting the tank under different scenarios and find the corresponding measures to reduce this risk, such as increase the tank level low limit or the number of running chillers.

REFERENCES

Ahn, B. C., and J. W. Mitchell. 2001. Optimal control development for chilled water plants using a quadratic representation. *Energy and Buildings* 33(4): 371-78.

Andrepont, J. S. 2006. Developments in thermal energy storage large applications, low temps, high efficiency, and capital savings. *Energy and Engineering* 103(4): 7-18.

ARI. 2001. *ARI 410: 2001 Forced-circulation Air-heating and Air-cooling Coils* Arlington, VA: Air-Conditioning and Refrigeration Institute.

Armstrong. 2006. Ultra-efficient chilled water integrated plant package. From http://www.armstrongpumps.com/Data/pdfbrochures/Links/02_10_002/12-3_IPP_CHW_brochure.pdf.

Armstrong, P. R., T. N. Bechtel, C. E. Hancock, S. E. Jarvis, J. E. Seem, et al. 1989. *Environment for structured implementation of general and advanced HVAC controls—Phase II final report*. Washington, DC: Department of Energy.

ASHRAE. 1996. *ASHRAE Handbook—HVAC Systems and Equipment, Chapter 38 Centrifugal Pumps*. Atlanta, GA: American Society of Heating, Refrigerating and Air-Conditioning Engineers, Inc.

ASHRAE. 2003a. *ASHRAE Handbook—HVAC Applications Chapter 34 Thermal Storage*. Atlanta, GA: American Society of Heating, Refrigerating and Air-Conditioning Engineers, Inc.

ASHRAE. 2003b. *ASHRAE Handbook—HVAC Applications Chapter 41 Supervisory Control Strategies and Optimization*. Atlanta, GA: American Society of Heating, Refrigerating and Air-Conditioning Engineers, Inc.

ASHRAE. 2005. *ASHRAE Handbook—Fundamentals Chapter 28 Climatic Design Information*. Atlanta, GA: American Society of Heating, Refrigerating and Air-Conditioning Engineers, Inc.

ASHRAE. 2006. *RP-1054 cool storage operating and control strategies*. Atlanta, GA: American Society of Heating, Refrigerating and Air-Conditioning Engineers, Inc.

Bahnfleth, W. P., and W. S. Joyce. 1994. Energy use in a district cooling system with stratified chilled-water storage. *ASHRAE Transactions* 100(1): 1767-1778.

Bahnfleth, W. P., and A. Musser. 1998. Thermal performance of a full-scale stratified chilled-water thermal storage tank. *ASHRAE Transactions* 104(2): 377-388.

Bahnfleth, W. P., and E. B. Peyer. 2006. Energy use and economic comparison of chilled-water pumping system alternatives. *ASHRAE Transactions* 112(2): 198-208.

Bahnfleth, W. P., and E. B. Peyer. 2007. Energy use characteristics of variable primary flow chilled water pumping systems. Washington, DC: International Congress of Refrigeration.

Barbosa, R. M., and N. Mendes. 2008. Combined simulation of central HVAC systems with a whole-building hygrothermal model. *Energy and Buildings* 40(3): 276-288.

Bellman, R. 1957. *Dynamic Programming*. Princeton, NJ: Princeton University Press.

Bernier, M. A., and B. Bourret. 1999. Pumping energy and variable frequency drives. *ASHRAE Journal* 41(12): 37-40.

Bradford, J. D. 1998. Optimal supervisory control of cooling plants without storage. Ph.D. Dissertation, Department of Civil, Environmental and Architectural Engineering, University of Colorado.

Braun, J. E. 1988. Methodologies for the design and control of central cooling plants. Ph.D. Dissertation, Department of Mechanical Engineering, University of Wisconsin-Madison.

Braun, J. E. 1989. Effectiveness models for cooling towers and cooling coils. *ASHRAE Transactions* 96(2): 164-174.

Braun, J. E. 1992. A comparison of chiller-priority, storage-priority, and optimal control of an ice system. *ASHRAE Transactions* 98(1): 893-902.

Braun, J. E. 2007a. A near-optimal control strategy for cool storage systems with dynamic electric rates. *HVAC&R Research* 13(4): 557-580.

Braun, J. E. 2007b. Impact of control on operating costs for cool storage systems with dynamic electric rates. *ASHRAE Transactions* 113(2): 343-354.

Braun, J. E., and G. T. Diderrich. 1990. Near-optimal control of cooling towers for chilled-water systems. *ASHRAE Transactions* 96(2): 806-813.

Braun, J. E., S. A. Klein, J. W. Mitchell, and W. A. Beckman. 1989b. Applications of optimal control to chilled water systems without storage. *ASHRAE Transactions* 95(1): 663-675.

Braun, J. E., S. A. Klein, J. W. Mitchell, and W. A. Beckman. 1989c. Methodologies for optimal control to chilled water systems without storage. *ASHRAE Transactions* 95(1): 652-662.

Braun, J. E., J. W. Mitchell, S. A. Klein, and W. A. Beckman. 1987. Performance and control characteristics of a large central cooling system. *ASHRAE Transactions* 93(1): 1830-1852.

Caldwell, J. S., and W. P. Bahnfleth. 1997. Chilled water thermal energy storage without electric rate incentives or rebates. *Journal of Architectural Engineering* 3(3): 133-140.

Caldwell, J. S., and W. P. Bahnfleth. 1998. Identification of mixing effects in stratified chilled-water storage tanks by analysis of time series temperature data. *ASHRAE Transactions* 104(2): 366-376.

Chang, Y. 2004. A novel energy conservation method—Optimal chiller loading. *Electric Power Systems Research* 69(2-3): 221-226.

Chang, Y. 2006. An innovative approach for demand side management—optimal chiller loading by simulated annealing. *Energy* 31(12): 1883-1896.

Chang, Y., F. Lin, and C. Lin. 2005. Optimal chiller sequencing by branch and bound method for saving energy. *Energy Conversion and Management* 46(13-14): 2158-2172.

Chow, T. T., G. Q. Zhang, Z. Lin, and C. L. Song. 2002. Global optimization of absorption chiller system by genetic algorithm and neural network. *Energy and Buildings* 34(1): 103-109.

Cumali, Z. 1988. Global optimization of HVAC system operations in real time. *ASHRAE Transactions* 94(1): 1729-1744.

Dorgan, C. B. 2001. A descriptive framework for cool storage operating and control strategies. Atlanta, GA: 2001 ASHRAE Winter Meeting.

Dorgan, C. E., and J. S. Elleson. 1993. *Design Guide for Cool Thermal Storage*. Atlanta, GA: American Society of Heating, Refrigerating and Air-Conditioning Engineers, Inc.

Drees, K. H. 1994. Modeling and control of area-constrained ice storage systems. M.S. Thesis, Department of Mechanical Engineering, Purdue University.

Drees, K. H., and J. E. Braun. 1995. Modeling and control of area constrained ice storage systems. *HVAC&R Research* 1(1): 143-159.

Drees, K. H., and J. E. Braun. 1996. Development and evaluation of a rule-based control strategy for ice storage systems. *HVAC&R Research* 2(4): 312-336.

Durkin, T. H. 2005. Evolving design of chiller plants. *ASHRAE Journal* 47(11): 40-50.

Erpelding, B. 2006. Ultra efficient all-variable-speed chilled water plants. *Heating Piping Air Conditioning* 78(3): 35-43.

Flake, B. A. 1998. Parameter estimation and optimal supervisory control of chilled water plants. Ph.D. Dissertation, Department of Mechanical Engineering, University of Wisconsin-Madison.

Forrester, J. R., and W. J. Wepfer. 1984. Formulation of a load prediction algorithm for a large commercial building. *ASHRAE Transactions* 90(2B): 536-551.

Furlong, J. W., and F. T. Morrison. 2005. Optimization of water-cooled chiller-cooling tower combinations. *CTI Journal* 26(1): 12-19.

Gordon, J. M., and K. C. Ng. 2000. *Cool Thermodynamics*. Cambridge, UK: Cambridge International Science Publishing.

Graves, R. D. 2003. Thermodynamic modelling and optimization of a screw compressor chiller and cooling tower system. M.S. Thesis, Department of Mechanical Engineering, Texas A&M University.

Gretarsson, S. P., C. O. Pedersen, and R. K. Strand. 1994. Development of a fundamentally based stratified thermal storage tank model for energy analysis calculations. *ASHRAE Transactions* 100(1): 1213-1220.

Hackner, R. J., J. W. Mitchell, and W. A. Bechman. 1985. HVAC system dynamics and energy use in buildings- Part II. *ASHRAE Transactions* 91(1): 781-795.

Hajiah, A. E. H. 2000. Development and implementation of an optimal controller of a central cooling plant using ice storage system and building thermal mass. Ph.D. Dissertation, Department of Civil Engineering, and Architecture Engineering, University of Colorado at Boulder.

Hartman, T. B. 1993. *Direct Digital Controls for HVAC Systems, Chapter 1*. New York: McGraw-Hill.

Hartman, T. B. 1995. Global optimization strategies for high-performance controls. *ASHRAE Transactions* 101(2): 679-687.

Hartman, T. B. 1996. Design issues of variable chilled water flow-through chillers. *ASHRAE Transactions*: SA-96-12-2.

Hartman, T. B. 1999a. Loop chiller plant dramatically lowers chilled water costs. Lahaina, Maui, HI: ASME International Conference Renewable and Advanced Energy Systems for the 21st Century.

Hartman, T. B. 1999b. Loop chiller plants benefit users & electric utilities. Madison, WI: EPRI Target Chillers Meeting '99 Technical Seminar.

Hartman, T. B. 2001a. All-variable speed centrifugal chiller plants. *ASHRAE Journal* 43(9): 43-52.

Hartman, T. B. 2001b. Ultra-efficient cooling with demand-based control. *HPAC Engineering* 73(12): 29-35.

Hartman, T. B. 2005. Designing efficient systems with the equal marginal performance principle. *ASHRAE Journal* 47(7): 64-70.

Hartman, T. B. 2006. New Vistas with Relational Control. From http://www.automatedbuildings.com/news/mar06/articles/hartman/060227054447hartman.htm.

Henze, G. P. 1995. Evaluation of optimal control for ice storage systems. Ph.D. Dissertation, Department of Civil Engineering, and Architecture Engineering, University of Colorado at Boulder.

Henze, G. P. 2003a. Impact of real-time pricing rate uncertainty on the annual performance of cool storage systems. *Energy and Buildings* 35(3): 313-325.

Henze, G. P. 2003b. An overview of optimal control for central cooling plants with ice thermal energy storage. *Journal of Solar Energy Engineering* 125(3): 302-309.

Henze, G. P., B. Biffar, D. Kohn, and M. P. Becker. 2008. Optimal design and operation of a thermal storage system for a chilled water plant serving pharmaceutical buildings. *Energy and Buildings* 40(6): 1004-4019.

Henze, G. P., R. H. Dodier, and M. Krarti. 1997a. Development of a predictive optimal controller for thermal energy storage systems. *HVAC&R Research* 3(3): 233-264.

Henze, G. P., M. Krarti, and M. J. Brandemuehl. 1997b. A simulation environment for the analysis of ice storage controls. *HVAC&R Research* 3(2): 128-148.

Henze, G. P., and J. Schoenmann. 2003c. Evaluation of reinforcement learning control for thermal energy storage systems. *HVAC&R Research* 9(3): 259-276.

Homan, K. O., C. W. Sohn, and S. L. Soo. 1996. Thermal performance of stratified chilled water storage tanks. *HVAC&R Research* 2(2): 150-170.

Hull, D. G. 2003. *Optimal Control Theory for Applications*. New York: Springer-Verlag, Inc.

Hyman, L. B., and D. Little. 2004. Overcoming low delta T, negative delta P at large university campus. *ASHRAE Journal* 46(2): 28-34.

Ihm, P., M. Krarti, and G. P. Henze. 2004. Development of a thermal energy storage model for EnergyPlus. *Energy and Buildings* 36(8): 807-814.

Isukapalli, S. S. 1999. Uncertainty analysis of transport-transformation models. Ph.D. Dissertation, Department of Chemical and Biochemical Engineering The State University of New Jersey

Jiang, W. 2005. Framework combining static optimization, dynamic scheduling and decision analysis applicable to complex primary HVAC&R systems. Ph.D. Dissertation, Department of Mechanical Engineering, Drexel University.

Jiang, W., and T. A. Reddy. 2003. Re-evaluation of the Gordon-Ng performance models for water-cooled chillers. *ASHRAE Transactions* 109(2): 272-287.

Kaya, A., and A. Sommer. 1985. Energy management of chillers by multilevel control and optimization. *Journal of Dynamic Systems, Measurement, and Control* 107(4): 270-277.

Kirsner, W. 1995. Troubleshooting chilled water distribution problems at the NASA Johnson Space Center. *Heating Piping Air Conditioning* 67(2): 51-59.

Kota, N. N., J. M. House, J. S. Arora, and T. F. Smith. 1996. Optimal control of HVAC systems using DDP and NLP techniques. *Optimal Control Applications & Methods* 17(1): 71-78.

Krarti, M., M. J. Brandemuehl, and G. P. Henze. 1995. *RP-809 -- Evaluation of Optimal Control for Ice Storage Systems*. Atlanta, GA: American Society of Heating, Refrigerating and Air-Conditioning Engineers, Inc.

Kreider, J. F., and J. S. Haberl. 1994. Predicting hourly building energy use: The great energy predictor shootout-overview and discussion of results. *ASHRAE Transactions* 100(2): 1104-1118.

Kreider, J. F., and X. A. Wang. 1991. Artificial neural networks demonstration for automated generation of energy use predictors for commercial buildings. *ASHRAE Transactions* 97(2): 775-779.

Lau, A. S. 1985. Development of computerized control strategies for a large chilled water plant. *ASHRAE Transactions* 91(1): 766-780.

Ling, K. V., and A. L. Dexter. 1994. Expert control of air-conditioning plant. *Automatica* 30(5): 761-773.

Lu, L., W. Cai, Y. S. Chai, and L. Xie. 2005a. Global optimization for overall HVAC systems—Part I problem formulation and analysis. *Energy Conversion and Management* 46(7-8): 999-1014.

Lu, L., W. Cai, Y. C. Soh, and L. Xie. 2005b. Global optimization for overall HVAC systems—Part II problem solution and simulations. *Energy Conversion and Management* 46(7-8): 1015-1028.

Lu, L., W. Cai, Y. C. Soh, L. Xie, and S. Li. 2004. HVAC system optimization—condenser water loop. *Energy Conversion and Management* 45(4): 613-630.

Lu, L., W. Cai, L. Xie, S. Li, and Y. C. Soh. 2005c. HVAC system optimization—in-building section. *Energy and Buildings* 37(1): 11-22.

Ma, D. L., S. H. Chung, and R. D. Braatz. 1999. Worst-case performance analysis of optimal batch control trajectories. *AIChE Journal* 45(7): 1469-1476.

Ma, Z., and S. Wang. 2009. An optimal control strategy for complex building central chilled water systems for practical and real-time applications. *Building and Environment* 44(6): 1188-1198.

Massie, D. D. 2002. Optimization of a building's cooling plant for operating cost and energy use. *International Journal of Thermal Sciences* 41(12): 1121-1129.

Moe, E. M. 2005. Applying pressure independent control to achieve high delta-T. Nashville, TN: International District Energy Association (IDEA) Annual Conference.

Montgomery, D. C., and G. C. Runger. 2002. *Applied Statistics and Probability for Engineers 3rd*. New York: John Wiley & Sons, Inc.

Moore, B. J., and D. S. Fisher. 2003. Pump differential pressure setpoint reset based on chilled water valve position. *ASHRAE Transactions* 109(1): 373-379.

Morgan, S. 2006. Experimental analysis of optimal control of passive and active building thermal storage inventory. M.S. Thesis, Department of Civil, Environmental, and Architectural Engineering, University of Colorado at Boulder.

Nassif, N., S. Kajl, and R. Sabourin. 2005. Optimization of HVAC control system strategy using two-objective genetic algorithm. *HVAC&R Research* 11(3): 459-486.

Nelles, O. 2001. *Nonlinear System Identification: From Classical Approaches to Neural Networks and Fuzzy Models*. Berlin: Springer-Verlag.

Nelson, J. E. B., A. R. Balakrishnan, and S. S. Murthy. 1999a. Experiments on stratified chilled-water tanks. *International Journal of Refrigeration* 22(3): 216-234.

Nelson, J. E. B., A. R. Balakrishnan, and S. S. Murthy. 1999b. Parametric studies on thermally stratified chilled water storage systems. *Applied Thermal Engineering* 19(1): 89-115.

Olson, R. T. 1993. A dynamic procedure for the optimal sequencing of plant equipment part1 algorithm fundametnals. *Engineering Optimization* 21(1): 63-78.

Phelan, J., M. J. Brandemuehl, and M. Krarti. 1997. In-situ performance testing of chillers for energy analysis. *ASHRAE Transactions* 103(1): 290-302.

Ramirez, W. F. 1994. *Process Control and Identification*. Boston: Academic Press, Inc.

Reddy, T. A., and K. K. Andersen. 2002a. An evaluation of classical steady-state off-line linear parameter estimation methods applied to chiller performance data. *HVAC&R Research* 8(1): 101-124.

Rishel, J. B. 2002. Connecting buildings to central chilled water plants. *ASHRAE Journal* 44(11): 24-31.

Rishel, J. B. B. 2003. Control of variable speed pumps for HVAC water systems. *ASHRAE Transactions* 109(1): 380-389.

Roth, K., R. Zogg, and J. Brodrick. 2006. Cool thermal energy storage. *ASHRAE Journal* 48(9): 94-96.

Seem, J. E., and J. E. Braun. 1991. Adaptive methods for real-time forecasting of building electrical demand. *ASHRAE Transactions* 97(1): 710-721.

Sreedharan, P., and P. Haves. 2001. Comparison of chiller models for use in model-based fault detection. Austin, TX: International Conference for Enhanced Building Operations(ICEBO).

Sun, C., K. Temple, T. Rossi, and J. E. Braun. 2006. *Final Report for RP-1252: Interaction between dynamic electric rates and thermal energy storage control*. Atlanta, GA: American Society of Heating, Refrigerating and Air-Conditioning Engineers, Inc.

Sun, J., and A. Reddy. 2005. Optimal control of building HVAC&R systems using complete simulation based sequential quadratic programming (CSB-SQP). *Building and Environment* 40(5): 657-669.

Taylor, S. T. 2002. Degrading chilled water plant delta-T causes and mitigation. *ASHRAE Transactions* 108(1): 641-653.

Taylor, S. T. 2006. Chilled water plant retrofit—a case study. *ASHRAE Transactions* 112(2): 187-197.

Tran, N., J. F. Kreider, and P. Brothers. 1989. Field measurement of chilled water storage thermal performance. *ASHRAE Transactions* 95(1): 1106-1112.

Wang, S. W. 2008. Supervisory and optimal control of building HVAC systems a review. *HVAC&R Research* 14(1): 3-32.

Wang, S. W., and J. Burnett. 2001. Online adaptive control for optimizing variable-speed pumps of indirect water-cooled chilling systems. *Applied Thermal Engineering* 21(11): 1083-1103.

Wang, Y.-W., W.-J. Cai, Y.-C. Soh, S.-J. Li, L. Lu, et al. 2004. A simplified modeling of cooling coils for control and optimization of HVAC systems. *Energy Conversion and Management* 45(18-19): 2915-2930.

Wei, G., M. Liu, Y. Sakurai, D. E. Claridge, and W. D. Turner. 2002. Practical optimization of full thermal storage system operation. *ASHRAE Transactions* 108(2): 360-368.

Wildin, M. W., and C. R. Truman. 1985. A summary of experience with stratified chilled water tanks. *ASHRAE Transactions* 91(1B): 956-976.

Xu, J., P. B. Luh, W. E. Blankson, R. Jerdonek, and K. Shaikh. 2005. An optimization-based approach for facility energy management with uncertainties. *HVAC&R Research* 11(2): 215-237.

Yao, Y. 2004. Optimal operation of a large cooling system based on an empirical model. *Applied Thermal Engineering* 24(16): 2303-2321.

Yoshida, H., and Y. Goto. 1999. Development of optimal operation of thermal storage tank and the validation by simulation tool. Kyoto, Japan: Building Simulation 1999.

Yoshida, H., and H. Yamaguti. 2001. Optimal operation of a HVAC systm with a thermal storage water tank. Rio de Janeiro, Brazil: Seventh International IBPSA Conference.

Yu, F. W., and K. T. Chan. 2007. Optimum load sharing strategy for multiple-chiller systems serving air-conditioned buildings. *Building and Environment* 42(4): 1581-1593.

Yu, F. W., and K. T. Chan. 2008. Environmental performance and economic analysis of all-variable speed chiller systems with load-based speed control. *Applied Thermal Engineering* 29(8-9): 1721-1729.

Yu, F. W., and K. T. Chan. 2008. Optimization of water-cooled chiller system with load-based speed control. *Applied Energy* 85(10): 931-950.

Zaheer-uddin, M., and R. V. Patel. 1993. The design and simulation of a sub-optimal controller for space heating. *ASHRAE Transactions* 99(1): 554-564.

Zaheer-uddin, M., and G. R. Zheng. 2000. Optimal control of time-scheduled heating, ventilating and air conditioning processes in building. *Energy Conversion and Management* 41(1): 49-60.

Zaheer-uddin, M., and G. R. Zheng. 2001. Multistage optimal operating strategies for HVAC systems. *ASHRAE Transactions* 107(2): 346-352.

APPENDIX A. DFW: SIMULATION RESULTS FOR ENERGY PLAZA

	Without TES (Scenario 6, Baseline)														
Month	Monthly Billing cost ($)	Energy cost ($)	Demand cost ($)	On-peak energy (kWh)	Off-peak energy (kWh)	Charged 4CP kW	Charged NCP kW	Current month 4CP kW	Current month NCP kW	On-peak CHW production (Ton-hr)	Off-peak CHW production (Ton-hr)	Noff	Non	ChW leaving temp (F)	ΔT approach (F)
3	$ 573,506	$ 476,485	$ 97,021	840,496	4,995,421	20,635	17,112	13,312	13,312	5,308,200	888,103	3	3	36.0	6.0
4	$ 540,835	$ 443,813	$ 97,021	816,600	4,835,130	20,635	17,112	15,690	15,949	5,241,329	866,755	3	3	36.0	6.0
5	$ 738,075	$ 641,053	$ 97,021	1,144,275	7,019,202	20,635	17,112	16,824	16,886	7,192,280	1,164,919	3	3	36.0	6.0
6	$ 869,079	$ 765,921	$ 103,159	1,354,931	8,398,663	20,635	20,190	20,107	20,190	8,406,076	1,346,545	4	4	36.0	6.0
7	$ 935,384	$ 821,312	$ 114,072	1,468,786	8,990,188	20,635	21,390	21,390	21,390	8,892,785	1,446,194	4	4	36.0	6.0
8	$1,029,173	$ 917,953	$ 111,220	1,626,279	10,063,368	20,635	21,108	21,034	21,108	9,908,221	1,595,767	4	4	36.0	6.0
9	$ 837,365	$ 734,250	$ 103,115	1,344,384	8,005,904	20,635	20,199	20,008	20,199	8,021,684	1,333,783	4	4	36.0	6.0
10	$ 661,379	$ 557,523	$ 103,855	1,041,838	6,057,929	20,635	19,395	19,395	19,395	6,280,129	1,061,604	4	4	36.0	6.0
11	$ 481,615	$ 385,502	$ 96,113	744,067	4,165,093	20,635	17,112	13,577	13,577	4,432,440	769,741	3	3	36.0	6.0
12	$ 383,306	$ 287,192	$ 96,113	534,515	3,122,726	20,635	17,112	13,034	13,034	3,463,093	580,385	2	2	36.0	6.0
1	$ 353,690	$ 257,577	$ 96,113	467,948	2,812,160	20,635	17,112	11,256	11,256	3,072,704	504,434	2	2	36.0	6.0
2	$ 372,033	$ 275,920	$ 96,113	537,801	2,975,895	20,635	17,112	11,745	11,745	3,237,833	574,484	2	2	36.0	6.0
Total	**$ 7,775,439**	**$ 6,564,501**	**$ 1,210,938**	**11,921,919**	**71,441,679**			**20,635**	**21,390**	**73,456,775**	**12,132,715**				

	Storage priority control strategy (Scenario 5)														
Month	Monthly Billing cost ($)	Energy cost ($)	Demand cost ($)	On-peak energy (kWh)	Off-peak energy (kWh)	Charged 4CP kW	Charged NCP kW	Current month 4CP kW	Current month NCP kW	On-peak CHW production (Ton-hr)	Off-peak CHW production (Ton-hr)	Noff	Non	ChW leaving temp (F)	ΔT approach (F)
3	$ 557,698	$ 482,166	$ 75,532	226,602	5,678,895	3,584	19,506	7,676	12,777	6,187,356	33,847	2	1	36.0	6.0
4	$ 519,795	$ 444,263	$ 75,532	277,635	5,379,822	3,584	19,506	18,205	18,205	5,982,490	115,479	2	3	36.0	6.0
5	$ 726,848	$ 651,316	$ 75,532	234,747	8,059,425	3,584	19,506	3,117	18,295	8,386,411	0	3	0	36.0	6.0
6	$ 863,514	$ 775,341	$ 88,173	251,765	9,621,796	3,584	23,882	3,485	23,882	9,805,700	0	4	0	36.0	6.0
7	$ 918,951	$ 828,906	$ 90,046	266,143	10,289,535	3,584	24,383	3,513	24,383	10,374,558	0	4	0	36.0	6.0
8	$1,018,351	$ 927,439	$ 90,911	291,186	11,519,267	3,584	24,106	3,858	24,106	11,544,323	0	4	0	36.0	6.0
9	$ 831,095	$ 743,903	$ 87,192	255,464	9,217,747	3,584	23,923	3,482	23,923	9,411,443	0	4	0	36.0	6.0
10	$ 641,113	$ 568,335	$ 72,778	239,986	6,997,465	3,584	19,506	8,390	18,705	7,405,923	10,696	3	1	36.0	6.0
11	$ 459,559	$ 386,781	$ 72,778	177,077	4,748,381	3,584	19,506	2,951	13,279	5,252,346	0	2	0	36.0	6.0
12	$ 358,488	$ 285,710	$ 72,778	129,058	3,509,312	3,584	19,506	2,910	13,200	4,090,113	0	2	0	36.0	6.0
1	$ 327,930	$ 255,152	$ 72,778	112,577	3,136,646	3,584	19,506	2,753	12,997	3,614,985	0	2	0	36.0	6.0
2	$ 347,331	$ 274,553	$ 72,778	136,253	3,360,034	3,584	19,506	2,831	12,814	3,843,233	0	2	0	36.0	6.0
Total	**$7,570,673**	**$6,623,866**	**$946,807**	**2,598,493**	**81,518,323**			**3,584**	**24,383**	**85,898,883**	**160,021**				
Saving	$204,766	-$59,365	$264,131	9,323,427	-10,076,645					-12,442,107	11,972,693				

	Chiller priority control strategy (Scenario 4)														
Month	Monthly Billing cost ($)	Energy cost ($)	Demand cost ($)	On-peak energy (kWh)	Off-peak energy (kWh)	Charged 4CP kW	Charged NCP kW	Current month 4CP kW	Current month NCP kW	On-peak CHW production (Ton-hr)	Off-peak CHW production (Ton-hr)	Noff	Non	ChW leaving temp (F)	ΔT approach (F)
3	$ 564,664	$ 476,485	$ 88,179	840,496	4,995,421	19,029	15,416	13,312	13,312	5,308,200	888,103	3	3	36.0	6.0
4	$ 533,885	$ 443,813	$ 90,071	816,600	4,835,130	19,029	15,949	15,690	15,949	5,241,329	866,755	3	3	36.0	6.0
5	$ 734,448	$ 641,053	$ 93,394	1,144,275	7,019,202	19,029	16,886	16,824	16,886	7,192,280	1,164,919	3	3	36.0	6.0
6	$ 865,431	$ 768,092	$ 97,339	1,344,820	8,436,424	19,029	18,825	18,825	18,825	8,427,402	1,325,829	3	3	36.0	6.0
7	$ 923,822	$ 823,122	$ 100,700	1,456,443	9,025,587	19,029	19,211	19,211	19,211	8,910,506	1,422,138	3	3	36.0	6.0
8	$1,031,681	$ 930,460	$ 101,221	1,550,685	10,298,232	19,029	19,270	19,270	19,270	10,034,893	1,471,930	3	3	36.0	6.0
9	$ 834,094	$ 735,497	$ 98,597	1,339,864	8,026,300	19,029	19,074	18,811	19,074	8,032,352	1,323,580	3	3	36.0	6.0
10	$ 656,445	$ 557,882	$ 98,563	1,040,543	6,063,796	19,029	18,707	18,707	18,707	6,283,140	1,058,713	3	3	36.0	6.0
11	$ 472,901	$ 385,502	$ 87,399	744,067	4,165,093	19,029	15,416	13,577	13,577	4,432,440	769,741	3	3	36.0	6.0
12	$ 374,591	$ 287,192	$ 87,399	534,515	3,122,726	19,029	15,416	13,034	13,034	3,463,093	580,385	2	2	36.0	6.0
1	$ 344,976	$ 257,577	$ 87,399	467,948	2,812,160	19,029	15,416	11,256	11,256	3,072,704	504,434	2	2	36.0	6.0
2	$ 363,319	$ 275,920	$ 87,399	537,801	2,975,895	19,029	15,416	11,745	11,745	3,237,833	574,484	2	2	36.0	6.0
Total	**$7,700,258**	**$6,582,596**	**$1,117,662**	**11,818,057**	**71,775,966**			**19,029**	**19,270**	**73,636,171**	**11,951,012**				
Saving	$75,181	-$18,095	$93,276	103,863	-334,287					-179,396	181,703				

	Full storage control strategy (Scenario 3)														
Month	Monthly Billing cost ($)	Energy cost ($)	Demand cost ($)	On-peak energy (kWh)	Off-peak energy (kWh)	Charged 4CP kW	Charged NCP kW	Current month 4CP kW	Current month NCP kW	On-peak CHW production (Ton-hr)	Off-peak CHW production (Ton-hr)	Noff	Non	ChW leaving temp (F)	ΔT approach (F)
3	$ 558,452	$ 482,921	$ 75,532	199,554	5,715,184	3,584	19,506	2,783	17,812	6,237,966	0	3	0	36.0	6.0
4	$ 524,573	$ 449,041	$ 75,532	184,410	5,533,890	3,584	19,506	2,991	18,249	6,147,156	0	3	0	36.0	6.0
5	$ 726,848	$ 651,316	$ 75,532	234,747	8,059,425	3,584	19,506	3,117	18,295	8,386,411	0	3	0	36.0	6.0
6	$ 863,514	$ 775,341	$ 88,173	251,765	9,621,796	3,584	23,882	3,485	23,882	9,805,700	0	4	0	36.0	6.0
7	$ 918,951	$ 828,906	$ 90,046	266,143	10,289,535	3,584	24,383	3,513	24,383	10,374,558	0	4	0	36.0	6.0
8	$1,018,351	$ 927,439	$ 90,911	291,186	11,519,267	3,584	24,106	3,858	24,106	11,544,323	0	4	0	36.0	6.0
9	$ 831,095	$ 743,903	$ 87,192	255,464	9,217,747	3,584	23,923	3,482	23,923	9,411,443	0	4	0	36.0	6.0
10	$ 641,162	$ 568,384	$ 72,778	230,964	7,007,103	3,584	19,506	3,432	18,705	7,416,451	0	3	0	36.0	6.0
11	$ 459,559	$ 386,781	$ 72,778	177,077	4,748,381	3,584	19,506	2,951	13,279	5,252,346	0	2	0	36.0	6.0
12	$ 358,488	$ 285,710	$ 72,778	129,058	3,509,312	3,584	19,506	2,910	13,200	4,090,113	0	2	0	36.0	6.0
1	$ 327,930	$ 255,152	$ 72,778	112,577	3,136,646	3,584	19,506	2,753	12,997	3,614,985	0	2	0	36.0	6.0
2	$ 347,331	$ 274,553	$ 72,778	136,253	3,360,034	3,584	19,506	2,831	12,814	3,843,233	0	2	0	36.0	6.0
Total	**$7,576,254**	**$6,629,447**	**$946,807**	**2,469,198**	**81,718,319**			**3,584**	**24,383**	**86,124,686**	**0**				
Saving	$199,185	-$64,946	$264,131	9,452,721	-10,276,641					-12,667,911	12,132,715				

	Optimal control strategy without plant optimization (Scenario 2)														
Month	Monthly Billing cost ($)	Energy cost ($)	Demand cost ($)	On-peak energy (kWh)	Off-peak energy (kWh)	Charged 4CP kW	Charged NCP kW	Current month 4CP kW	Current month NCP kW	On-peak CHW production (Ton-hr)	Off-peak CHW production (Ton-hr)	Noff	Non	ChW leaving temp (F)	ΔT approach (F)
3	$ 527,276	$ 460,112	$ 67,164	199,554	5,435,827	3,584	17,148	2,783	13,824	6,234,990	0	3	0	36.0	6.0
4	$ 490,078	$ 422,914	$ 67,164	184,410	5,201,176	3,584	17,148	2,991	15,186	6,102,361	0	3	0	36.0	6.0
5	$ 698,559	$ 631,395	$ 67,164	496,796	7,543,688	3,584	17,148	16,378	16,851	8,029,746	332,426	3	3	36.0	6.0
6	$ 833,667	$ 758,218	$ 75,450	251,765	9,403,737	3,584	20,194	3,485	20,194	9,772,677	0	4	0	36.0	6.0
7	$ 892,360	$ 812,483	$ 79,878	266,143	10,080,397	3,584	21,436	3,513	21,436	10,352,795	0	4	0	36.0	6.0
8	$ 991,198	$ 909,795	$ 81,402	291,186	11,294,579	3,584	21,349	3,858	21,349	11,511,823	0	4	0	36.0	6.0
9	$ 801,155	$ 725,484	$ 75,671	255,464	8,983,197	3,584	20,526	3,482	20,526	9,374,835	0	4	0	36.0	6.0
10	$ 614,957	$ 540,099	$ 74,858	230,964	6,646,912	3,584	20,119	3,432	20,119	7,330,719	0	4	0	36.0	6.0
11	$ 431,834	$ 367,054	$ 64,780	177,077	4,497,157	3,584	17,148	2,951	14,330	5,226,851	0	3	0	36.0	6.0
12	$ 334,677	$ 269,896	$ 64,780	206,464	3,230,526	3,584	17,148	16,578	16,578	3,932,437	122,169	3	4	36.0	6.0
1	$ 305,436	$ 240,655	$ 64,780	112,577	2,952,041	3,584	17,148	2,753	10,480	3,583,340	0	2	0	36.0	6.0
2	$ 324,979	$ 260,198	$ 64,780	206,016	3,107,473	3,584	17,148	10,149	10,149	3,718,523	104,851	2	2	36.0	6.0
Total	**$7,246,175**	**$6,398,304**	**$847,871**	**2,878,416**	**78,376,710**			**3,584**	**21,436**	**85,171,097**	**559,447**				
Saving	$529,264	$166,198	$363,066	9,043,503	-6,935,031					-11,714,322	11,573,268				

	Optimal control strategy with plant optimization (Scenario 1)														
Month	Monthly Billing cost ($)	Energy cost ($)	Demand cost ($)	On-peak energy (kWh)	Off-peak energy (kWh)	Charged 4CP kW	Charged NCP kW	Current month 4CP kW	Current month NCP kW	On-peak CHW production (Ton-hr)	Off-peak CHW production (Ton-hr)	Noff	Non	ChW leaving temp (F)	ΔT approach (F)
3	$ 507,562	$ 442,338	$ 65,224	210,513	5,207,181	3,744	16,523	2,908	13,082	6,343,352	0	3	0	43.5	4.6
4	$ 472,123	$ 406,899	$ 65,224	193,983	4,987,660	3,744	16,523	3,135	14,552	6,195,198	0	3	0	42.8	4.7
5	$ 678,620	$ 613,396	$ 65,224	559,494	7,251,778	3,744	16,523	15,912	16,379	8,007,623	427,326	3	3	40.3	4.8
6	$ 816,189	$ 739,902	$ 76,287	257,960	9,164,301	3,744	20,449	3,584	20,449	9,817,257	0	4	0	39.3	4.7
7	$ 858,703	$ 782,197	$ 76,506	280,923	9,679,940	3,744	20,266	3,745	20,266	10,452,526	0	4	0	42.0	4.7
8	$ 961,067	$ 881,847	$ 79,220	303,185	10,926,673	3,744	20,653	4,006	20,653	11,588,419	0	4	0	40.7	4.8
9	$ 774,267	$ 700,443	$ 73,825	265,707	8,654,059	3,744	19,895	3,642	19,895	9,446,183	0	4	0	41.1	4.8
10	$ 592,072	$ 519,666	$ 72,405	241,315	6,376,364	3,744	19,309	3,638	19,309	7,416,188	0	4	0	42.2	4.6
11	$ 416,077	$ 353,124	$ 62,952	185,397	4,311,455	3,744	16,523	3,060	13,601	5,303,138	0	3	0	43.0	4.8
12	$ 323,240	$ 259,469	$ 63,771	224,638	3,079,563	3,744	16,764	16,764	16,764	3,986,745	149,818	3	4	44.0	4.6
1	$ 297,200	$ 234,248	$ 62,952	115,851	2,867,172	3,744	16,523	2,858	10,425	3,630,117	0	2	0	41.0	4.6
2	$ 313,320	$ 250,367	$ 62,952	196,780	2,991,516	3,744	16,523	9,695	9,695	3,796,718	85,416	2	2	43.3	4.6
Total	**$7,010,439**	**$6,183,896**	**$826,543**	**3,035,747**	**75,497,661**			**3,744**	**20,653**	**85,983,464**	**662,559**				
Saving	$765,000	$380,605	$384,395	8,886,173	-4,055,983					-12,526,689	11,470,155				

APPENDIX B. TFC: ORIGINAL RATE STRUCTURE OF FOUR PLANTS

At present, CPP is charged under the State Large Primary Service Optional Time-of-Use Rate (E16). SFA is charged under the State Large Primary Service Rate (E15). REJ and WPC are charged under the State General Service - Demand Rate (E14). Following is a brief description of each rate from the Austin Energy website (www.austinenergy.com).

State Large Primary Service

Application: This rate is applicable to electric service required for buildings, facilities, and other establishments occupied and operated by the State of Texas. The customer shall furnish, install, own, maintain, and operate all facilities and equipment on the customer's side of the point of delivery. This rate is applicable to the State of Texas accounts that receive service at 12,500 volts (nominal) or higher and whose demand for power meets or exceeds 3,000 kilowatts for any two months within the previous twelve months or as determined by the City of Austin. Rider TOU-Thermal Energy Storage and the Optional Time-of-Use Rate may be attached to this rate.

Rate (E15):	**Winter Billing Months November through April**	**Summer Billing Months May through October**
Energy Rate (E15)	1.07¢ per kWh, for all kWh	1.07¢ per kWh, for all kWh
Demand Rate (ELD)	$10.94 per kW	$11.64 per kW

Character of Service: The Character of Service provided under this rate shall be alternating current, 60 cycles, single phase or three phases, in accordance with the Utilities Criteria Manual prescribed by the City of Austin which may be amended from

time to time. Electric service of one standard character will be delivered to one point on the customer's premises and measured through one meter.

Fuel Adjustment Clause (FAC) - plus an adjustment for variable costs, calculated according to the Fuel Adjustment Clause Tariff, multiplied by all kWh.

Minimum Bill: Customer will be assessed a monthly Minimum Bill of $12.00 if the above calculations result in a charge of less than $12.00.

Billing Demand: The kilowatt demand during the fifteen-minute interval of greatest use during the current billing month as indicated or recorded by metering equipment installed by the City of Austin. When power factor during the interval of greatest use is less than 85%, Billing Demand shall be determined by multiplying the indicated demand by 85% and dividing by the lower peak power factor

Optional Time-of-Use Rate:

At the option of the customer, a separate agreement may be entered into between the City and the customer for a time-of-use incentive rate. The customer shall permit the City to install all equipment necessary for time-of-use metering and to permit reasonable access to all electric service facilities installed by the City for inspection, maintenance, repair, removal, or data recording purposes.

Fuel Adjustment Clause (FAC) - plus an adjustment for variable costs, calculated according to the Fuel Adjustment Clause Tariff, multiplied by all kWh.

On-Peak: 1:00 p.m. to 9:00 p.m., Monday through Friday; May 1 through October 31. 8:00 a.m. to 10:00 p.m., Monday through Sunday; November 1 through April 30.

Off-Peak: 9:00 p.m. to 1:00 p.m., Monday through Friday; all day Saturday, Sunday, Memorial Day, Independence Day, and Labor Day; May 1 through October 31. 10:00 p.m. to 8:00 a.m. Monday through Sunday; November 1 through April 30.

Energy Rate (E16)	**Winter Billing Months November through April**	**Summer Billing Months May through October**
On-Peak	1.67 ¢ per kWh	2.37 ¢ per kWh
Off-Peak	(0 .33 ¢) per kWh	0 .52 ¢ per kWh
Demand Rate (ELD)		
On-Peak	$10.94 per kW	$11.64 per kW
Off-Peak	$0.00 per kW	$0.00 per kW

Terms and Conditions: Upon request, customers receiving service under this tariff will be provided dual feed service with reserve capacity, except that the customer will be responsible for the initial assessment fee, customer requested changes to the initial assessment, and facilities design and construction costs, as established in the fee schedule. Dual feed service with reserve capacity is electric service provided to the customer's premise(s) through two (or more) independent distribution feeders, with one feeder in normal service and the other in back-up service. Capacity is reserved for the second feeder, and is placed into service upon an outage of the primary feeder.

State General Service - Demand

Application:

This rate is applicable to electric service required for buildings, facilities, and other establishments occupied and operated by the State of Texas. This rate is applicable to State of Texas accounts only whose demand for power meets or exceeds 20 kilowatts

for any month within the most recent six summer billing months or as determined by the City of Austin.

This rate classification shall be applied for a term of not less than one year (twelve months) following the month in which the criteria is met. If a customer has made significant changes in his connected load which prevents the customer from meeting or exceeding 20 kilowatts in any summer billing month and if the change has been certified by the Electric Utility Department, the City of Austin may waive the one year requirement. The contract with the State of Texas, dated August 22, 1995, as amended effective October 1, 2002, is incorporated by reference into this tariff. Rider TOU-Thermal Energy Storage may be attached to this rate.

Character of Service: The Character of Service provided under this rate shall be alternating current, 60 cycles, single phase or three phases, in accordance with the Utilities Criteria Manual prescribed by the City of Austin which may be amended from time to time. Electric service of one standard character will be delivered to one point of service on the customer's premises and measured through one meter.

Rate (E14):	**Winter Billing Months November through April**	**Summer Billing Months May through October**
Energy Rate (E14)	1.07¢ per kWh, for all kWh	1.07¢ per kWh, for all kWh
Demand Rate (ELD)	$10.94 per kW	$11.64 per kW

Fuel Adjustment Clause (FAC) - plus an adjustment for variable costs, calculated according to the Fuel Adjustment Clause Tariff, multiplied by all kWh.

Minimum Bill: Customer will be assessed a monthly Minimum Bill of $12.00 if the above calculations result in a charge of less than $12.00.

Billing Demand: The kilowatt demand during the fifteen-minute interval of greatest use during the current billing month as indicated or recorded by metering equipment installed by the City of Austin. When power factor during the interval of greatest use is less than 85%, Billing Demand shall be determined by multiplying the indicated demand by 85% and dividing by the lower peak power factor.

Rider TOU - Thermal Energy Storage

Application:

This rate is applicable to any customer on the General Service - Demand, Primary Service, Large Primary Service (including Time-of-Use), Large Primary Special Contract Rider (including Time-of-Use), State General Service - Demand, State Primary Service, State Large Primary Service (including Time-of-Use), or Independent School Districts General Service - Demand (including Time-of-Use) rate who shifts to off-peak time periods no less than the lesser of 20% of the customer's normal on-peak summer billed demand or 2,500 kW through the use of Thermal Energy Storage technology. The normal on-peak Summer Billed Demand shall be the maximum Summer Billed Demand recorded prior to attaching this rider, or as may be determined by the City of Austin.

Rate: The customer shall continue to be billed under the applicable current rate ordinance with the following provisions:

Summer Billed Demand: From May through October, the Summer Billed Demand shall be the highest fifteen-minute demand recorded during the on-peak period. The Summer Billed Demand shall not be less than 50% of the normal on-peak Summer Billed Demand. If more than 50% of the customer's load is attributable to cooling, the 50% floor will be waived.

Winter Billed Demand: From November through April, the Winter Billed Demand shall be the highest fifteen-minute demand recorded during the month, or 90% of the Summer Billed Demand set in the previous summer; whichever is less.

On-Peak: 4:00 p.m. to 8:00 p.m., Monday through Friday; May 1 through October 31.

Off-Peak: 8:00 p.m. to 4:00 p.m., Monday through Friday; all day Saturday, Sunday, Memorial Day, Independence Day, and Labor Day; May 1 through October 31, All day November 1 through April 30.

Conditions of Service:

A. The customer shall enter into a separate agreement with the City of Austin for this rider.

B. The customer shall continue to be served under the terms and conditions of, and shall continue to comply with, all rules and regulations of the City of Austin as amended from time to time during the term of this agreement.

C. The on-peak load shall be shifted to off-peak; not eliminated or replaced by alternative fuels.

D. The customer shall permit the City to install all equipment necessary for time-of-use metering and to permit reasonable access to all electric service facilities installed by the City for inspection, maintenance, repair, removal, or data recording purposes.

APPENDIX C. TFC: MONTHLY BUILDING ELECTRICITY, PLANT ELECTRICITY, AND ELECTRIC UTILITY RATES

The following tables show the estimation of electricity fed to buildings from each of the four plants.

Month	CPP total Elec.	ARC	SHB	JHR Elec. from CPP	CPP Elec. to buildings	CPP Non-ChW Elec.	Total CPP ChW Elec.	Bldg Elec. Usage excl. ChW Plant
	kWh/month	kWh/day	kWh/day	kWh/day	kWh/day	kWh	kWh	W/sf-day
Jan-08	2,297,710	7,138	10,970	6,439	24,547	760,954	1,536,756	64.2
Feb-08	2,205,300	7,495	11,519	6,831	25,845	749,494	1,455,806	67.4
Mar-08	2,383,353	7,557	11,615	7,053	26,225	812,983	1,570,370	67.9
Apr-08	2,502,682	7,622	11,714	7,016	26,352	790,562	1,712,120	68.5
May-08	2,852,478	7,648	11,753	6,989	26,390	818,090	2,034,389	68.7
Jun-08	2,982,158	7,749	11,909	7,113	26,771	803,136	2,179,022	69.7
Jul-08	3,124,155	8,205	12,610	7,726	28,542	884,809	2,239,346	73.8
Aug-08	3,133,715	8,099	12,447	7,506	28,051	869,585	2,264,130	72.8
Sep-08	2,677,689	8,170	12,556	7,549	28,275	848,252	1,829,437	73.4
Oct-08	2,474,879	8,343	12,822	7,823	28,988	898,628	1,576,251	75.0
Nov-08	2,241,463	7,624	11,717	7,088	26,429	792,877	1,448,586	68.5
Dec-08	2,204,868	7,505	11,534	7,006	26,045	807,385	1,397,483	67.5

Month	REJ total Elec.	REJ BLDG	Total REJ ChW ELEC	SFA total Elec.	SFA BLDG	Total SFA Non-ChW ELEC	Total SFA ChW ELEC	Bldg Elec. Usage excl. ChW Plant
	kWh/ Mon	kWh/day	kWh/Mon	kWh/ Mon	kWh/day	kWh	kWh/Mon	W/sf-day
Jan-08	658,041	16,093	159,166	1,528,330	22,775	706,032	822,297	64.2
Feb-08	624,289	16,763	138,153	1,542,908	23,360	677,433	865,475	67.4
Mar-08	670,277	16,641	154,401	1,735,655	27,049	838,509	897,145	67.9
Apr-08	668,200	17,241	150,961	1,722,984	30,519	915,556	807,428	68.5
May-08	705,609	16,731	186,940	1,768,798	31,348	971,784	797,014	68.7
Jun-08	722,411	16,936	214,325	1,634,633	31,451	943,521	691,111	69.7
Jul-08	754,354	16,465	243,925	1,691,185	29,342	909,593	781,592	73.8
Aug-08	768,571	16,625	253,201	1,678,709	29,565	916,517	762,192	72.8
Sep-08	711,342	15,429	248,467	1,543,787	29,185	875,550	668,237	73.4
Oct-08	718,948	16,767	199,159	1,523,202	25,828	800,664	722,538	75.0
Nov-08	645,795	15,974	166,568	1,337,054	22,878	686,340	650,713	68.5
Dec-08	650,272	15,840	159,228	1,411,150	18,969	588,044	823,106	67.5

Month	WPC total Elec.	WPC BLDG	Total WPC ChW ELEC	Bldg Elec. Usage excl. ChW Plant
	kWh/ Mon	kWh/day	kWh/ Mon	W/sf-day
Jan-08	1,198,755	30,758	245,268	64.2
Feb-08	1,053,031	28,970	212,889	67.4
Mar-08	1,098,954	27,775	237,926	67.9
Apr-08	1,031,303	26,623	232,625	68.5
May-08	1,131,477	27,207	288,067	68.7
Jun-08	1,180,637	28,346	330,266	69.7
Jul-08	1,202,234	26,657	375,878	73.8
Aug-08	1,192,253	25,874	390,173	72.8
Sep-08	1,099,555	23,889	382,877	73.4
Oct-08	1,091,631	25,314	306,895	75.0
Nov-08	1,028,459	25,726	256,674	68.5
Dec-08	1,191,744	30,528	245,364	67.5

The following tables show the utility rates in 2008 and the rates used in the baseline and TES simulations when the fuel charge is added on to the energy base price.

Month	Utility rates used in 2008							
	SFA (E15)		REJ/WPC (E14)		CPP (E16)			
	cent / kWh	$/kW	cent / kWh	$/kW	On-peak cent / kWh	On-peak $/kW	Off-peak cent / kWh	Off-peak $/kW
Jan-08	4.61	$ 10.94	4.72	$ 10.94	5.21	10.94	3.21	$ 0
Feb-08	4.61	$ 10.94	4.72	$ 10.94	5.21	10.94	3.21	$ 0
Mar-08	4.61	$ 10.94	4.72	$ 10.94	5.21	10.94	3.21	$ 0
Apr-08	4.61	$ 10.94	4.72	$ 10.94	5.21	10.94	3.21	$ 0
May-08	4.61	$ 11.64	4.72	$ 11.64	5.91	11.64	4.06	$ 0
Jun-08	4.61	$ 11.64	4.72	$ 11.64	5.91	11.64	4.06	$ 0
Jul-08	4.61	$ 11.64	4.72	$ 11.64	5.91	11.64	4.06	$ 0
Aug-08	4.61	$ 11.64	4.72	$ 11.64	5.91	11.64	4.06	$ 0
Sep-08	4.61	$ 11.64	4.72	$ 11.64	5.91	11.64	4.06	$ 0
Oct-08	4.61	$ 11.64	4.72	$ 11.64	5.91	11.64	4.06	$ 0
Nov-08	4.61	$ 10.94	4.72	$ 10.94	5.21	10.94	3.21	$ 0
Dec-08	4.61	$ 10.94	4.72	$ 10.94	5.21	10.94	3.21	$ 0

Month	Utility rate used in the baseline and TES simulation			
	REJ SFA WPC CPP (E16)			
	On-peak cent / kWh	On-peak $/kW	Off-peak cent / kWh	Off-peak $/kW
Jan-08	5.49	$ 10.94	3.49	$ 0
Feb-08	5.49	$ 10.94	3.49	$ 0
Mar-08	5.49	$ 10.94	3.49	$ 0
Apr-08	5.49	$ 10.94	3.49	$ 0
May-08	6.19	$ 11.64	4.34	$ 0
Jun-08	6.19	$ 11.64	4.34	$ 0
Jul-08	6.19	$ 11.64	4.34	$ 0
Aug-08	6.19	$ 11.64	4.34	$ 0
Sep-08	6.19	$ 11.64	4.34	$ 0
Oct-08	6.19	$ 11.64	4.34	$ 0
Nov-08	5.49	$ 10.94	3.49	$ 0
Dec-08	5.49	$ 10.94	3.49	$ 0

APPENDIX D. TFC: PLANT BILLING COST AND LOAD BASELINES

	Billing cost				Energy charge				Demand charge			
Month	CPP	SFA	REJ	WPC	CPP	SFA	REJ	WPC	CPP	SFA	REJ	WPC
1	$ 136,989	$ 94,986	$ 45,694	$ 86,199	$ 93,792	$ 66,611	$ 32,924	$ 59,959	$ 43,197	$ 28,375	$ 12,770	$ 26,240
2	$ 134,209	$ 96,731	$ 44,180	$ 78,091	$ 90,408	$ 66,840	$ 31,225	$ 52,768	$ 43,800	$ 29,891	$ 12,954	$ 25,323
3	$ 141,684	$ 106,613	$ 46,644	$ 80,910	$ 97,565	$ 76,018	$ 33,515	$ 54,982	$ 44,119	$ 30,596	$ 13,129	$ 25,929
4	$ 151,545	$ 107,436	$ 46,789	$ 73,020	$ 102,242	$ 76,298	$ 33,440	$ 51,595	$ 49,304	$ 31,138	$ 13,349	$ 21,425
5	$ 175,041	$ 112,854	$ 49,481	$ 81,728	$ 118,995	$ 78,703	$ 35,300	$ 56,561	$ 56,046	$ 34,151	$ 14,181	$ 25,167
6	$ 181,243	$ 105,473	$ 51,090	$ 84,350	$ 124,654	$ 73,147	$ 36,134	$ 59,068	$ 56,589	$ 32,326	$ 14,956	$ 25,283
7	$ 188,977	$ 106,571	$ 53,084	$ 85,499	$ 131,325	$ 74,926	$ 37,721	$ 60,146	$ 57,652	$ 31,645	$ 15,363	$ 25,353
8	$ 186,403	$ 106,455	$ 53,782	$ 85,043	$ 130,423	$ 74,619	$ 38,478	$ 59,663	$ 55,980	$ 31,836	$ 15,304	$ 25,380
9	$ 167,133	$ 99,904	$ 50,330	$ 79,808	$ 112,361	$ 68,925	$ 35,586	$ 55,047	$ 54,773	$ 30,979	$ 14,744	$ 24,761
10	$ 154,294	$ 96,470	$ 51,036	$ 79,314	$ 104,603	$ 67,371	$ 35,976	$ 54,613	$ 49,691	$ 29,099	$ 15,060	$ 24,701
11	$ 136,092	$ 86,130	$ 46,447	$ 74,547	$ 92,062	$ 59,024	$ 32,340	$ 51,392	$ 44,029	$ 27,105	$ 14,107	$ 23,155
12	$ 134,623	$ 87,527	$ 45,902	$ 87,838	$ 90,873	$ 60,521	$ 32,444	$ 59,520	$ 43,750	$ 27,007	$ 13,458	$ 28,317
Sum	$ 1,888,233	$ 1,207,150	$ 584,457	$ 976,348	$ 1,289,304	$ 843,003	$ 415,082	$ 675,314	$ 598,930	$ 364,147	$ 169,375	$ 301,034
Total	$ 4,656,188				$ 3,222,703				$ 1,433,486			

	Monthly Total kWh				Monthly demand kW							
Month	CPP	SFA	REJ	WPC	CPP onpeak	CPP offpeak	SFA onpeak	SFA offpeak	REJ onpeak	REJ offpeak	WPC onpeak	WPC offpeak
1	1,990,347	1,363,298	658,091	1,198,463	3,873	3,249	2,544	2,160	1,145	1,020	2,349	2,353
2	1,912,989	1,367,983	624,132	1,054,735	3,928	3,200	2,680	2,295	1,162	1,029	2,129	2,271
3	2,067,627	1,555,831	669,904	1,098,972	3,956	3,394	2,743	2,431	1,177	1,033	2,189	2,325
4	2,163,388	1,561,569	668,400	1,031,273	4,421	3,468	2,792	2,453	1,197	1,064	1,888	1,921
5	2,462,298	1,610,786	705,578	1,130,549	4,729	4,654	2,881	2,842	1,196	1,195	2,121	2,123
6	2,586,153	1,497,073	722,240	1,180,644	4,775	4,686	2,727	2,714	1,262	1,248	2,133	2,129
7	2,712,851	1,533,485	753,968	1,202,200	4,864	4,807	2,670	2,657	1,296	1,284	2,139	2,135
8	2,719,554	1,527,191	769,095	1,192,542	4,723	4,675	2,686	2,675	1,291	1,261	2,136	2,141
9	2,323,030	1,410,671	711,283	1,100,276	4,619	4,768	2,614	2,593	1,244	1,241	2,089	2,087
10	2,159,711	1,378,867	719,084	1,091,612	4,192	4,232	2,455	2,415	1,271	1,216	2,069	2,084
11	1,953,593	1,208,028	646,409	1,027,228	3,948	3,176	2,431	2,062	1,265	1,067	2,076	2,065
12	1,925,117	1,238,652	648,485	1,189,693	3,923	3,135	2,422	1,946	1,207	1,003	2,539	2,465
Sum	26,976,658	17,253,433	8,296,670	13,498,186	4,864	4,807	2,881		1,296		2,139	
Total	66,024,946 kWh				10,970 kW							

	Monthly Total cooling load (TonHr)				ChW Production ELEC consumption (kWh)				Non-ChW production ELEC consumption (kWh)			
Month	CPP	SFA	REJ	WPC	CPP	SFA	REJ	WPC	CPP	SFA	REJ	WPC
1	1,229,398	657,562	144,707	222,916	1,229,398	657,562	159,178	245,208	760,949	705,736	498,914	953,254
2	1,163,946	691,455	125,562	193,849	1,163,946	691,455	138,119	213,234	749,044	676,528	486,013	841,502
3	1,255,293	717,534	140,286	216,300	1,255,293	717,534	154,315	237,930	812,334	838,297	515,589	861,042
4	1,372,655	645,972	137,279	211,472	1,372,655	645,972	151,007	232,619	790,733	915,597	517,393	798,655
5	1,644,881	638,162	169,938	261,665	1,644,881	638,162	186,932	287,831	817,416	972,624	518,646	842,718
6	1,782,921	553,134	194,795	300,244	1,782,921	553,134	214,274	330,268	803,232	943,939	507,966	850,375
7	1,828,565	624,711	221,636	341,698	1,828,565	624,711	243,800	375,867	884,286	908,774	510,168	826,332
8	1,849,624	610,121	230,340	354,789	1,849,624	610,121	253,374	390,267	869,931	917,070	515,721	802,274
9	1,473,639	534,791	225,860	348,299	1,473,639	534,791	248,446	383,129	849,391	875,880	462,837	717,148
10	1,261,049	578,103	181,088	278,991	1,261,049	578,103	199,196	306,890	898,662	800,765	519,888	784,722
11	1,159,966	521,052	151,569	233,061	1,159,966	521,052	166,726	256,367	793,627	686,975	479,683	770,861
12	1,117,838	650,932	143,293	221,078	1,117,838	650,932	157,623	243,186	807,278	587,719	490,862	946,507
Sum	17,139,775	7,423,529	2,066,354	3,184,360	17,139,775	7,423,529	2,272,990	3,502,796	9,836,883	9,829,904	6,023,680	9,995,390
Total	29,814,018 TonHr				30,339,090 kWh				35,685,857 kWh			

APPENDIX E. TFC: COST ESTIMATIONS OF TANK, AVOIDED CHILLER IN WPC, AND NEW PIPING

The breakdown of the overall cost for different size tanks:

Tank size (Gal)	Tank cost ($)	Foundation ($)	Pinping, Valves, Insulation, ect.($)	Test and Balance ($)	Instrumentation and Controls ($)	Contg($)	Contractor mark-up ($)	Design/CA ($)	Overall TES cost ($)
1,000,000	$ 750,000	$ 150,000	$ 350,000	$ 35,000	$ 75,600	$ 183,180	$ 198,445	$ 99,223	$1,841,448
2,000,000	$ 1,500,000	$ 300,000	$ 350,000	$ 35,000	$ 75,600	$ 228,180	$ 247,195	$123,598	$2,859,573
3,000,000	$ 2,250,000	$ 450,000	$ 350,000	$ 35,000	$ 75,600	$ 273,180	$ 295,945	$147,973	$3,877,698
3,500,000	$ 2,625,000	$ 525,000	$ 350,000	$ 35,000	$ 75,600	$ 295,680	$ 320,320	$160,160	$4,386,760
4,000,000	$ 3,000,000	$ 600,000	$ 350,000	$ 35,000	$ 75,600	$ 318,180	$ 344,695	$172,348	$4,895,823
5,000,000	$ 3,750,000	$ 750,000	$ 350,000	$ 35,000	$ 75,600	$ 363,180	$ 393,445	$196,723	$5,913,948
6,000,000	$ 4,500,000	$ 900,000	$ 350,000	$ 35,000	$ 75,600	$ 408,180	$ 442,195	$221,098	$6,932,073
7,000,000	$ 5,250,000	$1,050,000	$ 350,000	$ 35,000	$ 75,600	$ 453,180	$ 490,945	$245,473	$7,950,198

Estimation of avoided chiller replacement cost in WPC:

Project Name:	TFC TES+LOOP Evaluation						
Location	Austin, Texas						
System Discription	WPC Plant avoided chiller replacement cost						
Task Discription	**QUANTITY**		**LABOR**		**MATERIALS**		**TOTAL COSTS**
	NO/UNIT	**UNIT**	**UNIT PRICE**	**COST**	**UNIT PRICE**	**COST**	
1. Chillers							
Chiller Demolition	2	EA	$ 15,000	$ 30,000	$ -	$ -	$ 30,000
800 Ton Chiller	2	EA	$ 16,000	$ 32,000	$ 336,000	$ 672,000	$ 704,000
2. Primary Pump							
Pump (1200 gpm)	0	EA	$ 8,250	$ -	$ 16,100	$ -	$ -
Pump (2900 gpm)	0	EA	$ 17,900	$ -	$ 45,100	$ -	$ -
Pump Demo	0	EA	$ 5,000	$ -	$ -	$ -	$ -
5. Miscellaneous							
Mechanical	2	EA	$ -	$ -	$ 91,000	$ 182,000	$ 182,000
Electrical	2	EA	$ -	$ -	$ 45,500	$ 91,000	$ 91,000
Plumbing	2	EA	$ -	$ -	$ 8,531	$ 17,062	$ 17,062
Controls	2	EA	$ -	$ -	$ 14,219	$ 28,438	$ 28,438
SUBTOTAL				$ 62,000		$ 990,500	$ 1,052,500
CONTINGENCIES		30.0%					$ 315,750
CONTRACTOR MARK-UP		25.0%					$ 342,063
DESIGN/CA		10.0%					$ 171,031
TOTAL							$ 1,881,344

Piping cost estimation for connecting four downtown energy plants:

Project Name:	TFC TES+LOOP Evaluation						
Location	Austin, Texas						
System Discription	Piping construction cost estimation						
Task Discription	**QUANTITY**		**LABOR**		**MATERIALS**		**TOTAL COSTS**
	NO/UNIT	**UNIT**	**UNIT PRICE**	**COST**	**UNIT PRICE**	**COST**	
1. Piping							
Material	3096	ft	$ 1,000	$ 3,096,000	$ 1,000	$ 3,096,000	$ 6,192,000
SUBTOTAL				$ 3,096,000		$ 3,096,000	$ 6,192,000
CONTINGENCIES		30.0%					$ 1,857,600
CONTRACTOR MARK-UP		0.0%					$ -
DESIGN/CA		10.0%					$ 804,960
TOTAL							$ 8,854,560

APPENDIX F. TFC: MONTHLY PROFILES FOR DIFFERENT SIZE TANKS

Tank size: 1.0 M gallon

	Billing cost				Energy charge				Demand charge			
Month	CPP	SFA	REJ	WPC	CPP	SFA	REJ	WPC	CPP	SFA	REJ	WPC
1	$ 154,059	$ 80,797	$ 32,707	$ 60,038	$ 111,606	$ 53,847	$ 23,509	$ 44,645	$ 42,452	$ 26,950	$ 9,199	$ 15,393
2	$ 149,245	$ 81,620	$ 32,164	$ 54,838	$ 106,402	$ 54,577	$ 22,927	$ 39,458	$ 42,843	$ 27,043	$ 9,236	$ 15,381
3	$ 157,313	$ 91,708	$ 33,595	$ 55,866	$ 114,212	$ 63,338	$ 24,287	$ 40,484	$ 43,100	$ 28,370	$ 9,309	$ 15,383
4	$ 153,804	$ 100,117	$ 33,743	$ 53,098	$ 110,919	$ 71,537	$ 24,397	$ 37,786	$ 42,885	$ 28,580	$ 9,345	$ 15,312
5	$ 162,681	$ 123,221	$ 35,143	$ 58,866	$ 117,272	$ 89,488	$ 24,992	$ 40,801	$ 45,409	$ 33,733	$ 10,151	$ 18,064
6	$ 158,751	$ 127,593	$ 34,476	$ 58,617	$ 114,121	$ 94,262	$ 24,425	$ 41,098	$ 44,630	$ 33,331	$ 10,051	$ 17,519
7	$ 166,531	$ 130,075	$ 34,873	$ 56,827	$ 121,194	$ 98,480	$ 24,668	$ 40,166	$ 45,337	$ 31,595	$ 10,204	$ 16,661
8	$ 163,982	$ 131,269	$ 34,709	$ 54,952	$ 119,454	$ 99,406	$ 24,721	$ 38,672	$ 44,529	$ 31,863	$ 9,988	$ 16,280
9	$ 163,308	$ 112,747	$ 31,702	$ 50,281	$ 116,592	$ 80,531	$ 22,373	$ 34,897	$ 46,717	$ 32,216	$ 9,329	$ 15,384
10	$ 168,927	$ 80,226	$ 35,996	$ 55,266	$ 120,587	$ 63,392	$ 25,186	$ 38,180	$ 48,340	$ 16,833	$ 10,810	$ 17,086
11	$ 152,925	$ 75,315	$ 32,091	$ 51,488	$ 109,470	$ 47,640	$ 22,594	$ 36,161	$ 43,455	$ 27,675	$ 9,497	$ 15,327
12	$ 156,355	$ 69,011	$ 32,294	$ 59,680	$ 113,026	$ 44,010	$ 23,121	$ 44,256	$ 43,330	$ 25,001	$ 9,174	$ 15,424
Sum	$1,907,880	$1,203,699	$ 403,493	$ 669,817	$1,374,854	$ 860,508	$ 287,200	$ 476,605	$ 533,026	$ 343,191	$ 116,293	$ 193,213
Total	$4,184,890				$2,999,167				$1,185,723			
Saving ($	$ 471,298				$ 223,536				$ 247,762			

	Monthly Total kWh				Monthly demand kW							
Month	CPP	SFA	REJ	WPC	CPP onpeak	CPP offpeak	SFA onpeak	SFA offpeak	REJ onpeak	REJ offpeak	WPC onpeak	WPC offpeak
1	2,389,200	1,160,805	498,914	953,254	3,807	0	2,417	0	824	0	1,371	0
2	2,274,820	1,169,756	486,013	841,502	3,841	0	2,425	0	827	0	1,371	0
3	2,443,010	1,366,853	515,589	861,042	3,864	0	2,543	0	833	0	1,371	0
4	2,371,052	1,536,838	517,393	798,655	3,844	3,404	2,543	3,560	836	720	1,371	935
5	2,445,870	1,855,976	518,646	842,718	3,831	3,791	2,826	3,964	856	880	1,523	1,583
6	2,385,006	1,959,517	507,966	850,375	3,766	3,695	2,791	3,964	847	888	1,477	1,536
7	2,519,485	2,039,821	510,168	826,332	3,825	3,808	2,645	3,827	861	877	1,405	1,470
8	2,505,189	2,074,709	515,721	802,274	3,757	3,727	2,667	3,858	842	866	1,372	1,441
9	2,425,410	1,664,336	462,837	717,148	3,941	3,977	2,698	3,842	787	809	1,297	1,362
10	2,505,868	1,304,565	519,888	784,722	4,079	4,076	1,384	3,422	912	919	1,441	1,498
11	2,346,192	1,029,581	479,683	770,861	3,896	0	2,482	0	850	0	1,371	0
12	2,419,596	948,512	490,862	946,507	3,883	0	2,242	0	821	0	1,371	0
Sum	29,030,697	18,111,269	6,023,680	9,995,390	4,079	4,076	2,826	3,964	912	919	1,523	1,583
Total	63,161,037 kWh				8,638 kW							
Saving	2,863,909 kWh				2,059 kW							

	Monthly Total cooling load (TonHr)				ChW Production ELEC consumption (kWh)				Non-ChW production ELEC consumption (kWh)			
Month	CPP	SFA	REJ	WPC	CPP	SFA	REJ	WPC	CPP	SFA	REJ	WPC
1	2,160,537	568,836	0	0	1,628,251	455,069	0	0	760,949	705,736	498,914	953,254
2	2,024,320	616,536	0	0	1,525,776	493,229	0	0	749,044	676,528	486,013	841,502
3	2,163,623	660,695	0	0	1,630,676	528,556	0	0	812,334	838,297	515,589	861,042
4	2,096,686	776,551	0	0	1,580,319	621,241	0	0	790,733	915,597	517,393	798,655
5	2,160,980	1,104,191	0	0	1,628,454	883,353	0	0	817,416	972,624	518,646	842,718
6	2,099,257	1,269,472	0	0	1,581,774	1,015,578	0	0	803,232	943,939	507,966	850,375
7	2,170,137	1,413,809	0	0	1,635,200	1,131,047	0	0	884,286	908,774	510,168	826,332
8	2,170,251	1,447,048	0	0	1,635,258	1,157,639	0	0	869,931	917,070	515,721	802,274
9	2,091,874	985,571	0	0	1,576,019	788,456	0	0	849,391	875,880	462,837	717,148
10	2,132,471	629,750	0	0	1,607,206	503,800	0	0	898,662	800,765	519,888	784,722
11	2,060,397	428,257	0	0	1,552,565	342,605	0	0	793,627	686,975	479,683	770,861
12	2,139,595	450,991	0	0	1,612,318	360,793	0	0	807,278	587,719	490,862	946,507
Sum	25,470,129	10,351,707	0	0	19,193,815	8,281,366	0	0	9,836,883	9,829,904	6,023,680	9,995,390
Total	35,821,836	TonHr			27,475,180	kWh			35,685,857	kWh		
Saving	-6,007,818	TonHr			2,863,909	kWh			0	kWh		

Month	Elec. Energy saving (kWh)	Energy cost saving	Demand cost saving	Control strategy	off-peak num	on-peak num
1	208,026	$ 19,679	$ 16,588	Storage-priority	3	3
2	187,748	$ 17,878	$ 17,466	Storage-priority	3	3
3	205,839	$ 19,759	$ 17,611	Storage-priority	3	3
4	200,693	$ 18,935	$ 19,094	Storage-priority	4	4
5	246,000	$ 17,005	$ 22,188	Storage-priority	4	3
6	283,246	$ 19,096	$ 23,622	Storage-priority	4	3
7	306,696	$ 19,610	$ 26,215	Storage-priority	4	3
8	310,490	$ 20,930	$ 25,840	Storage-priority	4	3
9	275,530	$ 17,527	$ 21,611	Storage-priority	4	3
10	234,231	$ 15,219	$ 25,481	Storage-priority	4	2
11	208,940	$ 18,953	$ 12,443	Storage-priority	3	3
12	196,469	$ 18,945	$ 19,603	Storage-priority	3	3
Total	2,863,909	$ 223,536	$ 247,762			

Tank size: 2.0 M gallon

	Billing cost				Energy charge				Demand charge			
Month	CPP	SFA	REJ	WPC	CPP	SFA	REJ	WPC	CPP	SFA	REJ	WPC
1	$ 151,924	$ 70,886	$ 32,707	$ 60,038	$ 110,216	$ 53,191	$ 23,509	$ 44,645	$ 41,708	$ 17,695	$ 9,199	$ 15,393
2	$ 147,328	$ 71,158	$ 32,164	$ 54,838	$ 105,593	$ 53,456	$ 22,927	$ 39,458	$ 41,735	$ 17,702	$ 9,236	$ 15,381
3	$ 155,497	$ 79,807	$ 33,595	$ 55,866	$ 113,512	$ 62,079	$ 24,287	$ 40,484	$ 41,986	$ 17,728	$ 9,309	$ 15,383
4	$ 152,246	$ 87,689	$ 33,743	$ 53,098	$ 110,470	$ 69,934	$ 24,397	$ 37,786	$ 41,776	$ 17,755	$ 9,345	$ 15,312
5	$ 159,293	$ 113,251	$ 35,143	$ 58,866	$ 113,530	$ 92,315	$ 24,992	$ 40,801	$ 45,764	$ 20,936	$ 10,151	$ 18,064
6	$ 156,591	$ 116,367	$ 34,476	$ 58,617	$ 111,610	$ 95,833	$ 24,425	$ 41,098	$ 44,982	$ 20,534	$ 10,051	$ 17,519
7	$ 165,054	$ 117,905	$ 34,873	$ 56,827	$ 119,365	$ 99,107	$ 24,668	$ 40,166	$ 45,689	$ 18,798	$ 10,204	$ 16,661
8	$ 162,723	$ 119,107	$ 34,709	$ 54,952	$ 117,844	$ 100,042	$ 24,721	$ 38,672	$ 44,879	$ 19,066	$ 9,988	$ 16,280
9	$ 159,337	$ 103,431	$ 31,702	$ 50,281	$ 112,271	$ 84,013	$ 22,373	$ 34,897	$ 47,066	$ 19,419	$ 9,329	$ 15,384
10	$ 149,840	$ 86,295	$ 35,996	$ 55,266	$ 113,829	$ 69,462	$ 25,186	$ 38,180	$ 36,011	$ 16,833	$ 10,810	$ 17,086
11	$ 149,551	$ 65,707	$ 32,091	$ 51,488	$ 107,215	$ 47,995	$ 22,594	$ 36,161	$ 42,336	$ 17,713	$ 9,497	$ 15,327
12	$ 153,505	$ 61,289	$ 32,294	$ 59,680	$ 111,295	$ 43,815	$ 23,121	$ 44,256	$ 42,209	$ 17,473	$ 9,174	$ 15,424
Sum	$1,862,889	$1,092,892	$ 403,493	$ 669,817	$1,346,749	$ 871,241	$ 287,200	$ 476,605	$ 516,140	$ 221,651	$ 116,293	$ 193,213
Total	$4,029,092				$2,981,794				$1,047,297			
Saving ($	$ 627,097				$ 240,909				$ 386,188			

	Monthly Total kWh				Monthly demand kW							
Month	CPP	SFA	REJ	WPC	CPP onpeak	CPP offpeak	SFA onpeak	SFA offpeak	REJ onpeak	REJ offpeak	WPC onpeak	WPC offpeak
1	2,363,864	1,199,087	498,914	953,254	3,739	0	1,554	0	824	0	1,371	0
2	2,260,073	1,196,102	486,013	841,502	3,740	0	1,554	0	827	0	1,371	0
3	2,430,234	1,392,855	515,589	861,042	3,762	0	1,554	0	833	0	1,371	0
4	2,362,872	1,555,058	517,393	798,655	3,743	3,404	1,554	3,560	836	720	1,371	935
5	2,376,107	1,942,292	518,646	842,718	3,861	3,791	1,726	3,964	856	880	1,523	1,583
6	2,335,770	2,023,426	507,966	850,375	3,795	3,695	1,692	3,964	847	888	1,477	1,536
7	2,482,790	2,089,942	510,168	826,332	3,855	3,808	1,545	3,827	861	877	1,405	1,470
8	2,470,555	2,124,543	515,721	802,274	3,787	3,727	1,568	3,858	842	866	1,372	1,441
9	2,346,283	1,761,057	462,837	717,148	3,971	3,977	1,598	3,842	787	809	1,297	1,362
10	2,387,632	1,444,541	519,888	784,722	3,019	4,076	1,384	3,422	912	919	1,441	1,498
11	2,305,151	1,086,102	479,683	770,861	3,793	0	1,554	0	850	0	1,371	0
12	2,388,648	992,071	490,862	946,507	3,781	0	1,554	0	821	0	1,371	0
Sum	28,509,978	18,807,076	6,023,680	9,995,390	3,971	4,076	1,726	3,964	912	919	1,523	1,583
Total	63,336,124 kWh				7,570 kW							
Saving	2,688,822 kWh				3,127 kW							

	Monthly Total cooling load (TonHr)				ChW Production ELEC consumption (kWh)				Non-ChW production ELEC consumption (kWh)			
Month	CPP	SFA	REJ	WPC	CPP	SFA	REJ	WPC	CPP	SFA	REJ	WPC
1	2,115,660	616,689	0	0	1,602,914	493,351	0	0	760,949	705,736	498,914	953,254
2	1,994,503	649,468	0	0	1,511,029	519,574	0	0	749,044	676,528	486,013	841,502
3	2,135,983	693,198	0	0	1,617,900	554,558	0	0	812,334	838,297	515,589	861,042
4	2,075,457	799,326	0	0	1,572,139	639,461	0	0	790,733	915,597	517,393	798,655
5	2,056,606	1,212,085	0	0	1,558,690	969,668	0	0	817,416	972,624	518,646	842,718
6	2,022,540	1,349,359	0	0	1,532,538	1,079,487	0	0	803,232	943,939	507,966	850,375
7	2,109,569	1,476,460	0	0	1,598,504	1,181,168	0	0	884,286	908,774	510,168	826,332
8	2,112,431	1,509,341	0	0	1,600,625	1,207,473	0	0	869,931	917,070	515,721	802,274
9	1,975,303	1,106,472	0	0	1,496,892	885,177	0	0	849,391	875,880	462,837	717,148
10	1,963,563	804,720	0	0	1,488,970	643,776	0	0	898,662	800,765	519,888	784,722
11	1,994,597	498,908	0	0	1,511,524	399,126	0	0	793,627	686,975	479,683	770,861
12	2,087,441	505,439	0	0	1,581,370	404,351	0	0	807,278	587,719	490,862	946,507
Sum	24,643,653	11,221,465	0	0	18,673,096	8,977,172	0	0	9,836,883	9,829,904	6,023,680	9,995,390
Total	35,865,117	TonHr			27,650,268	kWh			35,685,857	kWh		
Saving	-6,051,099	TonHr			2,688,822	kWh			0	kWh		

Month	Elec. Energy saving (kWh)	Energy cost saving	Demand cost saving	Control strategy	off-peak num	on-peak num
1	195,080	$ 21,725	$ 26,587	Storage-priority	4	3
2	176,150	$ 19,808	$ 27,916	Storage-priority	4	3
3	192,613	$ 21,719	$ 29,368	Storage-priority	4	3
4	190,653	$ 20,987	$ 31,029	Storage-priority	4	3
5	229,448	$ 17,920	$ 34,630	Storage-priority	4	2
6	268,572	$ 20,037	$ 36,068	Storage-priority	4	2
7	293,271	$ 20,812	$ 38,660	Storage-priority	4	2
8	295,289	$ 21,904	$ 38,286	Storage-priority	4	2
9	257,936	$ 18,365	$ 34,059	Storage-priority	4	2
10	212,491	$ 15,907	$ 37,810	Storage-priority	4	1
11	193,461	$ 20,854	$ 23,525	Storage-priority	4	3
12	183,858	$ 20,870	$ 28,251	Storage-priority	3	3
Total	2,688,822	$ 240,909	$ 386,188			

Tank size: 3.0 M gallon

	Billing cost				Energy charge				Demand charge			
Month	CPP	SFA	REJ	WPC	CPP	SFA	REJ	WPC	CPP	SFA	REJ	WPC
1	$ 138,134	$ 70,844	$ 32,707	$ 60,038	$ 108,299	$ 53,149	$ 23,509	$ 44,645	$ 29,835	$ 17,695	$ 9,199	$ 15,393
2	$ 133,648	$ 71,138	$ 32,164	$ 54,838	$ 103,788	$ 53,437	$ 22,927	$ 39,458	$ 29,860	$ 17,702	$ 9,236	$ 15,381
3	$ 141,475	$ 79,790	$ 33,595	$ 55,866	$ 111,436	$ 62,062	$ 24,287	$ 40,484	$ 30,039	$ 17,728	$ 9,309	$ 15,383
4	$ 138,892	$ 87,242	$ 33,743	$ 53,098	$ 109,007	$ 69,487	$ 24,397	$ 37,786	$ 29,885	$ 17,755	$ 9,345	$ 15,312
5	$ 140,518	$ 119,123	$ 35,143	$ 58,866	$ 106,914	$ 98,187	$ 24,992	$ 40,801	$ 33,603	$ 20,936	$ 10,151	$ 18,064
6	$ 137,986	$ 122,256	$ 34,476	$ 58,617	$ 105,087	$ 101,722	$ 24,425	$ 41,098	$ 32,900	$ 20,534	$ 10,051	$ 17,519
7	$ 145,910	$ 124,916	$ 34,873	$ 56,827	$ 112,310	$ 105,931	$ 24,668	$ 40,166	$ 33,600	$ 18,985	$ 10,204	$ 16,661
8	$ 143,547	$ 126,158	$ 34,709	$ 54,952	$ 110,709	$ 106,914	$ 24,721	$ 38,672	$ 32,838	$ 19,244	$ 9,988	$ 16,280
9	$ 125,804	$ 111,936	$ 31,702	$ 50,281	$ 103,139	$ 92,332	$ 22,373	$ 34,897	$ 22,665	$ 19,604	$ 9,329	$ 15,384
10	$ 131,231	$ 91,767	$ 35,996	$ 55,266	$ 107,549	$ 74,934	$ 25,186	$ 38,180	$ 23,682	$ 16,833	$ 10,810	$ 17,086
11	$ 134,326	$ 67,010	$ 32,091	$ 51,488	$ 104,038	$ 49,298	$ 22,594	$ 36,161	$ 30,288	$ 17,713	$ 9,497	$ 15,327
12	$ 138,379	$ 62,562	$ 32,294	$ 59,680	$ 108,175	$ 44,918	$ 23,121	$ 44,256	$ 30,204	$ 17,644	$ 9,174	$ 15,424
Sum	$1,649,850	$1,134,743	$ 403,493	$ 669,817	$1,290,451	$ 912,370	$ 287,200	$ 476,605	$ 359,400	$ 222,373	$ 116,293	$ 193,213
Total	$3,857,903				$2,966,625				$ 891,278			
Saving ($	$ 798,285				$ 256,078				$ 542,207			

	Monthly Total kWh				Monthly demand kW							
Month	CPP	SFA	REJ	WPC	CPP onpeak	CPP offpeak	SFA onpeak	SFA offpeak	REJ onpeak	REJ offpeak	WPC onpeak	WPC offpeak
1	2,328,911	1,247,472	498,914	953,254	2,653	0	1,554	0	824	0	1,371	0
2	2,227,177	1,243,417	486,013	841,502	2,654	0	1,554	0	827	0	1,371	0
3	2,392,402	1,444,237	515,589	861,042	2,670	0	1,554	0	833	0	1,371	0
4	2,336,200	1,596,087	517,393	798,655	2,656	3,404	1,554	3,560	836	720	1,371	935
5	2,259,875	2,077,701	518,646	842,718	2,818	3,791	1,726	3,964	856	880	1,523	1,583
6	2,219,538	2,158,974	507,966	850,375	2,759	3,695	1,692	3,964	847	888	1,477	1,536
7	2,359,096	2,234,305	510,168	826,332	2,818	3,793	1,545	4,710	861	877	1,405	1,470
8	2,343,760	2,270,816	515,721	802,274	2,753	3,714	1,568	4,698	842	866	1,372	1,441
9	2,189,971	1,942,176	462,837	717,148	1,875	3,977	1,598	4,716	787	809	1,297	1,362
10	2,280,418	1,570,740	519,888	784,722	1,960	4,076	1,384	3,422	912	919	1,441	1,498
11	2,247,479	1,159,262	479,683	770,861	2,691	0	1,554	0	850	0	1,371	0
12	2,331,626	1,065,468	490,862	946,507	2,683	0	1,554	0	821	0	1,371	0
Sum	27,516,453	20,010,654	6,023,680	9,995,390	2,818	4,076	1,726	4,716	912	919	1,523	1,583
Total	63,546,177 kWh				6,353 kW							
Saving	2,478,769 kWh				4,345 kW							

	Monthly Total cooling load (TonHr)				ChW Production ELEC consumption (kWh)				Non-ChW production ELEC consumption (kWh)			
Month	CPP	SFA	REJ	WPC	CPP	SFA	REJ	WPC	CPP	SFA	REJ	WPC
1	2,058,011	677,170	0	0	1,567,962	541,736	0	0	760,949	705,736	498,914	953,254
2	1,940,060	708,611	0	0	1,478,134	566,889	0	0	749,044	676,528	486,013	841,502
3	2,073,869	757,425	0	0	1,580,068	605,940	0	0	812,334	838,297	515,589	861,042
4	2,028,974	850,612	0	0	1,545,467	680,490	0	0	790,733	915,597	517,393	798,655
5	1,890,560	1,381,346	0	0	1,442,458	1,105,077	0	0	817,416	972,624	518,646	842,718
6	1,856,494	1,518,793	0	0	1,416,306	1,215,035	0	0	803,232	943,939	507,966	850,375
7	1,933,503	1,656,914	0	0	1,474,810	1,325,531	0	0	884,286	908,774	510,168	826,332
8	1,932,071	1,692,182	0	0	1,473,830	1,353,746	0	0	869,931	917,070	515,721	802,274
9	1,752,000	1,332,871	0	0	1,340,580	1,066,297	0	0	849,391	875,880	462,837	717,148
10	1,810,400	962,470	0	0	1,381,756	769,976	0	0	898,662	800,765	519,888	784,722
11	1,906,579	590,358	0	0	1,453,852	472,286	0	0	793,627	686,975	479,683	770,861
12	1,999,777	597,186	0	0	1,524,348	477,749	0	0	807,278	587,719	490,862	946,507
Sum	23,182,299	12,725,938	0	0	17,679,570	10,180,750	0	0	9,836,883	9,829,904	6,023,680	9,995,390
Total	35,908,237	TonHr			27,860,321	kWh			35,685,857	kWh		
Saving	-6,094,219	TonHr			2,478,769	kWh			0	kWh		

Month	Elec. Energy saving (kWh)	Energy cost saving	Demand cost saving	Control strategy	off-peak num	on-peak num
1	181,648	$ 23,685	$ 38,460	Storage-priority	4	3
2	161,731	$ 21,632	$ 39,791	Storage-priority	4	3
3	179,064	$ 23,811	$ 41,314	Storage-priority	4	3
4	176,296	$ 22,897	$ 42,919	Storage-priority	4	3
5	210,271	$ 18,665	$ 46,791	Storage-priority	4	1
6	249,257	$ 20,670	$ 48,150	Storage-priority	4	1
7	272,602	$ 21,043	$ 50,562	Storage-priority	5	1
8	275,811	$ 22,167	$ 50,150	Storage-priority	5	1
9	233,129	$ 19,178	$ 58,275	Full storage	5	0
10	193,506	$ 16,715	$ 50,138	Full storage	4	0
11	177,973	$ 22,728	$ 35,573	Storage-priority	4	3
12	167,483	$ 22,888	$ 40,086	Storage-priority	4	3
Total	2,478,769	$ 256,078	$ 542,207			

Tank size: 3.5 M gallon

	Billing cost				Energy charge				Demand charge			
Month	CPP	SFA	REJ	WPC	CPP	SFA	REJ	WPC	CPP	SFA	REJ	WPC
1	$ 127,134	$ 72,092	$ 32,707	$ 60,038	$ 106,129	$ 54,384	$ 23,509	$ 44,645	$ 21,004	$ 17,708	$ 9,199	$ 15,393
2	$ 123,814	$ 70,764	$ 32,164	$ 54,838	$ 102,789	$ 52,820	$ 22,927	$ 39,458	$ 21,025	$ 17,945	$ 9,236	$ 15,381
3	$ 131,093	$ 80,489	$ 33,595	$ 55,866	$ 109,941	$ 62,737	$ 24,287	$ 40,484	$ 21,151	$ 17,752	$ 9,309	$ 15,383
4	$ 129,173	$ 87,230	$ 33,743	$ 53,098	$ 108,129	$ 69,451	$ 24,397	$ 37,786	$ 21,044	$ 17,779	$ 9,345	$ 15,312
5	$ 124,994	$ 122,662	$ 35,143	$ 58,866	$ 103,536	$ 101,538	$ 24,992	$ 40,801	$ 21,458	$ 21,124	$ 10,151	$ 18,064
6	$ 121,528	$ 126,472	$ 34,476	$ 58,617	$ 100,691	$ 105,756	$ 24,425	$ 41,098	$ 20,838	$ 20,716	$ 10,051	$ 17,519
7	$ 128,652	$ 129,223	$ 34,873	$ 56,827	$ 107,127	$ 110,237	$ 24,668	$ 40,166	$ 21,525	$ 18,985	$ 10,204	$ 16,661
8	$ 126,493	$ 130,617	$ 34,709	$ 54,952	$ 105,681	$ 111,372	$ 24,721	$ 38,672	$ 20,812	$ 19,244	$ 9,988	$ 16,280
9	$ 125,804	$ 111,987	$ 31,702	$ 50,281	$ 103,139	$ 92,383	$ 22,373	$ 34,897	$ 22,665	$ 19,604	$ 9,329	$ 15,384
10	$ 131,231	$ 91,767	$ 35,996	$ 55,266	$ 107,549	$ 74,934	$ 25,186	$ 38,180	$ 23,682	$ 16,833	$ 10,810	$ 17,086
11	$ 122,780	$ 68,560	$ 32,091	$ 51,488	$ 101,452	$ 50,847	$ 22,594	$ 36,161	$ 21,327	$ 17,713	$ 9,497	$ 15,327
12	$ 126,776	$ 64,314	$ 32,294	$ 59,680	$ 105,504	$ 46,662	$ 23,121	$ 44,256	$ 21,272	$ 17,652	$ 9,174	$ 15,424
Sum	$1,519,472	$1,156,176	$ 403,493	$ 669,817	$1,261,668	$ 933,121	$ 287,200	$ 476,605	$ 257,804	$ 223,055	$ 116,293	$ 193,213
Total	$3,748,958				$2,958,594				$ 790,364			
Saving ($	$ 907,231				$ 264,109				$ 643,121			

	Monthly Total kWh				Monthly demand kW							
Month	CPP	SFA	REJ	WPC	CPP onpeak	CPP offpeak	SFA onpeak	SFA offpeak	REJ onpeak	REJ offpeak	WPC onpeak	WPC offpeak
1	2,289,362	1,295,861	498,914	953,254	1,846	0	1,554	0	824	0	1,371	0
2	2,208,965	1,267,836	486,013	841,502	1,846	0	1,554	0	827	0	1,371	0
3	2,365,153	1,483,122	515,589	861,042	1,857	0	1,554	0	833	0	1,371	0
4	2,320,195	1,618,070	517,393	798,655	1,848	3,404	1,554	3,560	836	720	1,371	935
5	2,203,762	2,144,236	518,646	842,718	1,774	3,791	1,726	4,852	856	880	1,523	1,583
6	2,146,376	2,241,933	507,966	850,375	1,723	3,688	1,692	4,822	847	888	1,477	1,536
7	2,272,924	2,333,629	510,168	826,332	1,780	3,793	1,545	4,710	861	877	1,405	1,470
8	2,258,590	2,373,645	515,721	802,274	1,720	3,714	1,568	4,698	842	866	1,372	1,441
9	2,189,971	1,943,345	462,837	717,148	1,875	3,977	1,598	4,716	787	809	1,297	1,362
10	2,280,418	1,570,740	519,888	784,722	1,960	4,076	1,384	3,422	912	919	1,441	1,498
11	2,200,435	1,212,401	479,683	770,861	1,872	0	1,554	0	850	0	1,371	0
12	2,282,975	1,124,504	490,862	946,507	1,866	0	1,554	0	821	0	1,371	0
Sum	27,019,127	20,609,322	6,023,680	9,995,390	1,960	4,076	1,726	4,852	912	919	1,523	1,583
Total	63,647,519 kWh				5,661 kW							
Saving	2,377,427 kWh				5,036 kW							

	Monthly Total cooling load (TonHr)				ChW Production ELEC consumption (kWh)				Non-ChW production ELEC consumption (kWh)			
Month	CPP	SFA	REJ	WPC	CPP	SFA	REJ	WPC	CPP	SFA	REJ	WPC
1	1,999,497	737,657	0	0	1,528,413	590,125	0	0	760,949	705,736	498,914	953,254
2	1,907,489	739,136	0	0	1,459,922	591,309	0	0	749,044	676,528	486,013	841,502
3	2,031,903	806,031	0	0	1,552,819	644,825	0	0	812,334	838,297	515,589	861,042
4	2,002,526	878,090	0	0	1,529,462	702,472	0	0	790,733	915,597	517,393	798,655
5	1,810,400	1,464,516	0	0	1,386,346	1,171,612	0	0	817,416	972,624	518,646	842,718
6	1,752,000	1,622,492	0	0	1,343,144	1,297,994	0	0	803,232	943,939	507,966	850,375
7	1,810,400	1,781,069	0	0	1,388,638	1,424,855	0	0	884,286	908,774	510,168	826,332
8	1,810,400	1,820,719	0	0	1,388,660	1,456,575	0	0	869,931	917,070	515,721	802,274
9	1,752,000	1,334,332	0	0	1,340,580	1,067,465	0	0	849,391	875,880	462,837	717,148
10	1,810,400	962,470	0	0	1,381,756	769,976	0	0	898,662	800,765	519,888	784,722
11	1,837,997	656,783	0	0	1,406,808	525,426	0	0	793,627	686,975	479,683	770,861
12	1,928,863	670,981	0	0	1,475,697	536,784	0	0	807,278	587,719	490,862	946,507
Sum	22,453,874	13,474,273	0	0	17,182,244	10,779,419	0	0	9,836,883	9,829,904	6,023,680	9,995,390
Total	35,928,147	TonHr			27,961,663	kWh			35,685,857	kWh		
Saving	-6,114,129	TonHr			2,377,427	kWh			0	kWh		

Month	Elec. Energy saving (kWh)	Energy cost saving	Demand cost saving	Control strategy	off-peak num	on-peak num
1	172,807	$ 24,619	$ 47,278	Storage-priority	4	3
2	155,522	$ 23,248	$ 48,383	Storage-priority	5	2
3	167,428	$ 24,631	$ 50,178	Storage-priority	4	3
4	170,318	$ 23,811	$ 51,736	Storage-priority	4	3
5	199,848	$ 18,692	$ 58,747	Full storage	5	0
6	239,460	$ 21,032	$ 60,030	Full storage	5	0
7	259,450	$ 21,919	$ 62,638	Full storage	5	0
8	258,152	$ 22,736	$ 62,176	Full storage	5	0
9	231,960	$ 19,127	$ 58,275	Full storage	5	0
10	193,506	$ 16,715	$ 50,138	Full storage	4	0
11	171,877	$ 23,764	$ 44,533	Storage-priority	4	2
12	157,098	$ 23,816	$ 49,010	Storage-priority	4	2
Total	2,377,427	$ 264,109	$ 643,121			

Tank size: 4.0 M gallon

	Billing cost				Energy charge				Demand charge			
Month	CPP	SFA	REJ	WPC	CPP	SFA	REJ	WPC	CPP	SFA	REJ	WPC
1	$ 124,283	$ 74,105	$ 32,707	$ 60,038	$ 103,279	$ 56,394	$ 23,509	$ 44,645	$ 21,004	$ 17,711	$ 9,199	$ 15,393
2	$ 122,000	$ 72,190	$ 32,164	$ 54,838	$ 100,975	$ 54,245	$ 22,927	$ 39,458	$ 21,025	$ 17,945	$ 9,236	$ 15,381
3	$ 128,716	$ 81,783	$ 33,595	$ 55,866	$ 107,565	$ 63,813	$ 24,287	$ 40,484	$ 21,151	$ 17,971	$ 9,309	$ 15,383
4	$ 127,866	$ 87,791	$ 33,743	$ 53,098	$ 106,816	$ 69,793	$ 24,397	$ 37,786	$ 21,050	$ 17,998	$ 9,345	$ 15,312
5	$ 124,994	$ 122,760	$ 35,143	$ 58,866	$ 103,536	$ 101,636	$ 24,992	$ 40,801	$ 21,458	$ 21,124	$ 10,151	$ 18,064
6	$ 121,528	$ 126,472	$ 34,476	$ 58,617	$ 100,691	$ 105,756	$ 24,425	$ 41,098	$ 20,838	$ 20,716	$ 10,051	$ 17,519
7	$ 128,652	$ 129,223	$ 34,873	$ 56,827	$ 107,127	$ 110,237	$ 24,668	$ 40,166	$ 21,525	$ 18,985	$ 10,204	$ 16,661
8	$ 126,493	$ 130,617	$ 34,709	$ 54,952	$ 105,681	$ 111,372	$ 24,721	$ 38,672	$ 20,812	$ 19,244	$ 9,988	$ 16,280
9	$ 125,805	$ 111,393	$ 31,702	$ 50,281	$ 103,139	$ 91,971	$ 22,373	$ 34,897	$ 22,665	$ 19,423	$ 9,329	$ 15,384
10	$ 131,231	$ 91,767	$ 35,996	$ 55,266	$ 107,549	$ 74,934	$ 25,186	$ 38,180	$ 23,682	$ 16,833	$ 10,810	$ 17,086
11	$ 119,773	$ 70,710	$ 32,091	$ 51,488	$ 98,446	$ 52,997	$ 22,594	$ 36,161	$ 21,327	$ 17,713	$ 9,497	$ 15,327
12	$ 123,653	$ 66,636	$ 32,294	$ 59,680	$ 102,381	$ 48,967	$ 23,121	$ 44,256	$ 21,272	$ 17,669	$ 9,174	$ 15,424
Sum	$1,504,994	$1,165,447	$ 403,493	$ 669,817	$1,247,184	$ 942,116	$ 287,200	$ 476,605	$ 257,810	$ 223,331	$ 116,293	$ 193,213
Total	$3,743,752				$2,953,105				$ 790,647			
Saving ($	$ 912,437				$ 269,598				$ 642,838			

	Monthly Total kWh				Monthly demand kW							
Month	CPP	SFA	REJ	WPC	CPP onpeak	CPP offpeak	SFA onpeak	SFA offpeak	REJ onpeak	REJ offpeak	WPC onpeak	WPC offpeak
1	2,237,401	1,357,029	498,914	953,254	1,846	0	1,554	0	824	0	1,371	0
2	2,175,899	1,308,734	486,013	841,502	1,846	0	1,554	0	827	0	1,371	0
3	2,321,840	1,531,360	515,589	861,042	1,857	0	1,554	0	833	0	1,371	0
4	2,296,257	1,652,799	517,393	798,655	1,848	3,404	1,554	4,705	836	720	1,371	935
5	2,203,762	2,146,504	518,646	842,718	1,774	3,791	1,726	4,852	856	880	1,523	1,583
6	2,146,376	2,241,933	507,966	850,375	1,723	3,688	1,692	4,822	847	888	1,477	1,536
7	2,272,924	2,333,629	510,168	826,332	1,780	3,793	1,545	4,710	861	877	1,405	1,470
8	2,258,590	2,373,645	515,721	802,274	1,720	3,714	1,568	4,698	842	866	1,372	1,441
9	2,189,971	1,943,345	462,837	717,148	1,875	3,977	1,598	3,861	787	809	1,297	1,362
10	2,280,418	1,570,740	519,888	784,722	1,960	4,076	1,384	3,422	912	919	1,441	1,498
11	2,145,694	1,274,068	479,683	770,861	1,872	0	1,554	0	850	0	1,371	0
12	2,226,151	1,190,652	490,862	946,507	1,866	0	1,554	0	821	0	1,371	0
Sum	26,755,284	20,924,436	6,023,680	9,995,390	1,960	4,076	1,726	4,852	912	919	1,523	1,583
Total	63,698,790 kWh				5,661 kW							
Saving	2,326,156 kWh				5,036 kW							

	Monthly Total cooling load (TonHr)				ChW Production ELEC consumption (kWh)				Non-ChW production ELEC consumption (kWh)			
Month	CPP	SFA	REJ	WPC	CPP	SFA	REJ	WPC	CPP	SFA	REJ	WPC
1	1,924,720	814,116	0	0	1,476,451	651,293	0	0	760,949	705,736	498,914	953,254
2	1,860,251	790,258	0	0	1,426,856	632,207	0	0	749,044	676,528	486,013	841,502
3	1,967,320	866,329	0	0	1,509,505	693,063	0	0	812,334	838,297	515,589	861,042
4	1,964,454	921,501	0	0	1,505,524	737,201	0	0	790,733	915,597	517,393	798,655
5	1,810,400	1,467,350	0	0	1,386,346	1,173,880	0	0	817,416	972,624	518,646	842,718
6	1,752,000	1,622,492	0	0	1,343,144	1,297,994	0	0	803,232	943,939	507,966	850,375
7	1,810,400	1,781,069	0	0	1,388,638	1,424,855	0	0	884,286	908,774	510,168	826,332
8	1,810,400	1,820,719	0	0	1,388,660	1,456,575	0	0	869,931	917,070	515,721	802,274
9	1,752,000	1,334,332	0	0	1,340,580	1,067,465	0	0	849,391	875,880	462,837	717,148
10	1,810,400	962,470	0	0	1,381,756	769,976	0	0	898,662	800,765	519,888	784,722
11	1,759,779	733,865	0	0	1,352,067	587,092	0	0	793,627	686,975	479,683	770,861
12	1,847,658	753,665	0	0	1,418,873	602,932	0	0	807,278	587,719	490,862	946,507
Sum	22,069,783	13,868,166	0	0	16,918,401	11,094,532	0	0	9,836,883	9,829,904	6,023,680	9,995,390
Total	35,937,948	TonHr			28,012,934	kWh			35,685,857	kWh		
Saving	-6,123,930	TonHr			2,326,156	kWh			0	kWh		

Month	Elec. Energy saving (kWh)	Energy cost saving	Demand cost saving	Control strategy	off-peak num	on-peak num
1	163,601	$ 25,460	$ 47,275	Storage-priority	4	3
2	147,691	$ 23,636	$ 48,383	Storage-priority	5	2
3	162,503	$ 25,932	$ 49,959	Storage-priority	5	2
4	159,527	$ 24,782	$ 51,511	Storage-priority	5	3
5	197,581	$ 18,594	$ 58,747	Full storage	5	0
6	239,460	$ 21,032	$ 60,030	Full storage	5	0
7	259,450	$ 21,919	$ 62,638	Full storage	5	0
8	258,152	$ 22,736	$ 62,176	Full storage	5	0
9	231,960	$ 19,539	$ 58,456	Full storage	4	0
10	193,506	$ 16,715	$ 50,138	Full storage	4	0
11	164,951	$ 24,621	$ 44,532	Storage-priority	4	2
12	147,775	$ 24,633	$ 48,994	Storage-priority	4	2
Total	2,326,156	$ 269,598	$ 642,838			

Tank size: 5.0 M gallon

	Billing cost				Energy charge				Demand charge			
Month	CPP	SFA	REJ	WPC	CPP	SFA	REJ	WPC	CPP	SFA	REJ	WPC
1	$ 117,751	$ 79,103	$ 32,707	$ 60,038	$ 96,747	$ 61,165	$ 23,509	$ 44,645	$ 21,004	$ 17,938	$ 9,199	$ 15,393
2	$ 116,173	$ 76,508	$ 32,164	$ 54,838	$ 95,149	$ 58,563	$ 22,927	$ 39,458	$ 21,025	$ 17,945	$ 9,236	$ 15,381
3	$ 122,505	$ 86,427	$ 33,595	$ 55,866	$ 101,353	$ 68,456	$ 24,287	$ 40,484	$ 21,151	$ 17,971	$ 9,309	$ 15,383
4	$ 123,248	$ 90,492	$ 33,743	$ 53,098	$ 102,198	$ 72,494	$ 24,397	$ 37,786	$ 21,050	$ 17,998	$ 9,345	$ 15,312
5	$ 124,994	$ 122,340	$ 35,143	$ 58,866	$ 103,536	$ 101,400	$ 24,992	$ 40,801	$ 21,458	$ 20,940	$ 10,151	$ 18,064
6	$ 121,528	$ 126,472	$ 34,476	$ 58,617	$ 100,691	$ 105,756	$ 24,425	$ 41,098	$ 20,838	$ 20,716	$ 10,051	$ 17,519
7	$ 128,652	$ 129,223	$ 34,873	$ 56,827	$ 107,127	$ 110,237	$ 24,668	$ 40,166	$ 21,525	$ 18,985	$ 10,204	$ 16,661
8	$ 126,493	$ 130,617	$ 34,709	$ 54,952	$ 105,681	$ 111,372	$ 24,721	$ 38,672	$ 20,812	$ 19,244	$ 9,988	$ 16,280
9	$ 125,805	$ 111,393	$ 31,702	$ 50,281	$ 103,139	$ 91,971	$ 22,373	$ 34,897	$ 22,665	$ 19,423	$ 9,329	$ 15,384
10	$ 131,231	$ 91,767	$ 35,996	$ 55,266	$ 107,549	$ 74,934	$ 25,186	$ 38,180	$ 23,682	$ 16,833	$ 10,810	$ 17,086
11	$ 113,338	$ 75,601	$ 32,091	$ 51,488	$ 92,010	$ 57,646	$ 22,594	$ 36,161	$ 21,327	$ 17,956	$ 9,497	$ 15,327
12	$ 116,936	$ 71,795	$ 32,294	$ 59,680	$ 95,664	$ 53,908	$ 23,121	$ 44,256	$ 21,272	$ 17,887	$ 9,174	$ 15,424
Sum	$1,468,654	$1,191,737	$ 403,493	$ 669,817	$1,210,844	$ 967,902	$ 287,200	$ 476,605	$ 257,810	$ 223,835	$ 116,293	$ 193,213
Total	$3,733,701				$2,942,550				$ 791,151			
Saving ($	$ 922,487				$ 280,153				$ 642,335			

	Monthly Total kWh				Monthly demand kW							
Month	CPP	SFA	REJ	WPC	CPP onpeak	CPP offpeak	SFA onpeak	SFA offpeak	REJ onpeak	REJ offpeak	WPC onpeak	WPC offpeak
1	2,118,335	1,497,665	498,914	953,254	1,846	0	1,554	0	824	0	1,371	0
2	2,069,687	1,432,597	486,013	841,502	1,846	0	1,554	0	827	0	1,371	0
3	2,208,614	1,664,570	515,589	861,042	1,857	0	1,554	0	833	0	1,371	0
4	2,212,085	1,752,278	517,393	798,655	1,848	3,404	1,554	4,705	836	720	1,371	935
5	2,203,763	2,151,039	518,646	842,718	1,774	3,791	1,726	3,984	856	880	1,523	1,583
6	2,146,376	2,241,933	507,966	850,375	1,723	3,688	1,692	4,822	847	888	1,477	1,536
7	2,272,924	2,333,629	510,168	826,332	1,780	3,793	1,545	4,710	861	877	1,405	1,470
8	2,258,590	2,373,645	515,721	802,274	1,720	3,714	1,568	4,698	842	866	1,372	1,441
9	2,189,971	1,943,345	462,837	717,148	1,875	3,977	1,598	3,861	787	809	1,297	1,362
10	2,280,418	1,570,740	519,888	784,722	1,960	4,076	1,384	3,422	912	919	1,441	1,498
11	2,028,320	1,407,424	479,683	770,861	1,872	0	1,554	0	850	0	1,371	0
12	2,103,595	1,332,373	490,862	946,507	1,866	0	1,554	0	821	0	1,371	0
Sum	26,092,679	21,701,238	6,023,680	9,995,390	1,960	4,076	1,726	4,822	912	919	1,523	1,583
Total	63,812,987 kWh				5,661 kW							
Saving	2,211,959 kWh				5,036 kW							

	Monthly Total cooling load (TonHr)				ChW Production ELEC consumption (kWh)				Non-ChW production ELEC consumption (kWh)			
Month	CPP	SFA	REJ	WPC	CPP	SFA	REJ	WPC	CPP	SFA	REJ	WPC
1	1,754,037	989,911	0	0	1,357,386	791,929	0	0	760,949	705,736	498,914	953,254
2	1,708,520	945,086	0	0	1,320,644	756,069	0	0	749,044	676,528	486,013	841,502
3	1,805,569	1,032,842	0	0	1,396,279	826,273	0	0	812,334	838,297	515,589	861,042
4	1,840,783	1,045,850	0	0	1,421,352	836,680	0	0	790,733	915,597	517,393	798,655
5	1,810,400	1,473,019	0	0	1,386,346	1,178,415	0	0	817,416	972,624	518,646	842,718
6	1,752,000	1,622,492	0	0	1,343,144	1,297,994	0	0	803,232	943,939	507,966	850,375
7	1,810,400	1,781,069	0	0	1,388,638	1,424,855	0	0	884,286	908,774	510,168	826,332
8	1,810,400	1,820,719	0	0	1,388,660	1,456,575	0	0	869,931	917,070	515,721	802,274
9	1,752,000	1,334,332	0	0	1,340,580	1,067,465	0	0	849,391	875,880	462,837	717,148
10	1,810,400	962,470	0	0	1,381,756	769,976	0	0	898,662	800,765	519,888	784,722
11	1,592,119	900,561	0	0	1,234,693	720,449	0	0	793,627	686,975	479,683	770,861
12	1,672,609	930,817	0	0	1,296,317	744,654	0	0	807,278	587,719	490,862	946,507
Sum	21,119,236	14,839,168	0	0	16,255,796	11,871,334	0	0	9,836,883	9,829,904	6,023,680	9,995,390
Total	35,958,403	TonHr			28,127,130	kWh			35,685,857	kWh		
Saving	-6,144,385	TonHr			2,211,959	kWh			0	kWh		

Month	Elec. Energy saving (kWh)	Energy cost saving	Demand cost saving	Control strategy	off-peak num	on-peak num
1	142,031	$ 27,221	$ 47,048	Storage-priority	5	2
2	130,040	$ 25,145	$ 48,383	Storage-priority	5	2
3	142,519	$ 27,500	$ 49,959	Storage-priority	5	2
4	144,220	$ 26,699	$ 51,511	Storage-priority	5	2
5	193,045	$ 18,830	$ 58,931	Full storage	4	0
6	239,460	$ 21,032	$ 60,030	Full storage	5	0
7	259,450	$ 21,919	$ 62,638	Full storage	5	0
8	258,152	$ 22,736	$ 62,176	Full storage	5	0
9	231,960	$ 19,539	$ 58,456	Full storage	4	0
10	193,506	$ 16,715	$ 50,138	Full storage	4	0
11	148,969	$ 26,408	$ 44,290	Storage-priority	5	2
12	128,609	$ 26,409	$ 48,775	Storage-priority	5	2
Total	2,211,959	$ 280,153	$ 642,335			

Tank size: 6.0 M gallon

	Billing cost				Energy charge				Demand charge			
Month	CPP	SFA	REJ	WPC	CPP	SFA	REJ	WPC	CPP	SFA	REJ	WPC
1	$ 111,045	$ 84,072	$ 32,707	$ 60,038	$ 90,040	$ 66,134	$ 23,509	$ 44,645	$ 21,004	$ 17,938	$ 9,199	$ 15,393
2	$ 110,126	$ 80,999	$ 32,164	$ 54,838	$ 89,102	$ 63,044	$ 22,927	$ 39,458	$ 21,025	$ 17,955	$ 9,236	$ 15,381
3	$ 115,963	$ 91,305	$ 33,595	$ 55,866	$ 94,812	$ 73,311	$ 24,287	$ 40,484	$ 21,151	$ 17,995	$ 9,309	$ 15,383
4	$ 117,257	$ 94,949	$ 33,743	$ 53,098	$ 96,206	$ 76,927	$ 24,397	$ 37,786	$ 21,050	$ 18,022	$ 9,345	$ 15,312
5	$ 124,994	$ 122,573	$ 35,143	$ 58,866	$ 103,536	$ 101,633	$ 24,992	$ 40,801	$ 21,458	$ 20,940	$ 10,151	$ 18,064
6	$ 121,531	$ 125,931	$ 34,476	$ 58,617	$ 100,692	$ 105,397	$ 24,425	$ 41,098	$ 20,839	$ 20,534	$ 10,051	$ 17,519
7	$ 128,652	$ 129,223	$ 34,873	$ 56,827	$ 107,127	$ 110,237	$ 24,668	$ 40,166	$ 21,525	$ 18,985	$ 10,204	$ 16,661
8	$ 126,493	$ 130,617	$ 34,709	$ 54,952	$ 105,681	$ 111,372	$ 24,721	$ 38,672	$ 20,812	$ 19,244	$ 9,988	$ 16,280
9	$ 125,805	$ 111,393	$ 31,702	$ 50,281	$ 103,139	$ 91,971	$ 22,373	$ 34,897	$ 22,665	$ 19,423	$ 9,329	$ 15,384
10	$ 131,231	$ 91,767	$ 35,996	$ 55,266	$ 107,549	$ 74,934	$ 25,186	$ 38,180	$ 23,682	$ 16,833	$ 10,810	$ 17,086
11	$ 106,857	$ 80,239	$ 32,091	$ 51,488	$ 85,530	$ 62,283	$ 22,594	$ 36,161	$ 21,327	$ 17,956	$ 9,497	$ 15,327
12	$ 110,191	$ 76,790	$ 32,294	$ 59,680	$ 88,924	$ 58,895	$ 23,121	$ 44,256	$ 21,267	$ 17,895	$ 9,174	$ 15,424
Sum	$1,430,145	$1,219,858	$ 403,493	$ 669,817	$1,172,338	$ 996,138	$ 287,200	$ 476,605	$ 257,806	$ 223,720	$ 116,293	$ 193,213
Total	$3,723,313				$2,932,281				$ 791,032			
Saving ($	$ 932,876				$ 290,422				$ 642,454			

	Monthly Total kWh				Monthly demand kW							
Month	CPP	SFA	REJ	WPC	CPP onpeak	CPP offpeak	SFA onpeak	SFA offpeak	REJ onpeak	REJ offpeak	WPC onpeak	WPC offpeak
1	1,996,091	1,640,224	498,914	953,254	1,846	0	1,554	0	824	0	1,371	0
2	1,959,467	1,561,133	486,013	841,502	1,846	0	1,554	0	827	0	1,371	0
3	2,089,376	1,803,817	515,589	861,042	1,857	0	1,554	0	833	0	1,371	0
4	2,102,867	1,879,452	517,393	798,655	1,848	3,404	1,554	4,705	836	720	1,371	935
5	2,203,763	2,155,574	518,646	842,718	1,774	3,791	1,726	3,984	856	880	1,523	1,583
6	2,146,392	2,241,938	507,966	850,375	1,723	3,695	1,692	3,964	847	888	1,477	1,536
7	2,272,924	2,333,629	510,168	826,332	1,780	3,793	1,545	4,710	861	877	1,405	1,470
8	2,258,590	2,373,645	515,721	802,274	1,720	3,714	1,568	4,698	842	866	1,372	1,441
9	2,189,971	1,943,345	462,837	717,148	1,875	3,977	1,598	3,861	787	809	1,297	1,362
10	2,280,418	1,570,740	519,888	784,722	1,960	4,076	1,384	3,422	912	919	1,441	1,498
11	1,910,257	1,540,450	479,683	770,861	1,872	0	1,554	0	850	0	1,371	0
12	1,980,970	1,475,438	490,862	946,507	1,866	0	1,554	0	821	0	1,371	0
Sum	25,391,087	22,519,385	6,023,680	9,995,390	1,960	4,076	1,726	4,710	912	919	1,523	1,583
Total	63,929,542 kWh				5,661 kW							
Saving	2,095,404 kWh				5,036 kW							

	Monthly Total cooling load (TonHr)				ChW Production ELEC consumption (kWh)				Non-ChW production ELEC consumption (kWh)			
Month	CPP	SFA	REJ	WPC	CPP	SFA	REJ	WPC	CPP	SFA	REJ	WPC
1	1,579,403	1,168,109	0	0	1,235,142	934,487	0	0	760,949	705,736	498,914	953,254
2	1,551,063	1,105,757	0	0	1,210,424	884,605	0	0	749,044	676,528	486,013	841,502
3	1,635,229	1,206,900	0	0	1,277,041	965,520	0	0	812,334	838,297	515,589	861,042
4	1,684,757	1,204,818	0	0	1,312,134	963,854	0	0	790,733	915,597	517,393	798,655
5	1,810,400	1,478,688	0	0	1,386,346	1,182,950	0	0	817,416	972,624	518,646	842,718
6	1,752,000	1,622,499	0	0	1,343,160	1,297,999	0	0	803,232	943,939	507,966	850,375
7	1,810,400	1,781,069	0	0	1,388,638	1,424,855	0	0	884,286	908,774	510,168	826,332
8	1,810,400	1,820,719	0	0	1,388,660	1,456,575	0	0	869,931	917,070	515,721	802,274
9	1,752,000	1,334,332	0	0	1,340,580	1,067,465	0	0	849,391	875,880	462,837	717,148
10	1,810,400	962,470	0	0	1,381,756	769,976	0	0	898,662	800,765	519,888	784,722
11	1,423,441	1,066,843	0	0	1,116,630	853,475	0	0	793,627	686,975	479,683	770,861
12	1,497,371	1,109,648	0	0	1,173,692	887,719	0	0	807,278	587,719	490,862	946,507
Sum	20,116,863	15,861,852	0	0	15,554,204	12,689,481	0	0	9,836,883	9,829,904	6,023,680	9,995,390
Total	35,978,715	TonHr			28,243,685	kWh			35,685,857	kWh		
Saving	-6,164,696	TonHr			2,095,404	kWh			0	kWh		

Month	Elec. Energy saving (kWh)	Energy cost saving	Demand cost saving	Control strategy	off-peak num	on-peak num
1	121,716	$ 28,958	$ 47,048	Storage-priority	5	2
2	111,724	$ 26,711	$ 48,372	Storage-priority	5	2
3	122,510	$ 29,187	$ 49,935	Storage-priority	5	2
4	126,264	$ 28,258	$ 51,487	Storage-priority	5	2
5	188,510	$ 18,597	$ 58,931	Full storage	4	0
6	239,438	$ 21,391	$ 60,211	Full storage	4	0
7	259,450	$ 21,919	$ 62,638	Full storage	5	0
8	258,152	$ 22,736	$ 62,176	Full storage	5	0
9	231,960	$ 19,539	$ 58,456	Full storage	4	0
10	193,506	$ 16,715	$ 50,138	Full storage	4	0
11	134,006	$ 28,251	$ 44,290	Storage-priority	5	2
12	108,169	$ 28,162	$ 48,772	Storage-priority	5	2
Total	2,095,404	$ 290,422	$ 642,454			

Tank size: 7.0 M gallon

	Billing cost				Energy charge				Demand charge			
Month	CPP	SFA	REJ	WPC	CPP	SFA	REJ	WPC	CPP	SFA	REJ	WPC
1	$ 105,658	$ 88,018	$ 32,707	$ 60,038	$ 84,653	$ 70,064	$ 23,509	$ 44,645	$ 21,004	$ 17,954	$ 9,199	$ 15,393
2	$ 105,619	$ 84,348	$ 32,164	$ 54,838	$ 84,594	$ 66,390	$ 22,927	$ 39,458	$ 21,025	$ 17,958	$ 9,236	$ 15,381
3	$ 112,116	$ 94,205	$ 33,595	$ 55,866	$ 90,964	$ 76,210	$ 24,287	$ 40,484	$ 21,151	$ 17,995	$ 9,309	$ 15,383
4	$ 114,783	$ 96,767	$ 33,743	$ 53,098	$ 93,733	$ 78,745	$ 24,397	$ 37,786	$ 21,050	$ 18,022	$ 9,345	$ 15,312
5	$ 124,994	$ 122,770	$ 35,143	$ 58,866	$ 103,536	$ 101,830	$ 24,992	$ 40,801	$ 21,458	$ 20,940	$ 10,151	$ 18,064
6	$ 121,531	$ 125,931	$ 34,476	$ 58,617	$ 100,692	$ 105,397	$ 24,425	$ 41,098	$ 20,839	$ 20,534	$ 10,051	$ 17,519
7	$ 128,652	$ 129,223	$ 34,873	$ 56,827	$ 107,127	$ 110,237	$ 24,668	$ 40,166	$ 21,525	$ 18,985	$ 10,204	$ 16,661
8	$ 126,493	$ 130,617	$ 34,709	$ 54,952	$ 105,681	$ 111,372	$ 24,721	$ 38,672	$ 20,812	$ 19,244	$ 9,988	$ 16,280
9	$ 125,805	$ 111,393	$ 31,702	$ 50,281	$ 103,139	$ 91,971	$ 22,373	$ 34,897	$ 22,665	$ 19,423	$ 9,329	$ 15,384
10	$ 131,231	$ 91,767	$ 35,996	$ 55,266	$ 107,549	$ 74,934	$ 25,186	$ 38,180	$ 23,682	$ 16,833	$ 10,810	$ 17,086
11	$ 100,864	$ 84,454	$ 32,091	$ 51,488	$ 79,614	$ 66,497	$ 22,594	$ 36,161	$ 21,250	$ 17,957	$ 9,497	$ 15,327
12	$ 103,803	$ 81,520	$ 32,294	$ 59,680	$ 82,614	$ 63,608	$ 23,121	$ 44,256	$ 21,189	$ 17,912	$ 9,174	$ 15,424
Sum	$1,401,547	$1,241,012	$ 403,493	$ 669,817	$1,143,896	$1,017,256	$ 287,200	$ 476,605	$ 257,651	$ 223,756	$ 116,293	$ 193,213
Total	$3,715,869				$2,924,957				$ 790,912			
Saving ($	$ 940,319				$ 297,746				$ 642,573			

	Monthly Total kWh				Monthly demand kW							
Month	CPP	SFA	REJ	WPC	CPP onpeak	CPP offpeak	SFA onpeak	SFA offpeak	REJ onpeak	REJ offpeak	WPC onpeak	WPC offpeak
1	1,897,895	1,752,956	498,914	953,254	1,846	0	1,554	0	824	0	1,371	0
2	1,877,303	1,657,127	486,013	841,502	1,846	0	1,554	0	827	0	1,371	0
3	2,019,236	1,887,001	515,589	861,042	1,857	0	1,554	0	833	0	1,371	0
4	2,057,777	1,931,601	517,393	798,655	1,848	3,404	1,554	4,705	836	720	1,371	935
5	2,203,763	2,160,109	518,646	842,718	1,774	3,791	1,726	3,984	856	880	1,523	1,583
6	2,146,392	2,241,938	507,966	850,375	1,723	3,695	1,692	3,964	847	888	1,477	1,536
7	2,272,924	2,333,629	510,168	826,332	1,780	3,793	1,545	4,710	861	877	1,405	1,470
8	2,258,590	2,373,645	515,721	802,274	1,720	3,714	1,568	4,698	842	866	1,372	1,441
9	2,189,971	1,943,345	462,837	717,148	1,875	3,977	1,598	3,861	787	809	1,297	1,362
10	2,280,418	1,570,740	519,888	784,722	1,960	4,076	1,384	3,422	912	919	1,441	1,498
11	1,802,638	1,661,338	479,683	770,861	1,872	0	1,554	0	850	0	1,371	0
12	1,866,067	1,610,637	490,862	946,507	1,866	0	1,554	0	821	0	1,371	0
Sum	24,872,975	23,124,066	6,023,680	9,995,390	1,960	4,076	1,726	4,710	912	919	1,523	1,583
Total	64,016,111 kWh				5,661 kW							
Saving	2,008,835 kWh				5,036 kW							

	Monthly Total cooling load (TonHr)				ChW Production ELEC consumption (kWh)				Non-ChW production ELEC consumption (kWh)			
Month	CPP	SFA	REJ	WPC	CPP	SFA	REJ	WPC	CPP	SFA	REJ	WPC
1	1,439,123	1,309,025	0	0	1,136,946	1,047,220	0	0	760,949	705,736	498,914	953,254
2	1,433,686	1,225,749	0	0	1,128,260	980,599	0	0	749,044	676,528	486,013	841,502
3	1,535,029	1,310,881	0	0	1,206,901	1,048,704	0	0	812,334	838,297	515,589	861,042
4	1,620,343	1,270,004	0	0	1,267,044	1,016,003	0	0	790,733	915,597	517,393	798,655
5	1,810,400	1,484,357	0	0	1,386,346	1,187,486	0	0	817,416	972,624	518,646	842,718
6	1,752,000	1,622,499	0	0	1,343,160	1,297,999	0	0	803,232	943,939	507,966	850,375
7	1,810,400	1,781,069	0	0	1,388,638	1,424,855	0	0	884,286	908,774	510,168	826,332
8	1,810,400	1,820,719	0	0	1,388,660	1,456,575	0	0	869,931	917,070	515,721	802,274
9	1,752,000	1,334,332	0	0	1,340,580	1,067,465	0	0	849,391	875,880	462,837	717,148
10	1,810,400	962,470	0	0	1,381,756	769,976	0	0	898,662	800,765	519,888	784,722
11	1,269,643	1,217,953	0	0	1,009,011	974,363	0	0	793,627	686,975	479,683	770,861
12	1,333,193	1,278,647	0	0	1,058,789	1,022,917	0	0	807,278	587,719	490,862	946,507
Sum	19,376,615	16,617,703	0	0	15,036,092	13,294,162	0	0	9,836,883	9,829,904	6,023,680	9,995,390
Total	35,994,318	TonHr			28,330,255	kWh			35,685,857	kWh		
Saving	-6,180,300	TonHr			2,008,835	kWh			0	kWh		

Month	Elec. Energy saving (kWh)	Energy cost saving	Demand cost saving	Control strategy	off-peak num	on-peak num
1	107,180	$ 30,415	$ 47,032	Storage-priority	5	2
2	97,894	$ 27,872	$ 48,370	Storage-priority	5	2
3	109,466	$ 30,135	$ 49,935	Storage-priority	5	2
4	119,205	$ 28,913	$ 51,487	Storage-priority	5	2
5	183,975	$ 18,400	$ 58,931	Full storage	4	0
6	239,438	$ 21,391	$ 60,211	Full storage	4	0
7	259,450	$ 21,919	$ 62,638	Full storage	5	0
8	258,152	$ 22,736	$ 62,176	Full storage	5	0
9	231,960	$ 19,539	$ 58,456	Full storage	4	0
10	193,506	$ 16,715	$ 50,138	Full storage	4	0
11	120,736	$ 29,952	$ 44,366	Storage-priority	5	1
12	87,874	$ 29,759	$ 48,834	Storage-priority	5	1
Total	2,008,835	$ 297,746	$ 642,573			

VITA

Name: Zhiqin Zhang

Address: Energy Systems Laboratory

Department of Mechanical Engineering

Texas A&M University

College Station, TX 77843-3581

Email Address: zhangzhiqin@neo.tamu.edu

Education: B.S., Building Sciences, Tsinghua University, 2001

M.S., Building Sciences, Tsinghua University, 2004